Title
The Molecular Mechanisms of Lifespan Extension by Alpha-Ketoglutarate in Caenorhabditis elegans

Author
Chin, Randall

Publication Date
2014

Peer reviewed|Thesis/dissertation

UNIVERSITY OF CALIFORNIA

Los Angeles

The Molecular Mechanisms of Lifespan Extension by Alpha-Ketoglutarate in *Caenorhabditis elegans*

A dissertation submitted in partial satisfaction of the
requirements for the degree Doctor of Philosophy
in Molecular Biology

By

Randall Marcelo Chin

2014

ABSTRACT OF THE DISSERTATION

The Molecular Mechanisms of Lifespan Extension by

Alpha-Ketoglutarate in *Caenorhabditis elegans*

by

Randall Marcelo Chin

Doctor of Philosophy in Molecular Biology

University of California, Los Angeles, 2014

Professor Jing Huang, Chair

As the elderly population is now the fastest growing age group in the United States, there is an imminent need to understand the molecular mechanisms of aging and develop new approaches to counter aging and the maladies that come with it. Modulation of metabolism, either by dietary restriction or pharmacologic or genetic alteration of metabolic pathways, can extend lifespan and delay age-related diseases in evolutionarily diverse organisms. Here we demonstrate, for the first time, a role for alpha-ketoglutarate (α-KG) in the regulation of aging. α-KG serves many functions in the cell, including being an intermediate of the tricarboxylic acid cycle, a precursor for several amino acids, and a substrate for α-KG-dependent oxygenases. We show that α-KG extends the mean lifespan of adult *Caenorhabditis elegans* by about 50%, and provide evidence to suggest that this is not due to the metabolism of α-KG into other metabolites. Other metabolites have been shown to extend lifespan as well, but without a well defined mechanism. Research on small molecules in aging has been hindered by the inability to identify drug targets. We use a label-free, unbiased drug target identification strategy termed DARTS (drug affinity responsive target stability) to uncover a new binding target of α-KG, the beta subunit of the ATP

synthase. We reveal that α-KG inhibits ATP synthase in *in vitro* and *in vivo* assays using both worm and mammalian models. Consistently, genetic or pharmacological inhibition of ATP synthase yields the same phenotypes as α-KG: increased lifespan, decreased ATP levels, lower oxygen consumption rates, elevated levels of reactive oxygen species, and reduced target of rapamycin signaling. However, unlike genetic inhibition of ATP synthase, α-KG does not induce the mitochondrial unfolded protein response, cause larval arrest, or slow pharyngeal pumping rates. Remarkably, α-KG does not further increase the lifespan of dietary restricted animals and is elevated during starvation, a testament to it being a key regulator of dietary restriction mediated lifespan extension. Like dietary restriction, α-KG also induces autophagy, and we provide evidence to suggest that autophagy may play an essential role for the longevity of α-KG treated animals. Our findings posit α-KG as a key regulator of metabolic pathways in response to nutrient status, and suggest new strategies for the prevention and treatment of aging and age-related diseases.

The dissertation of Randall Marcelo Chin is approved.

Catherine F. Clarke

Alison R. Frand

Jing Huang, Committee Chair

University of California, Los Angeles

2014

To my dear family, for lending me their unconditional support through good and bad times.

TABLE OF CONTENTS

LIST OF FIGURES AND TABLES

For Chapter 2 (reprint of previous publication):

LIST OF FIGURES AND TABLES

For Chapters 3 and 4:

ACKNOWLEDGEMENTS

First and foremost, I would like to thank my advisor, Jing Huang, for supporting me throughout these years. When I first joined her lab, I had a lot of crazy ideas that I wanted to test. I wanted to discover a novel compound or treatment that could extend lifespan in *C. elegans*, and then study the mechanism for the anti-aging effect. After 14 months of experimentation, I still did not have any fascinating data to show. However, Jing was supportive of my efforts, and I am very thankful for that. Eventually, Jing came up with the idea to test alpha-ketoglutarate for an effect on lifespan, and that day has changed my life. Without Jing, I would have never had this great project to work on, and I am really grateful for her guidance throughout graduate school.

I would like to thank my committee members, Steven Clarke, Catherine Clarke, Alison Frand, and David Walker. Through their insightful suggestions, they have helped me become a better scientist and well as a better person. In particular, I am grateful for all the help that Alison Frand and her lab gave to me, especially for the experiments involving confocal imaging, and for Catherine Clarke and her student Fernando Gomez for introducing me to the wonderful world of *Caenorhabditis elegans*. I want to thank all the members of the Jing Huang lab, including Mariam Valamehr, Ryosuke Watanabe, Nao Jonai, Heejun Hwang, Brett Lomenick, Simon Diep, Melody Pai, Gwanghyun Jung, and Xudong Fu. They been very helpful in teaching me how to do experiments, doing experiments for my project, and getting me through each day (emotionally and scientifically). I also want to thank my undergrads, Eileen Hu, Kimberly Yan, and Roger Wang. They did a lot of experiments for me, taught me how to train students, and kept me feeling young.

I need to thank Bin Lui and Vasili Chernishof, who introduced me to the world of basic research while I was an undergrad working in Ke Shuai's lab at UCLA. I also need to thank Dr. Hendrickson from Van Nuys High School, who inspired me to study biology in the first place. They were the ones who started it all.

As a graduate student, I was supported by funding from the predoctoral training program in genetic mechanisms (USPHS National Research Service Award GM07104) and the UCLA graduate division dissertation year fellowship.

Chapter 2 is a reprint of a previous publication published in *Nature* (Chin, R. M. *et al*. The metabolite alpha-ketoglutarate extends lifespan by inhibiting ATP synthase and TOR. *Nature*, doi:10.1038/nature13264 (2014)) that has been slightly modified to meet the specifications in the UCLA graduate division thesis and dissertation formatting and filing guide. I would like to acknowledge contributions from the following co-authors: X. Fu, M.Y. Pai, L. Vergnes, H. Hwang, G. Deng, S. Diep, B. Lomenick, V.S. Meli, G.C. Monsalve, E. Hu, S.A. Whelan, J.X. Wang, G. Jung, G.M. Solis, F. Fazlollahi, C. Kaweeteerawat, A. Quach, M. Nili, A.S. Krall, H.A. Godwin, H.R. Chang, K.F. Faull, F. Guo, M. Jiang, S.A. Trauger, A. Saghatelian, D. Braas, H.R. Christofk, C.F. Clarke, M.A. Teitell, M. Petrascheck, K. Reue, M.E. Jung, A.R. Frand, and J. Huang. J. Huang is the principle investigator of the work presented in Chapter 2; she provided ideas, helped design experiments and analyze results, and helped write the manuscript. As an author of this paper, I retain the copyrights to reprint and reuse without permission from *Nature*.

For Chapter 3, I would like to acknowledge contributions from: J. Wu, V.S. Meli, R. Wang, and J. Huang. Specifically, J. Wu executed heat resistance assays, V.S. Meli planned and performed fluorescence imaging experiments concerning the mitochondrial unfolded protein response, and R. Wang helped helped in western blot experiments concerning the mitochondrial unfolded protein response. I would also like to thank M. Hansen for gifting us the *hlh-30(tm1978)* strain. J. Huang is the principle investigator of the work presented in Chapter 3; she provided ideas, helped design experiments and analyze results, and helped write the manuscript.

For Chapter 4, I would like to acknowledge contributions from: E. Hu, K. Yan, R. Wang, X. Fu, D. Braas, H. Christofk, and J. Huang. Specifically, E. Hu, K. Yan, and R. Wang helped in

conducting and planning lifespan experiments, and X. Fu, D. Braas, and H. Christofk performed the metabolome experiment and analyzed its results. J. Huang is the principle investigator of the work presented in Chapter 4; she provided ideas, helped design experiments and analyze results, and helped write the manuscript.

VITA

EDUCATION

2004-2008	University of California, Los Angeles (UCLA)
	Bachelor of Science, Molecular, Cell, and Developmental Biology

HONORS AND AWARDS

2013-2014	UCLA dissertation year fellowship
2010-2011	Pre-doctoral training program in genetic mechanisms;
	USPHS national research service award GM07104
2008	Vice provost award (for best review article published in the UCLA
	Undergraduate Science Journal)
2007	Amgen scholars award
2005-2008	Dean's honors list, UCLA
2004-2008	College honors program, UCLA

PUBLICATIONS AND PRESENTATIONS

Chin RM, Fu X, Pai MY, Vergnes L, Hwang H, Deng G, Diep S, Lomenick B, Meli VS, Monsalve GC, Hu E, Whelan SA, Wang JX, Jung G, Solis GM, Fazlollahi F, Kaweeteerawat C, Quach A, Nili M, Krall AS, Godwin HA, Chang HR, Faull KF, Guo F, Jiang M, Trauger SA, Saghatelian A, Braas D, Christofk HR, Clarke CF, Teitell MA, Petrascheck M, Reue K, Jung ME, Frand AR, and Huang J. The metabolite alpha-ketoglutarate extends lifespan by inhibiting the ATP synthase and TOR. *Nature*, doi:10.1038/nature13264 (2014).

Chin RM. Small molecule regulators of aging in *Caenorhabditis elegans*. UCLA Worm Enthusiasts Meeting, Los Angeles, March 2013

Chin RM. Small molecule regulators of aging. UCLA Molecular and Medical Pharmacology Retreat, Huntington Beach, November 2012.

Chin RM. Chemical genetics of aging. Molecular and Medical Pharmacology M237, Los Angeles, October 2012.

Gomez F, Saiki R, **Chin R**, Srinivasan C, Clarke C. Restoring de novo coenzyme Q biosynthesis in *Caenorhabditis elegans coq-3* mutants yields profound rescue compared to exogenous coenzyme Q supplementation. *Gene* **506**, 106-116 (2012).

Chin R, Diep S, Lomenick B, Pai M, Fu X, Deng G, Jung G, Hu E, Yan K, Jung M, and Huang J. Small molecule regulators of aging. *Cell* Symposia, Genetics and Chemistry, Sharing a Language of Discovery, Boston, May 2012.

Chin RM. Lifespan extension in *Caenorhabditis elegans* by alpha ketoglutarate (α-KG) and other metabolites. UCLA Worm Group Meeting, Los Angeles, April 2012.

Lomenick B, Hao R, Jonai N, **Chin RM**, Aghajan M, Warburton S, Wang J, Wu RP, Gomez F, Loo JA, Wohlschlegel JA, Vondriska TM, Pelletier J, Herschman HR, Clardy J, Clarke CF, Huang J. Target identification using drug affinity responsive target stability (DARTS). *Proc Natl Acad Sci U S A*. **106**, 21984-21989 (2009).

Chin RM. Fountain of Youth? A Review of Aging Research. *UCLA Undergraduate Science Journal* **21**, 25-32 (2008).

CHAPTER 1

Introduction

Aging, or the accumulation of changes that occurs in an organism over time, is an intriguing subject that has boggled the mind for centuries. The Spanish explorer Juan Ponce de León, for example, was purportedly searching for the fountain of youth when he discovered Florida in 1513. Within the last few decades, we have seen an explosion in the amount of research in the aging field. It is important to study aging because the elderly population is now the fastest growing age group. For instance, by 2030, it is projected that 20% of the US population will be age 65 or older[1]. As age increases, the risk for age-related diseases, such as cancer, cardiovascular disease, and neurodegeneration, also increases[2]. Therefore, a study and understanding of the basic biology and mechanisms of aging is essential and can lead to new methods to treat or prevent aging and age related diseases.

DIETARY RESTRICTION

Dietary restriction (DR), also known as calorie restriction, is the reduction of food intake without malnutrition. In 1935, McCay et al. showed, for the first time, that the mean and maximal lifespan in rats could be extended by DR[3]. Since then, DR has been demonstrated to extend lifespan in multiple organisms, including yeast, worms, flies, mice, primates, and many others[4-12]. In *C. elegans*, there are several different ways to achieve DR, including bacterial dilution and genetic mutation of the *eat-2* gene, which slows pharyngeal pumping[5,13]. In addition to lifespan extension, it is also well documented that DR reduces the incidence of multiple age-related diseases[9,14-16]. In humans, it is difficult to conduct a well-controlled long-term survival study on

DR; however, DR has been shown to be beneficial with respect to age-related diseases in humans[17,18].

Many studies in the field of aging have been devoted to understanding the mechanisms by which DR extends lifespan. Nutrient-sensing pathways, such as the insulin/IGF-1 signaling (IIS), TOR (target of rapamycin), and AMP kinase signaling pathways, have long been suspected to regulate the response to DR in lifespan. Of these, TOR signaling has been most consistently linked to DR—supported by evidence in yeast, worms, flies, and mice[19,20].

GENETIC REGULATION OF AGING

In 1988, the first mutant gene found to extend lifespan (*age-1*) was named and mapped, with a reported 65% increase in mean lifespan[21]. This was a breakthrough finding because prior to this, people could not fathom that a mutation in just a single gene could result in such a robust long-life phenotype. Their finding inspired others to find other genes that regulate aging, and since then, many of these so-called longevity genes have been identified. Much of the work in the aging field has been done in the model organism *Caenorhabditis elegans*, due to its relatively short lifespan and ease of genetic manipulation. Massive RNAi Interference (RNAi) screens, as well as detailed genetic epistasis studies, have been conducted in *C. elegans* to identify genes that regulate aging and understand their mechanism. Here, we summarize the research done on several of the key aging regulatory pathways, focusing on their relationship to each other.

TOR pathway

The TOR kinase is a serine/threonine kinase that functions in two complexes, TOR complex 1 (TORC1) and TOR complex 2 (TORC2). TORC1 has been much more extensively studied than TORC2, and thus the upstream regulation and downstream outputs of TORC1 are better understood. TORC1 senses a variety of nutrient and small molecule cues (e.g., amino acids, ATP, glucose, oxygen, and growth factors) and regulates cell growth, division, motility,

autophagy, protein synthesis, nucleotide synthesis, fatty acid synthesis, and transcription[22]. Inhibition of TOR, either by genetic means or by rapamycin, has been demonstrated to extend lifespan in yeast, worms, flies, and mice[23]. TOR inhibition extends lifespan independently of the IIS pathway, as *daf-16*/FOXO null mutations do not abrogate the longevity by TOR inhibition[24,25]. TOR inhibition is closely linked with DR, and in yeast, worms and flies, the longevity produced by TOR inhibition is not further increased by DR[25-28].

A major downstream target of TORC1 is protein synthesis. The phosphorylation of S6 kinase (S6K) and the eukaryotic translation initiation factor 4E (eIF4E)-binding protein 1 (4E-BP1) by TORC1 leads to a massive increase in ribosome and mRNA production as well as the promotion of translation initiation and elongation[22]. Inhibition of protein synthesis alone is sufficient for lifespan extension[25,29]. Paradoxically, inhibition of S6K or translation initiation factors, both of which decrease protein synthesis, extend lifespan via seemingly different mechanisms[25].

Autophagy

Autophagy is an evolutionarily conserved process in which protein and organelles can be degraded via the lysosomal pathway. There are two main functions of autophagy: (1) to rid the cell of damaged or misfolded proteins and organelles and (2) to provide additional energy during times of starvation or stress. There are three types of autophagy: macroautophagy, microautophagy, and chaperone-mediated autophagy. Macroautophagy is more extensively studied and degrades more materials than the other two types of autophagy. In macroautophagy, double membrane structures called autophagosomes engulf entire regions of the cytoplasm (including proteins and organelles), and then fuse with secondary lysosomes to breakdown its contents. Out of the three types of autophagy, only macroautophagy has been studied in yeast, worms, flies, and mice with respect to aging. Therefore, only macroautophagy, henceforth referred to as autophagy, will be discussed here.

Autophagy is negatively regulated by TORC1. In general, when nutrients are abundant, TORC1 stimulates growth and blocks autophagy. But during starvation, TORC1 is downregulated and autophagy is activated. In mammals, TORC1 regulates autophagy through several different proteins, including the unc-51-like kinase 1 (ULK1) and the transcription factor EF (TFEB). Under nutrient-rich conditions, TORC1 phosphorylates and suppresses ULK1, a kinase required to initiate autophagy[22]. Likewise, when nutrients are abundant, TORC1 also phosphorylates TFEB to prevent its translocation into the nucleus[22]. TFEB controls the expression of multiple genes involved throughout the autophagy process, such as those playing a role in autophagosome formation, cargo degradation, fusion, and lysosomal degradation[22].

Enhancing autophagy, by overexpressing either TFEB or Atg5 (a protein essential for the early stages of autophagosome formation), is sufficient to extend lifespan[30,31]. Additionally, autophagy is required for the lifespan extension observed in multiple distinct longevity pathways, such as reduced IIS, TOR inhibition, DR, and mitochondrial inhibition[30,32-34], and in some studies, autophagy-defective animals did not exhibit a shortened lifespan[33]. Of all the aging-regulatory pathways, autophagy appears to be essential for the most longevity-promoting regimens.

Mitochondrial inhibition

A modest inhibition of the mitochondrial electron transport chain (ETC), either by genetic mutation, RNAi, or pharmacological perturbation, has been shown to extend lifespan in yeast, worms, flies, and mice[35-41]. Of the three methods, pharmacological perturbation of the ETC is the least studied with respect to lifespan extension, and genetic modulation of the ETC has yielded different results depending on whether mutation or RNAi is studied[42]. Therefore, the mechanism by which mitochondrial inhibition extends lifespan is not fully understood. The amount of lifespan extension is directly related to the degree of ETC inhibition[43], with too little inhibition resulting in no lifespan change, and too much inhibition resulting in death or severe disorders[44,45]. At least in worms, the mechanism by which mitochondrial inhibition extends

lifespan appears to be distinct from the IIS pathway, as ETC RNAi can increase the lifespan of *daf-16* and *daf-2* mutants[37]. On the other hand, the relationship between mitochondrial inhibition and DR is unclear. The mutations in the *clk-1* gene, encoding a step in the coenzyme Q biosynthetic pathway, extend lifespan[46], but do not further extend the lifespan of *eat-2* animals[5]. In contrast, life extending mutations in *nuo-6* (a complex I subunit) can further prolong the lifespan of *eat-2* animals[42]. As alluded to above, mitochondrial inhibition does not increase lifespan in autophagy defective strains[32].

Recently, it was reported that the mitochondrial unfolded protein response (UPR^{mt}) plays an important role in the extension of lifespan by ETC inhibition[47,48], but this remains controversial[49]. The UPR^{mt} is a stress response mechanism that, upon mitochondrial perturbation, activates the expression of nuclear-encoded mitochondrial-associated protein chaperones, such as HSP-6 and HSP-60[50]. Apparently, a stoichiometric imbalance between the levels of nuclear-encoded and mitochondrial-encoded mitochondrial proteins activates the UPR^{mt} [48]. The UPR^{mt} was shown to be activated by ETC RNAi, but whether the UPR^{mt} is required for the lifespan extension by ETC RNAi/mutants is debatable[47-49].

The long life caused by mitochondrial inhibition is a puzzling phenomenon, especially when considering the fact that mitochondrial function decreases with age[45] and DR increases mitochondrial biogenesis and respiration[51,52]. Intriguingly, increasing mitochondrial biogenesis or overexpressing complex I of the ETC also extends lifespan[53-55].

Insulin/IGF-1 signaling

The first gene found to extend lifespan, *age-1*, is part of the IIS pathway[21]. Reduced IIS results in lifespan extension in worms, flies, and mice[56-58]. The mechanisms of lifespan extension by the IIS pathway have been well characterized in *C. elegans*. Decreased IIS extends lifespan through the activation of three transcription factors (DAF-16, HSF-1, SKN-1), such that loss-of-function mutations in any one of the transcription factors can greatly (or fully) suppress the longevity of the long-lived *daf-2* (insulin/IGF-1 receptor) mutant[19,56,59,60]. These

transcription factors activate a myriad of longevity promoting genes, encoding stress response genes, antimicrobial peptides, catalases, chaperones, and many others[19].

In *C. elegans*, the relationship between DR and IIS is complicated, with *daf-16* being required for DR by bacterial dilution but not for DR by *eat-2* mutation[13]. Also, *eat-2;daf-2* double mutants live even longer than *daf-2* or *eat-2* mutants[5]. As with mitochondrial inhibition and reduced TOR signaling, autophagy-defective strains abrogate the lifespan extension by IIS mutations[33,34].

SMALL MOLECULE REGULATION OF AGING

Recently, researchers have begun to study small molecules in the modulation of aging. There are several advantages to studying small molecules. First, there are an endless amount of small molecules to study, including thousands of endogenous metabolites and infinite amounts of synthesized molecules. Second, small molecules can be readily tested in multiple model organisms. Lastly, as of now, the development of small molecules that delay aging has the most potential to be translated for human use. Many small molecules have been found to extend lifespan in *C. elegans*[61,62], and remarkably, some have even been shown to extend the lifespan of mammals[63].

The development of the metabolomics field has made it possible to study the steady state levels and flux of metabolites in organisms. The metabolome of long-lived mutants, dietary restricted animals, and longevity-drug treated animals, as well as old mice versus young mice, have been analyzed[64-67], and so it is exciting to speculate whether the supplementation of metabolites found in long-lived or young animals would delay aging. Of course, another viable approach is to first find metabolites that extend lifespan and then try to elucidate their mechanism. Recently, several metabolites have been shown to extend lifespan[68-70], but the molecular mechanisms by which they operate are largely unknown.

In this dissertation, we report that alpha-ketoglutarate (α-KG), a tricarboxylic acid cycle intermediate, extends lifespan. We use a novel, label-free, unbiased drug-target identification strategy[71] to show that α-KG binds to the beta subunit of ATP synthase, and we demonstrate that α-KG acts as an inhibitor of ATP synthase. We further show that α-KG inhibits TOR, and speculate that α-KG may be a key metabolite in DR-induced longevity. Finally, in the latter chapters, we investigate the role of other key aging-regulatory pathways in α-KG mediated lifespan extension and explore the effects of α-KG-related metabolites in aging.

References

1 US Department of Health and Human Services, A. o. A. *Projected future growth of the older population*, <http://www.aoa.gov/Aging_Statistics/future_growth/future_growth.aspx#age> (2008).

2 Niccoli, T. & Partridge, L. Ageing as a risk factor for disease. *Curr Biol* **22**, R741-752, doi:10.1016/j.cub.2012.07.024 (2012).

3 McCay, C. M., Crowell, M. F. & Maynard, L. A. The effect of retarded growth upon the length of life span and upon the ultimate body size. 1935. *Nutrition* **5**, 155-171; discussion 172 (1935).

4 Lin, S. J., Defossez, P. A. & Guarente, L. Requirement of NAD and SIR2 for life-span extension by calorie restriction in Saccharomyces cerevisiae. *Science* **289**, 2126-2128 (2000).

5 Lakowski, B. & Hekimi, S. The genetics of caloric restriction in Caenorhabditis elegans. *Proc Natl Acad Sci U S A* **95**, 13091-13096 (1998).

6 Avery, L. The genetics of feeding in Caenorhabditis elegans. *Genetics* **133**, 897-917 (1993).

7 Greer, E. L. *et al.* An AMPK-FOXO pathway mediates longevity induced by a novel method of dietary restriction in C. elegans. *Curr Biol* **17**, 1646-1656, doi:10.1016/j.cub.2007.08.047 (2007).

8 Partridge, L., Green, A. & Fowler, K. Effects of egg-production and of exposure to males on female survival in Drosophila melanogaster. *Journal of Insect Physiology* **33**, 745–749 (1987).

9 Colman, R. J. *et al.* Caloric restriction delays disease onset and mortality in rhesus monkeys. *Science* **325**, 201-204 (2009).

10 Colman, R. J. *et al.* Caloric restriction reduces age-related and all-cause mortality in rhesus monkeys. *Nat Commun* **5**, 3557, doi:10.1038/ncomms4557 (2014).

11 Weindruch, R. & Walford, R. L. Dietary restriction in mice beginning at 1 year of age: effect on life-span and spontaneous cancer incidence. *Science* **215**, 1415-1418 (1982).

12 Weindruch, R., Walford, R. L., Fligiel, S. & Guthrie, D. The retardation of aging in mice by dietary restriction: longevity, cancer, immunity and lifetime energy intake. *J Nutr* **116**, 641-654 (1986).

13 Greer, E. L. & Brunet, A. Different dietary restriction regimens extend lifespan by both independent and overlapping genetic pathways in C. elegans. *Aging Cell* **8**, 113-127 (2009).

14 Omodei, D. & Fontana, L. Calorie restriction and prevention of age-associated chronic disease. *FEBS Lett* **585**, 1537-1542, doi:10.1016/j.febslet.2011.03.015 (2011).

15 Lane, M. A., Ingram, D. K. & Roth, G. S. Calorie restriction in nonhuman primates: effects on diabetes and cardiovascular disease risk. *Toxicol Sci* **52**, 41-48 (1999).

16 Mattson, M. P. & Wan, R. Beneficial effects of intermittent fasting and caloric restriction on the cardiovascular and cerebrovascular systems. *J Nutr Biochem* **16**, 129-137, doi:10.1016/j.jnutbio.2004.12.007 (2005).

17 Fontana, L., Meyer, T. E., Klein, S. & Holloszy, J. O. Long-term calorie restriction is highly effective in reducing the risk for atherosclerosis in humans. *Proc Natl Acad Sci U S A* **101**, 6659-6663, doi:10.1073/pnas.0308291101 (2004).

18 Witte, A. V., Fobker, M., Gellner, R., Knecht, S. & Floel, A. Caloric restriction improves memory in elderly humans. *Proc Natl Acad Sci U S A* **106**, 1255-1260, doi:10.1073/pnas.0808587106 (2009).

19 Kenyon, C. J. The genetics of ageing. *Nature* **464**, 504-512 (2010).

20 Fontana, L., Partridge, L. & Longo, V. D. Extending healthy life span--from yeast to humans. *Science* **328**, 321-326, doi:10.1126/science.1172539 (2010).

21 Friedman, D. B. & Johnson, T. E. A mutation in the age-1 gene in Caenorhabditis elegans lengthens life and reduces hermaphrodite fertility. *Genetics* **118**, 75-86 (1988).

22 Laplante, M. & Sabatini, D. M. mTOR signaling in growth control and disease. *Cell* **149**, 274-293, doi:10.1016/j.cell.2012.03.017 (2012).

23 Johnson, S. C., Rabinovitch, P. S. & Kaeberlein, M. mTOR is a key modulator of ageing and age-related disease. *Nature* **493**, 338-345, doi:10.1038/nature11861 (2013).

24 Vellai, T. *et al.* Genetics: influence of TOR kinase on lifespan in C. elegans. *Nature* **426**, 620 (2003).

25 Hansen, M. *et al.* Lifespan extension by conditions that inhibit translation in Caenorhabditis elegans. *Aging Cell* **6**, 95-110 (2007).

26 Kaeberlein, M. *et al.* Regulation of yeast replicative life span by TOR and Sch9 in response to nutrients. *Science* **310**, 1193-1196 (2005).

27 Kapahi, P. *et al.* Regulation of lifespan in Drosophila by modulation of genes in the TOR signaling pathway. *Curr Biol* **14**, 885-890 (2004).

28 Bjedov, I. *et al.* Mechanisms of life span extension by rapamycin in the fruit fly Drosophila melanogaster. *Cell Metab* **11**, 35-46, doi:10.1016/j.cmet.2009.11.010 (2010).

29 Pan, K. Z. *et al.* Inhibition of mRNA translation extends lifespan in Caenorhabditis elegans. *Aging Cell* **6**, 111-119 (2007).

30 Lapierre, L. R. *et al.* The TFEB orthologue HLH-30 regulates autophagy and modulates longevity in Caenorhabditis elegans. *Nat Commun* **4**, 2267, doi:10.1038/ncomms3267 (2013).

31 Pyo, J. O. *et al.* Overexpression of Atg5 in mice activates autophagy and extends lifespan. *Nat Commun* **4**, 2300, doi:10.1038/ncomms3300 (2013).

32 Toth, M. L. *et al.* Longevity pathways converge on autophagy genes to regulate life span in Caenorhabditis elegans. *Autophagy* **4**, 330-338 (2008).

33 Hansen, M. *et al.* A role for autophagy in the extension of lifespan by dietary restriction in C. elegans. *PLoS Genet* **4**, e24, doi:10.1371/journal.pgen.0040024 (2008).

34 Melendez, A. *et al.* Autophagy genes are essential for dauer development and life-span extension in C. elegans. *Science* **301**, 1387-1391, doi:10.1126/science.1087782 (2003).

35 Chin, R. M. *et al.* The metabolite alpha-ketoglutarate extends lifespan by inhibiting ATP synthase and TOR. *Nature*, doi:10.1038/nature13264 (2014).

36 Schmeisser, S. *et al.* Neuronal ROS signaling rather than AMPK/sirtuin-mediated energy sensing links dietary restriction to lifespan extension. *Mol Metab* **2**, 92-102, doi:10.1016/j.molmet.2013.02.002 (2013).

37 Dillin, A. *et al.* Rates of behavior and aging specified by mitochondrial function during development. *Science* **298**, 2398-2401, doi:10.1126/science.1077780 (2002).

38 Curran, S. P. & Ruvkun, G. Lifespan regulation by evolutionarily conserved genes essential for viability. *PLoS Genet* **3**, e56 (2007).

39 Liu, X. *et al.* Evolutionary conservation of the clk-1-dependent mechanism of longevity: loss of mclk1 increases cellular fitness and lifespan in mice. *Genes Dev* **19**, 2424-2434, doi:10.1101/gad.1352905 (2005).

40 Copeland, J. M. *et al.* Extension of Drosophila life span by RNAi of the mitochondrial respiratory chain. *Curr Biol* **19**, 1591-1598, doi:10.1016/j.cub.2009.08.016 (2009).

41 Kirchman, P. A., Kim, S., Lai, C. Y. & Jazwinski, S. M. Interorganelle signaling is a determinant of longevity in Saccharomyces cerevisiae. *Genetics* **152**, 179-190 (1999).

42 Yang, W. & Hekimi, S. Two modes of mitochondrial dysfunction lead independently to lifespan extension in Caenorhabditis elegans. *Aging Cell* **9**, 433-447, doi:10.1111/j.1474-9726.2010.00571.x (2010).

43 Rea, S. L., Ventura, N. & Johnson, T. E. Relationship between mitochondrial electron transport chain dysfunction, development, and life extension in Caenorhabditis elegans. *PLoS Biol* **5**, e259, doi:10.1371/journal.pbio.0050259 (2007).

44 Schapira, A. H. Mitochondrial disease. *Lancet* **368**, 70-82, doi:10.1016/S0140-6736(06)68970-8 (2006).

45 Lin, M. T. & Beal, M. F. Mitochondrial dysfunction and oxidative stress in neurodegenerative diseases. *Nature* **443**, 787-795, doi:10.1038/nature05292 (2006).

46 Lakowski, B. & Hekimi, S. Determination of life-span in Caenorhabditis elegans by four clock genes. *Science* **272**, 1010-1013 (1996).

47 Durieux, J., Wolff, S. & Dillin, A. The cell-non-autonomous nature of electron transport chain-mediated longevity. *Cell* **144**, 79-91, doi:10.1016/j.cell.2010.12.016 (2011).

48 Houtkooper, R. H. *et al.* Mitonuclear protein imbalance as a conserved longevity mechanism. *Nature* **497**, 451-457, doi:10.1038/nature12188 (2013).

49 Bennett, C. F. *et al.* Activation of the mitochondrial unfolded protein response does not predict longevity in Caenorhabditis elegans. *Nat Commun* **5**, 3483, doi:10.1038/ncomms4483 (2014).

50 Yoneda, T. *et al.* Compartment-specific perturbation of protein handling activates genes encoding mitochondrial chaperones. *J Cell Sci* **117**, 4055-4066, doi:10.1242/jcs.01275 (2004).

51 Guarente, L. Mitochondria--a nexus for aging, calorie restriction, and sirtuins? *Cell* **132**, 171-176, doi:10.1016/j.cell.2008.01.007 (2008).

52 Civitarese, A. E. *et al.* Calorie restriction increases muscle mitochondrial biogenesis in healthy humans. *PLoS Med* **4**, e76, doi:10.1371/journal.pmed.0040076 (2007).

53 Rera, M. *et al.* Modulation of longevity and tissue homeostasis by the Drosophila PGC-1 homolog. *Cell Metab* **14**, 623-634, doi:10.1016/j.cmet.2011.09.013 (2011).

54 Bahadorani, S. *et al.* Neuronal expression of a single-subunit yeast NADH-ubiquinone oxidoreductase (Ndi1) extends Drosophila lifespan. *Aging Cell* **9**, 191-202, doi:10.1111/j.1474-9726.2010.00546.x (2010).

55 Hur, J. H. *et al.* Increased longevity mediated by yeast NDI1 expression in Drosophila intestinal stem and progenitor cells. *Aging (Albany NY)* **5**, 662-681 (2013).

56 Kenyon, C., Chang, J., Gensch, E., Rudner, A. & Tabtiang, R. A C. elegans mutant that lives twice as long as wild type. *Nature* **366**, 461-464 (1993).

57 Tatar, M. *et al.* A mutant Drosophila insulin receptor homolog that extends life-span and impairs neuroendocrine function. *Science* **292**, 107-110, doi:10.1126/science.1057987 (2001).

58 Holzenberger, M. *et al.* IGF-1 receptor regulates lifespan and resistance to oxidative stress in mice. *Nature* **421**, 182-187 (2003).

59 Tullet, J. M. *et al.* Direct inhibition of the longevity-promoting factor SKN-1 by insulin-like signaling in C. elegans. *Cell* **132**, 1025-1038, doi:10.1016/j.cell.2008.01.030 (2008).

60 Hsu, A. L., Murphy, C. T. & Kenyon, C. Regulation of aging and age-related disease by DAF-16 and heat-shock factor. *Science* **300**, 1142-1145 (2003).

61 Collins, J. J., Evason, K. & Kornfeld, K. Pharmacology of delayed aging and extended lifespan of Caenorhabditis elegans. *Exp Gerontol* **41**, 1032-1039, doi:10.1016/j.exger.2006.06.038 (2006).

62 Petrascheck, M., Ye, X. & Buck, L. B. An antidepressant that extends lifespan in adult Caenorhabditis elegans. *Nature* **450**, 553-556 (2007).

63 Harrison, D. E. *et al.* Rapamycin fed late in life extends lifespan in genetically heterogeneous mice. *Nature* **460**, 392-395 (2009).

64 Butler, J. A., Mishur, R. J., Bhaskaran, S. & Rea, S. L. A metabolic signature for long life in the Caenorhabditis elegans Mit mutants. *Aging Cell* **12**, 130-138, doi:10.1111/acel.12029 (2013).

65 Fuchs, S. *et al.* A metabolic signature of long life in Caenorhabditis elegans. *BMC Biol* **8**, 14, doi:10.1186/1741-7007-8-14 (2010).

66 Houtkooper, R. H. *et al.* The metabolic footprint of aging in mice. *Sci Rep* **1**, 134, doi:10.1038/srep00134 (2011).

67 Fok, W. C. *et al.* Combined treatment of rapamycin and dietary restriction has a larger effect on the transcriptome and metabolome of liver. *Aging Cell* **13**, 311-319, doi:10.1111/acel.12175 (2014).

68 Williams, D. S., Cash, A., Hamadani, L. & Diemer, T. Oxaloacetate supplementation increases lifespan in Caenorhabditis elegans through an AMPK/FOXO-dependent pathway. *Aging Cell* **8**, 765-768 (2009).

69 Mouchiroud, L. *et al.* Pyruvate imbalance mediates metabolic reprogramming and mimics lifespan extension by dietary restriction in Caenorhabditis elegans. *Aging Cell* **10**, 39-54 (2011).

70 Lucanic, M. *et al.* N-acylethanolamine signalling mediates the effect of diet on lifespan in Caenorhabditis elegans. *Nature* **473**, 226-229 (2011).

71 Lomenick, B. *et al.* Target identification using drug affinity responsive target stability (DARTS). *Proc Natl Acad Sci U S A* **106**, 21984-21989 (2009).

CHAPTER 2

The Metabolite Alpha-Ketoglutarate Extends Lifespan by Inhibiting ATP Synthase and TOR

(A reprint of “The metabolite α-ketoglutarate extends lifespan by inhibiting ATP synthase and TOR,” which was previously published in *Nature* (doi:10.1038/nature13264), is provided here as Chapter 2)

LETTER

doi:10.1038/nature13264

The metabolite α-ketoglutarate extends lifespan by inhibiting ATP synthase and TOR

Randall M. Chin[1], Xudong Fu[2], Melody Y. Pai[1]*, Laurent Vergnes[3]*, Heejun Hwang[2]*, Gang Deng[4], Simon Diep[2], Brett Lomenick[2], Vijaykumar S. Meli[5], Gabriela C. Monsalve[5], Eileen Hu[2], Stephen A. Whelan[6], Jennifer X. Wang[7], Gwanghyun Jung[2], Gregory M. Solis[8], Farbod Fazlollahi[9], Chitrada Kaweeteerawat[10], Austin Quach[2], Mahta Nili[11], Abby S. Krall[2], Hilary A. Godwin[10], Helena R. Chang[6], Kym F. Faull[9], Feng Guo[5], Meisheng Jiang[2], Sunia A. Trauger[7], Alan Saghatelian[12], Daniel Braas[2,13], Heather R. Christofk[2,13], Catherine F. Clarke[1,4], Michael A. Teitell[1,11], Michael Petrascheck[8], Karen Reue[1,3], Michael E. Jung[1,4], Alison R. Frand[5] & Jing Huang[1,2]

Metabolism and ageing are intimately linked. Compared with *ad libitum* feeding, dietary restriction consistently extends lifespan and delays age-related diseases in evolutionarily diverse organisms[1,2]. Similar conditions of nutrient limitation and genetic or pharmacological perturbations of nutrient or energy metabolism also have longevity benefits[3,4]. Recently, several metabolites have been identified that modulate ageing[5,6]; however, the molecular mechanisms underlying this are largely undefined. Here we show that α-ketoglutarate (α-KG), a tricarboxylic acid cycle intermediate, extends the lifespan of adult *Caenorhabditis elegans*. ATP synthase subunit β is identified as a novel binding protein of α-KG using a small-molecule target identification strategy termed drug affinity responsive target stability (DARTS)[7]. The ATP synthase, also known as complex V of the mitochondrial electron transport chain, is the main cellular energy-generating machinery and is highly conserved throughout evolution[8,9]. Although complete loss of mitochondrial function is detrimental, partial suppression of the electron transport chain has been shown to extend *C. elegans* lifespan[10–13]. We show that α-KG inhibits ATP synthase and, similar to ATP synthase knockdown, inhibition by α-KG leads to reduced ATP content, decreased oxygen consumption, and increased autophagy in both *C. elegans* and mammalian cells. We provide evidence that the lifespan increase by α-KG requires ATP synthase subunit β and is dependent on target of rapamycin (TOR) downstream. Endogenous α-KG levels are increased on starvation and α-KG does not extend the lifespan of dietary-restricted animals, indicating that α-KG is a key metabolite that mediates longevity by dietary restriction. Our analyses uncover new molecular links between a common metabolite, a universal cellular energy generator and dietary restriction in the regulation of organismal lifespan, thus suggesting new strategies for the prevention and treatment of ageing and age-related diseases.

To gain insight into the regulation of ageing by endogenous small molecules, we screened normal metabolites and aberrant disease-associated metabolites for their effects on adult lifespan using the *C. elegans* model. We discovered that the tricarboxylic acid (TCA) cycle intermediate α-KG (but not isocitrate or citrate) delays ageing and extends the lifespan of *C. elegans* by ~50% (Fig. 1a and Extended Data Fig. 1a). In the cell, α-KG (or 2-oxoglutarate; Fig. 1b) is produced from isocitrate by oxidative decarboxylation catalysed by isocitrate dehydrogenase (IDH). α-KG can also be produced anaplerotically from glutamate by oxidative deamination using glutamate dehydrogenase, and as a product of pyridoxal phosphate-dependent transamination reactions in which glutamate is a common amino donor. α-KG extended the lifespan of wild-type N2 worms in a concentration-dependent manner, with 8 mM α-KG producing the maximal lifespan extension (Fig. 1c); 8 mM was the concentration used in all subsequent *C. elegans* experiments. There is a ~50% increase in α-KG concentration in worms on 8 mM α-KG plates compared with those on vehicle plates (Extended Data Fig. 1b), or ~160 μM versus ~110 μM assuming homogenous distribution (Methods). α-KG not only extends lifespan, but also delays age-related phenotypes, such as the decline in rapid, coordinated body movement (Supplementary Videos 1 and 2). α-KG supplementation in the adult stage is sufficient for longevity (Extended Data Fig. 1c).

The dilution or killing of the *C. elegans* bacterial food source has been shown to extend worm lifespan[14], but the lifespan increase by α-KG is not due to altered bacterial proliferation or metabolism (Fig. 1d, e and Extended Data Fig. 1d). Animals also did not view α-KG-treated food as less favourable (Extended Data Fig. 1e, f), and there was no significant change in food intake, pharyngeal pumping, foraging behaviour, body size or brood size in the presence of α-KG (Extended Data Fig. 1e–h; data not shown).

In the cell, α-KG is decarboxylated to succinyl-CoA and CO_2 by α-KG dehydrogenase (encoded by *ogdh-1*), a key control point in the TCA cycle. Increasing α-KG levels by *ogdh-1* RNA interference (RNAi) (Extended Data Fig. 1b) also extends worm lifespan (Fig. 1f and Supplementary Notes), consistent with a direct effect of α-KG on longevity independent of bacterial food.

To investigate the molecular mechanism(s) of longevity by α-KG, we took advantage of an unbiased biochemical approach, DARTS[7]. As we proposed that key target(s) of α-KG are likely to be conserved and ubiquitously expressed, we used a human cell line (Jurkat) that is easy to culture as the protein source for DARTS (Fig. 2a). Mass spectrometry identified ATP5B, the β subunit of the catalytic core of the ATP synthase, among the most abundant and enriched proteins present in the α-KG-treated sample (Extended Data Table 1); the homologous α subunit ATP5A was also enriched but to a lesser extent. The interaction between α-KG and ATP5B was verified using additional cell lines (Fig. 2b; data not shown), and corroborated for the *C. elegans* orthologue ATP-2 (Extended Data Fig. 2a).

α-KG inhibits the activity of complex V, but not complex IV, from bovine heart mitochondria (Fig. 2c and Extended Data Fig. 2b; data not

[1]Molecular Biology Institute, University of California Los Angeles, Los Angeles, California 90095, USA. [2]Department of Molecular and Medical Pharmacology, University of California Los Angeles, Los Angeles, California 90095, USA. [3]Department of Human Genetics, University of California Los Angeles, Los Angeles, California 90095, USA. [4]Department of Chemistry and Biochemistry, University of California Los Angeles, Los Angeles, California 90095, USA. [5]Department of Biological Chemistry, University of California Los Angeles, Los Angeles, California 90095, USA. [6]Department of Surgery, University of California Los Angeles, Los Angeles, California 90095, USA. [7]Small Molecule Mass Spectrometry Facility, FAS Division of Science, Harvard University, Cambridge, Massachusetts 02138, USA. [8]Department of Chemical Physiology, The Scripps Research Institute, La Jolla, California 92037, USA. [9]Pasarow Mass Spectrometry Laboratory, Department of Psychiatry and Biobehavioral Sciences and Semel Institute for Neuroscience and Human Behavior, University of California Los Angeles, Los Angeles, California 90095, USA. [10]Department of Environmental Health Sciences, University of California Los Angeles, Los Angeles, California 90095, USA. [11]Department of Pathology and Laboratory Medicine, University of California Los Angeles, Los Angeles, California 90095, USA. [12]Department of Chemistry and Chemical Biology, Harvard University, Cambridge, Massachusetts 02138, USA. [13]UCLA Metabolomics Center, University of California Los Angeles, Los Angeles, California 90095, USA.
*These authors contributed equally to this work.

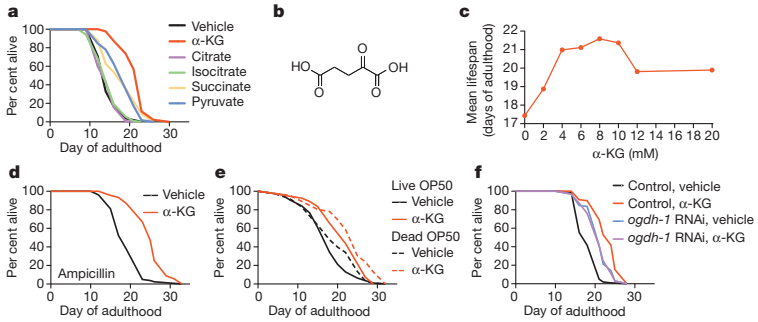

Figure 1 | α-KG extends the adult lifespan of *C. elegans*. **a**, α-KG extends the lifespan of adult worms in the metabolite longevity screen. All metabolites were given at a concentration of 8 mM. **b**, Structure of α-KG. **c**, Dose–response curve of the α-KG effect on longevity. **d**, **e**, α-KG extends the lifespan of worms fed bacteria that have been ampicillin arrested, mean lifespan (days of adulthood) with vehicle treatment (m_{veh}) = 19.4 (n = 80 animals tested), $m_{\alpha\text{-KG}}$ = 25.1 (n = 91), $P < 0.0001$ (log-rank test) (**d**); or γ-irradiation-killed, m_{veh} = 19.0 (n = 88), $m_{\alpha\text{-KG}}$ = 23.0 (n = 46), $P < 0.0001$ (log-rank test) (**e**). OP50, *E. coli* OP50 strain. **f**, α-KG does not further extend the lifespan of *ogdh-1* RNAi worms, m_{veh} = 21.2 (n = 98), $m_{\alpha\text{-KG}}$ = 21.1 (n = 100), P = 0.65 (log-rank test).

shown). This inhibition is also readily detected in live mammalian cells (Fig. 2d; data not shown) and in live nematodes (Fig. 2e), as evidenced by reduced ATP levels. Concomitantly, oxygen consumption rates are lowered (Fig. 2f, g), similar to with *atp-2* knockdown (Extended Data Fig. 2c). Specific inhibition of complex V—but not the other electron transport chain (ETC) complexes—by α-KG is further confirmed by respiratory control analysis[15] (Fig. 2h and Extended Data Fig. 2d–h). To understand the mechanism of inhibition by α-KG, we studied the enzyme inhibition kinetics of ATP synthase. α-KG (released from octyl α-KG) decreases both the effective velocity of the enzyme-catalysed reaction at an infinite concentration of the substrate (V_{max}) and the Michaelis constant (K_m) of ATP synthase, indicative of uncompetitive inhibition (Fig. 2i and Supplementary Notes).

To determine the significance of ATP-2 to the longevity by α-KG, we measured the lifespan of *atp-2* RNAi adults given α-KG. As reported previously[13], *atp-2* RNAi animals live longer than control RNAi animals (Fig. 3a). However, their lifespan is not further extended by α-KG (Fig. 3a), indicating that ATP-2 is required for the longevity benefit of

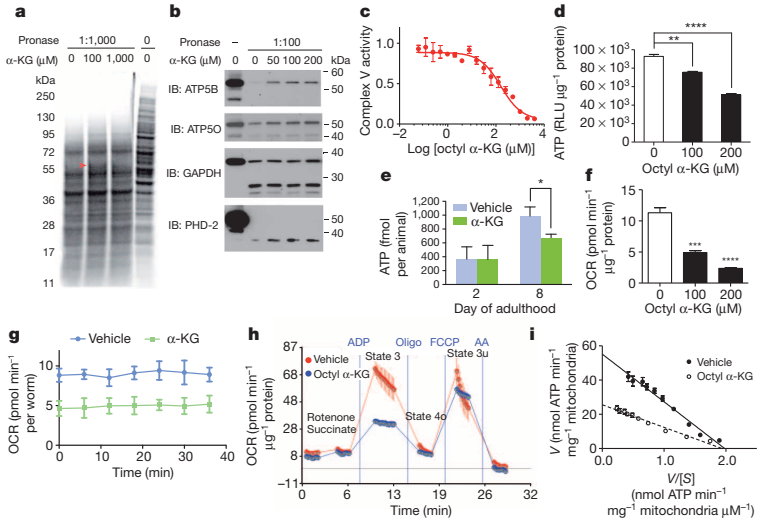

Figure 2 | α-KG binds and inhibits ATP synthase. **a**, DARTS identifies ATP5B as an α-KG-binding protein. Red arrowhead, protected band. **b**, DARTS confirms α-KG binding specifically to ATP5B. IB, immunoblot. **c**, Inhibition of ATP synthase by α-KG (released from octyl α-KG; Supplementary Notes). This inhibition was reversible (data not shown). **d**, **e**, Reduced ATP levels in octyl α-KG-treated normal human fibroblasts (**P = 0.0016, ****$P < 0.0001$; by t-test, two-tailed, two-sample unequal variance) (**d**) and α-KG-treated worms (day 2, P = 0.969; day 8, *P = 0.012; by t-test, two-tailed, two-sample unequal variance) (**e**). RLU, relative luminescence units. **f**, **g**, Decreased oxygen consumption rate (OCR) in octyl α-KG-treated cells (***P = 0.0004, ****$P < 0.0001$; by t-test, two-tailed, two-sample unequal variance) (**f**) and α-KG-treated worms ($P < 0.0001$; by t-test, two-tailed, two-sample unequal variance) (**g**). **h**, α-KG, released from octyl α-KG (800 μM), decreases state 3, but not state 4o or 3u (P = 0.997), respiration in mitochondria isolated from mouse liver. The respiratory control ratio is decreased in the octyl α-KG- (3.1 ± 0.6) versus vehicle-treated mitochondria (5.2 ± 1.0) (*P = 0.015; by t-test, two-tailed, two-sample unequal variance). Oligo, oligomycin; FCCP, carbonyl cyanide-4-(trifluoromethoxy)phenylhydrazone; AA, antimycin A. **i**, Eadie–Hofstee plot of steady-state inhibition kinetics of ATP synthase by α-KG (produced by *in situ* hydrolysis of octyl α-KG). [S] is the substrate (ADP) concentration, and V is the initial velocity of ATP synthesis in the presence of 200 μM octanol (vehicle control) or octyl α-KG. α-KG (produced from octyl α-KG) decreases the apparent V_{max} (53.9 to 26.7) and K_m (25.9 to 15.4), by nonlinear regression least-squares fit. **c**–**i**, Results were replicated in two independent experiments. Mean ± standard deviation (s.d.) is plotted in all cases.

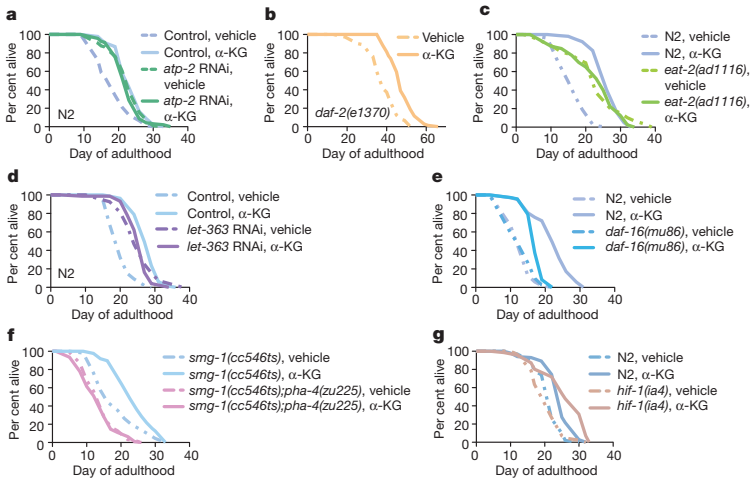

Figure 3 | α-KG longevity is mediated through ATP synthase and the dietary restriction/TOR axis. **a**–**g**, Effect of α-KG on the lifespan of mutant or RNAi worms. **a**, *atp-2* RNAi, $m_{veh} = 22.8$ ($n = 97$), $m_{\alpha\text{-KG}} = 22.5$ ($n = 94$), $P = 0.35$; or RNAi control, $m_{veh} = 18.6$ ($n = 94$), $m_{\alpha\text{-KG}} = 23.4$ ($n = 91$), $P < 0.0001$. **b**, *daf-2(e1370)*, $m_{veh} = 38.0$ ($n = 72$), $m_{\alpha\text{-KG}} = 47.6$ ($n = 69$), $P < 0.0001$. **c**, *eat-2(ad1116)*, $m_{veh} = 22.8$ ($n = 59$), $m_{\alpha\text{-KG}} = 22.9$ ($n = 40$), $P = 0.79$. **d**, *let-363* RNAi, $m_{veh} = 25.1$ ($n = 96$), $m_{\alpha\text{-KG}} = 25.7$ ($n = 74$), $P = 0.95$; or *gfp* RNAi control, $m_{veh} = 20.2$ ($n = 99$), $m_{\alpha\text{-KG}} = 27.7$ ($n = 81$), $P < 0.0001$. **e**, *daf-16(mu86)*, $m_{veh} = 13.4$ ($n = 71$), $m_{\alpha\text{-KG}} = 17.4$ ($n = 72$), $P < 0.0001$; or N2, $m_{veh} = 13.2$ ($n = 100$), $m_{\alpha\text{-KG}} = 22.3$ ($n = 104$), $P < 0.0001$. **f**, *pha-4(zu225)*, $m_{veh} = 14.2$ ($n = 94$), $m_{\alpha\text{-KG}} = 13.5$ ($n = 109$), $P = 0.55$. **g**, *hif-1(ia4)*, $m_{veh} = 20.5$ ($n = 85$), $m_{\alpha\text{-KG}} = 26.0$ ($n = 71$), $P < 0.0001$; or N2, $m_{veh} = 21.5$ ($n = 101$), $m_{\alpha\text{-KG}} = 24.6$ ($n = 102$), $P < 0.0001$. *P* values were determined by the log-rank test. Number of independent experiments: RNAi control (6), *atp-2* (2), *let-363* (3), *N2* (5), *daf-2* (2), *eat-2* (2), *pha-4* (2), *daf-16* (2), *hif-1* (5).

α-KG. This requirement is specific because, in contrast, the lifespan of the even longer-lived insulin/IGF-1 receptor *daf-2(e1370)* mutant worms[3] is further increased by α-KG (Fig. 3b). Remarkably, oligomycin, an inhibitor of ATP synthase, also extends the lifespan of adult worms (Extended Data Fig. 3a). Together, the direct binding of ATP-2 by α-KG, the related enzymatic inhibition, reduction in ATP levels and oxygen consumption, lifespan analysis, and other similarities (see also Supplementary Notes, Extended Data Fig. 4) to *atp-2* knockdown or oligomycin treatment demonstrate that α-KG probably extends lifespan primarily by targeting ATP-2.

The lower ATP content in α-KG-treated animals suggests that increased longevity by α-KG may involve a state similar to that induced by dietary restriction. Consistent with this idea, we found that α-KG does not extend the lifespan of *eat-2(ad1116)* animals (Fig. 3c), which is a model of dietary restriction with impaired pharyngeal pumping and therefore reduced food intake[16]. The longevity of *eat-2* mutants requires TOR (encoded by the *C. elegans* orthologue *let-363*)[17], an important mediator of the effects of dietary restriction on longevity[18]. Likewise, α-KG fails to increase the lifespan of *let-363* RNAi animals (Fig. 3d). The AMP-activated protein kinase (AMPK) is another conserved major sensor of cellular energy status[19]. Both AMPK (*C. elegans* orthologue *aak-2*) and the FoxO transcription factor DAF-16 mediate dietary-restriction-induced longevity in *C. elegans* fed diluted bacteria[20], but neither is required for lifespan extension in the *eat-2* model[16,20]. We found that in *aak-2* (Extended Data Fig. 5a) and *daf-16* (Fig. 3e) mutants the longevity effect of α-KG is smaller than in N2 animals ($P < 0.0001$), suggesting that α-KG longevity partially depends on AMPK and FoxO; nonetheless, lifespan is significantly increased by α-KG in *aak-2* (24.3%, $P < 0.0001$) and *daf-16* (29.5%, $P < 0.0001$) mutant or RNAi animals (Fig. 3e and Extended Data Fig. 5a, b; data not shown), indicating an AMPK- and FoxO-independent effect of α-KG in increasing longevity.

The inability of α-KG to extend further the lifespan of *let-363* RNAi animals suggests that α-KG treatment and TOR inactivation extend lifespan either through the same pathway (with α-KG acting on or upstream of TOR), or through independent mechanisms or parallel pathways that converge on a downstream effector. The first model predicts that the TOR pathway will be less active upon α-KG treatment, whereas if the latter model were true then TOR would be unaffected by α-KG treatment. In support of the first model, we found that TOR pathway activity is decreased in human cells treated with octyl α-KG (Fig. 4a and Extended Data Fig. 6a, b). However, α-KG does not interact with TOR directly (Extended Data Fig. 6d, e). Consistent with the involvement of TOR in α-KG longevity, the FoxA transcription factor PHA-4, which is required to extend adult lifespan in response to reduced TOR signalling[21] and for dietary-restriction-induced longevity in *C. elegans*[22], is likewise required for α-KG-induced longevity (Fig. 3f). Moreover, autophagy, which is activated both by TOR inhibition[18,23] and by dietary restriction[24], is markedly increased in worms treated with α-KG (or *ogdh-1* RNAi) and in *atp-2* RNAi animals (Fig. 4b, c, Extended Data Figs 6c, 7 and Supplementary Notes), as indicated by the prevalence of green fluorescent protein GFP::LGG-1 puncta (Methods). Autophagy was also induced in mammalian cells treated with octyl α-KG (Extended Data Fig. 6f). Furthermore, α-KG does not result in significantly more autophagy in either *atp-2* RNAi or *let-363* RNAi worms (Fig. 4b, c). The data provide further evidence that α-KG decreases TOR pathway activity through the inhibition of ATP synthase. Similarly, autophagy is induced by oligomycin, and oligomycin does not augment autophagy in *let-363* RNAi worms (Extended Data Fig. 3b, c).

α-KG is not only a metabolite, but also a co-substrate for a large family of dioxygenases[25]. The hypoxia inducible factor (HIF-1) is modified by one of these enzymes, the prolyl 4-hydroxylase (PHD) EGL-9, and thereafter degraded by the von Hippel–Lindau (VHL) protein[26,27]. α-KG extends the lifespan of animals with loss-of-function mutations in *hif-1*, *egl-9* and *vhl-1* (Fig. 3g and Extended Data Fig. 5c), suggesting that this pathway does not play a major part in lifespan extension by α-KG. However, it is prudent to acknowledge that the formal possibility of other α-KG-binding targets having an additional role in the extension of lifespan by α-KG cannot be eliminated at this time.

We show that ageing in *C. elegans* is delayed by α-KG supplementation in adult animals. This longevity effect is probably mediated by ATP synthase, which we identified as a direct target of α-KG, and TOR, a major effector of dietary restriction. Identification of new protein targets

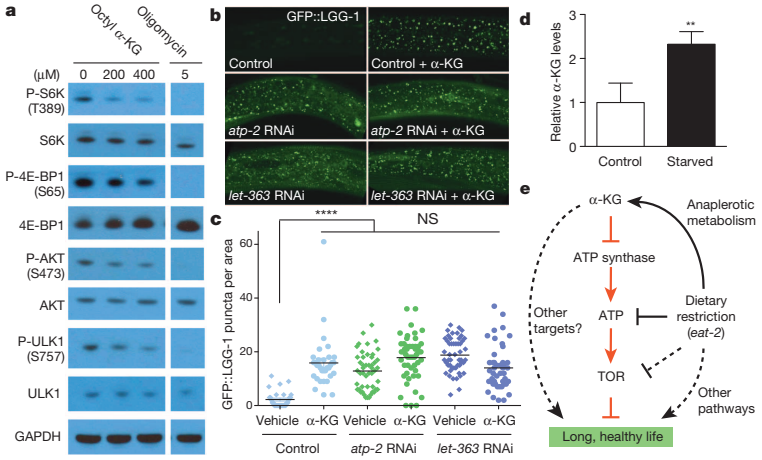

Figure 4 | Inhibition of ATP synthase by α-KG causes a conserved decrease in TOR pathway activity. **a**, Decreased phosphorylation of mammalian TOR substrates in U87 cells treated with octyl α-KG or oligomycin. Similar results were obtained in HEK-293 cells, normal human fibroblasts and mouse embryonic fibroblasts (data not shown). P, phospho. **b**, Increased autophagy in animals treated with α-KG or RNAi for *atp-2* or *let-363*. Photographs were taken at ×100 magnification. **c**, GFP::LGG-1 puncta quantified using ImageJ (Methods). Data show results of 2–3 independent experiments. Bars indicate the mean. ****$P < 0.0001$; NS, not significant (*t*-test, two-tailed, two-sample unequal variance). **d**, α-KG levels are increased in starved worms. **$P < 0.01$ (*t*-test, two-tailed, two-sample unequal variance). Mean ± s.d. is plotted. **e**, Model of α-KG-mediated longevity.

of α-KG illustrates that regulatory networks acted upon by metabolites are probably more complex than appreciated at present, and that DARTS is a useful method for discovering new protein targets and regulatory functions of metabolites. Our findings demonstrate a novel mechanism for extending lifespan that is mediated by the regulation of cellular energy metabolism by a key metabolite. Such moderation of ATP synthesis by metabolite(s) has probably evolved to ensure energy efficiency by the organism in response to nutrient availability. We suggest that this system may be exploited to confer a dietary-restriction-like state that favours maintenance over growth, and thereby delays ageing and prevents age-related diseases. In fact, the TOR pathway is often hyperactivated in human cancer; inhibition of TOR function by α-KG in normal human cells suggests an exciting role for α-KG as an endogenous tumour suppressor metabolite. Interestingly, physiological increases in α-KG levels have been reported in starved yeast and bacteria[28], in the liver of starved pigeons[29], and in humans after physical exercise[30]. The biochemical basis for this increase of α-KG is explained by starvation-based anaplerotic gluconeogenesis, which activates glutamate-linked transaminases in the liver to provide carbon derived from amino acid catabolism. Consistent with this idea, α-KG levels are elevated in starved *C. elegans* (Fig. 4d). These findings suggest a model in which α-KG is a key metabolite mediating lifespan extension by starvation/dietary restriction (Fig. 4e).

Longevity molecules that delay ageing and extend lifespan have long been a dream of humanity. Endogenous metabolites such as α-KG that can alter *C. elegans* lifespan suggest that an internal mechanism may exist that is accessible to intervention; whether this can translate into manipulating the ageing process in humans remains to be seen.

METHODS SUMMARY

Lifespan analysis. All lifespan assays were conducted at 20 °C on solid nematode growth media (NGM) and were replicated in at least two independent experiments. *P* values were determined by the log-rank (Mantel–Cox) test; survival curves were generated using GraphPad Prism. All lifespan data are available in Extended Data Table 2.

DARTS. Human Jurkat cell lysates were incubated with α-KG and digested using Pronase. Proteins protected from proteolysis by α-KG binding were analysed by liquid chromatography-tandem mass spectrometry (LC-MS/MS) as described previously[7], and identified by searching against the human Swissprot database (release 57.15) using Mascot with all peptides meeting a significance threshold of $P < 0.05$.

Online Content Any additional Methods, Extended Data display items and Source Data are available in the online version of the paper; references unique to these sections appear only in the online paper.

Received 3 October 2012; accepted 17 March 2014.
Published online 14 May 2014.

1. Colman, R. J. *et al.* Caloric restriction delays disease onset and mortality in rhesus monkeys. *Science* **325,** 201–204 (2009).
2. Mattison, J. A. *et al.* Impact of caloric restriction on health and survival in rhesus monkeys from the NIA study. *Nature* **489,** 318–321 (2012).
3. Kenyon, C. J. The genetics of ageing. *Nature* **464,** 504–512 (2010).
4. Harrison, D. E. *et al.* Rapamycin fed late in life extends lifespan in genetically heterogeneous mice. *Nature* **460,** 392–395 (2009).
5. Williams, D. S., Cash, A., Hamadani, L. & Diemer, T. Oxaloacetate supplementation increases lifespan in *Caenorhabditis elegans* through an AMPK/FOXO-dependent pathway. *Aging Cell* **8,** 765–768 (2009).
6. Lucanic, M. *et al.* N-acylethanolamine signalling mediates the effect of diet on lifespan in *Caenorhabditis elegans*. *Nature* **473,** 226–229 (2011).
7. Lomenick, B. *et al.* Target identification using drug affinity responsive target stability (DARTS). *Proc. Natl Acad. Sci. USA* **106,** 21984–21989 (2009).
8. Abrahams, J. P., Leslie, A. G., Lutter, R. & Walker, J. E. Structure at 2.8 Å resolution of F1-ATPase from bovine heart mitochondria. *Nature* **370,** 621–628 (1994).
9. Boyer, P. D. The ATP synthase—a splendid molecular machine. *Annu. Rev. Biochem.* **66,** 717–749 (1997).
10. Tsang, W. Y., Sayles, L. C., Grad, L. I., Pilgrim, D. B. & Lemire, B. D. Mitochondrial respiratory chain deficiency in *Caenorhabditis elegans* results in developmental arrest and increased life span. *J. Biol. Chem.* **276,** 32240–32246 (2001).
11. Dillin, A. *et al.* Rates of behavior and aging specified by mitochondrial function during development. *Science* **298,** 2398–2401 (2002).
12. Lee, S. S. *et al.* A systematic RNAi screen identifies a critical role for mitochondria in *C. elegans* longevity. *Nature Genet.* **33,** 40–48 (2002).
13. Curran, S. P. & Ruvkun, G. Lifespan regulation by evolutionarily conserved genes essential for viability. *PLoS Genet.* **3,** e56 (2007).
14. Gems, D. & Riddle, D. L. Genetic, behavioral and environmental determinants of male longevity in *Caenorhabditis elegans*. *Genetics* **154,** 1597–1610 (2000).
15. Brand, M. D. & Nicholls, D. G. Assessing mitochondrial dysfunction in cells. *Biochem. J.* **435,** 297–312 (2011).
16. Lakowski, B. & Hekimi, S. The genetics of caloric restriction in *Caenorhabditis elegans*. *Proc. Natl Acad. Sci. USA* **95,** 13091–13096 (1998).
17. Hansen, M. *et al.* Lifespan extension by conditions that inhibit translation in *Caenorhabditis elegans*. *Aging Cell* **6,** 95–110 (2007).
18. Stanfel, M. N., Shamieh, L. S., Kaeberlein, M. & Kennedy, B. K. The TOR pathway comes of age. *Biochim. Biophys. Acta* **1790,** 1067–1074 (2009).
19. Hardie, D. G., Scott, J. W., Pan, D. A. & Hudson, E. R. Management of cellular energy by the AMP-activated protein kinase system. *FEBS Lett.* **546,** 113–120 (2003).

20. Greer, E. L. & Brunet, A. Different dietary restriction regimens extend lifespan by both independent and overlapping genetic pathways in *C. elegans*. *Aging Cell* **8,** 113–127 (2009).
21. Sheaffer, K. L., Updike, D. L. & Mango, S. E. The target of rapamycin pathway antagonizes *pha-4/FoxA* to control development and aging. *Curr. Biol.* **18,** 1355–1364 (2008).
22. Panowski, S. H., Wolff, S., Aguilaniu, H., Durieux, J. & Dillin, A. PHA-4/Foxa mediates diet-restriction-induced longevity of *C. elegans*. *Nature* **447,** 550–555 (2007).
23. Wullschleger, S., Loewith, R. & Hall, M. N. TOR signaling in growth and metabolism. *Cell* **124,** 471–484 (2006).
24. Meléndez, A. *et al.* Autophagy genes are essential for dauer development and life-span extension in *C. elegans*. *Science* **301,** 1387–1391 (2003).
25. Loenarz, C. & Schofield, C. J. Expanding chemical biology of 2-oxoglutarate oxygenases. *Nature Chem. Biol.* **4,** 152–156 (2008).
26. Epstein, A. C. *et al. C. elegans* EGL-9 and mammalian homologs define a family of dioxygenases that regulate HIF by prolyl hydroxylation. *Cell* **107,** 43–54 (2001).
27. Zhang, Y., Shao, Z., Zhai, Z., Shen, C. & Powell-Coffman, J. A. The HIF-1 hypoxia-inducible factor modulates lifespan in *C. elegans*. *PLoS ONE* **4,** e6348 (2009).
28. Brauer, M. J. *et al.* Conservation of the metabolomic response to starvation across two divergent microbes. *Proc. Natl Acad. Sci. USA* **103,** 19302–19307 (2006).
29. Kaminsky, Y. G., Kosenko, E. A. & Kondrashova, M. N. Metabolites of citric acid cycle, carbohydrate and phosphorus metabolism, and related reactions, redox and phosphorylating states of hepatic tissue, liver mitochondria and cytosol of the pigeon, under normal feeding and natural nocturnal fasting conditions. *Comp. Biochem. Physiol. B* **73,** 957–963 (1982).
30. Brugnara, L. *et al.* Metabolomics approach for analyzing the effects of exercise in subjects with type 1 diabetes mellitus. *PLoS ONE* **7,** e40600 (2012).

Supplementary Information is available in the online version of the paper.

Acknowledgements We thank S. Lee, M. Hansen, B. Lemire, A. van der Bliek, S. Clarke, T. K. Blackwell, R. Johnson, J. E. Walker, A. G. W. Leslie, K. N. Houk, B. Martin, J. Lusis, J. Gober, Y. Wang and H. Sun for advice and discussions. J. Avruch for the *let-363* RNAi vector; J. Powell-Coffman for strains and advice; and K. Yan for technical assistance. Worm strains were provided by the *Caenorhabditis* Genetics Center, which is funded by the National Institutes of Health (NIH) Office of Research Infrastructure Programs (P40 OD010440). We thank the NIH for traineeship support of R.M.C. (T32 GM007104), M.Y.P. (T32 GM007185), B.L. (T32 GM008496) and M.N. (T32 CA009120). X.F. is a recipient of the China Scholarship Council Scholarship. G.C.M. was supported by Ford Foundation and National Science Foundation Graduate Research Fellowships.

Author Contributions Lifespan assays were performed by R.M.C., M.P. and E.H.; DARTS-mass spectrometry by S.D. and B.L.; DARTS-western blots by M.Y.P., H.H. and R.M.C.; mammalian cell experiments by X.F. and H.H.; mitochondrial respiration study design and analyses by L.V. and K.R.; enzyme kinetics and analyses by R.M.C. and J.H.; confocal microscopy by V.S.M., G.C.M. and A.R.F.; ultra-high-performance liquid chromatography-electrospray ionization-tandem mass spectrometry (UHPLC-ESI/MS/MS) by J.X.W. and S.A.T.; compound syntheses by G.D. and M.E.J.; other analyses by H.H., X.F., M.Y.P., D.B., R.M.C., E.H., G.J., G.M.S., C.K. and A.Q. S.A.W., F.F., M.N., A.S.K., H.A.G., H.R. Chang, K.F.F., F.G., M.J., S.A.T., A.S., D.B., H.R. Christofk, C.F.C., M.A.T., M.E.J., L.V., K.R., A.R.F. and M.P. provided guidance, specialized reagents and expertise. J.H. conceived the study. R.M.C. and J.H. wrote the paper. R.M.C., X.F. and J.H. analysed data. All authors discussed the results, commented on the studies and contributed to aspects of preparing the manuscript.

Author Information Reprints and permissions information is available at www.nature.com/reprints. The authors declare no competing financial interests. Readers are welcome to comment on the online version of the paper. Correspondence and requests for materials should be addressed to J.H. (jinghuang@mednet.ucla.edu).

METHODS

Nematode strains and maintenance. *C. elegans* strains were maintained using standard methods[31]. The following strains were used (strain, genotype): Bristol N2, wild type; DA1116, *eat-2(ad1116)*II; CB1370, *daf-2(e1370)*III; CF1038, *daf-16(mu86)*I; PD8120, *smg-1(cc546ts)*I; SM190, *smg-1(cc546ts)*I;*pha-4(zu225)*V; RB754, *aak-2(ok524)*X; ZG31, *hif-1(ia4)*V; ZG596, *hif-1(ia7)*V; JT307, *egl-9(sa307)*V; CB5602, *vhl-1(ok161)*X; DA2123, *adIs2122[lgg-1::GFP + rol-6(su1006)]*. They were all obtained from the *Caenorhabditis* Genetics Center (CGC).

RNAi in *C. elegans*. RNAi in *C. elegans* was accomplished by feeding worms HT115 (DE3) bacteria expressing target-gene double-stranded RNA (dsRNA) from the pL4440 vector[32]. dsRNA production was induced overnight on plates containing 1 mM isopropyl-β-D-thiogalactoside (IPTG). All RNAi feeding clones were obtained from the *C. elegans* ORF-RNAi Library (Thermo Scientific/Open Biosystems) unless otherwise stated. The *C. elegans* TOR (*let-363*) RNAi clone[33] was obtained from Joseph Avruch (MGH/Harvard). Efficient knockdown was confirmed by western blotting of the corresponding protein or by qRT–PCR of the mRNA. The primer sequences used for qRT–PCR are as follows. *atp-2* forward: TGACAACATTTTC CGTTTCACC; *atp-2* reverse: AAATAGCCTGGACGGATGTGAT; *let-363* forward: GATCCGAGACAAGATGAACGTG; *let-363* reverse: ACAATTTGGAAC CCAACCAATC; *ogdh-1* forward: TGATTTGGACCGAGAATTCCTT; *ogdh-1* reverse: GGATCAGACGTTTGAACAGCAC.

We validated the RNAi knockdown of both *ogdh-1* and *atp-2* by quantitative RT–PCR and also of *atp-2* by western blotting. Transcripts of *ogdh-1* were reduced by 85%, and transcripts and protein levels of *atp-2* were reduced by 52% and 83%, respectively, in larvae that were cultivated on bacteria that expressed the corresponding dsRNAs. In addition, RNAi of *atp-2* in this study was associated with delayed post-embryonic development and larval arrest, consistent with the phenotypes of *atp-2(ua2)* animals. Analysis by qRT–PCR indicated a modest but significant decrease by 26% in transcripts of *let-363* in larvae undergoing RNAi; moreover, molecular markers for autophagy were induced in these animals, and the lifespan of adults was extended, consistent with partial inactivation of the kinase.

In lifespan experiments, we used RNAi to inactivate *atp-2*, *ogdh-1* and *let-363* in mature animals in the presence or absence of exogenous α-KG. The concentration of α-KG used in these experiments (8 mM) was empirically determined to be most beneficial for wild-type animals (Fig. 1c). This approach enabled us to evaluate the contribution of essential proteins and pathways to the longevity conferred by supplementary α-KG. Specifically, we were able to substantially but not fully inactivate *atp-2* in adult animals that had completed embryonic and larval development. As described earlier, supplementation with 8 mM α-KG did not further extend (and in fact, on one occasion, even decreased) the lifespan of *atp-2* RNAi animals (Extended Data Table 2), indicating that *atp-2* is required for α-KG to promote longevity. On the other hand, a complete inactivation of *atp-2* would be lethal, and thereby mask the benefit of ATP synthase inhibition by α-KG.

Lifespan analysis. Lifespan assays were conducted at 20 °C on solid nematode growth media (NGM) using standard protocols and were replicated in at least two independent experiments. *C. elegans* were synchronized by performing either a timed egg lay[34] or an egg preparation (lysing ~100 gravid worms in 70 μl M9 buffer[31], 25 μl bleach (10% sodium hypochlorite solution) and 5 μl 10 N NaOH). Young adult animals were picked onto NGM assay plates containing 1.5% dimethyl sulfoxide (DMSO; Sigma, D8418), 49.5 μM 5-fluoro-2′-deoxyuridine[34] (FUDR; Sigma, F0503), and α-KG (Sigma, K1128) or vehicle control (H_2O). FUDR was included to prevent progeny production. Media containing α-KG were adjusted to pH 6.0 (that is, the same pH as the control plates) by the addition of NaOH. All compounds were mixed into the NGM media after autoclaving and before solidification of the media. Assay plates were seeded with OP50 (or a designated RNAi feeding clone, see later). Worms were moved to new assay plates every 4 days (to ensure sufficient food was present at all times and to reduce the risk of mould contamination). To assess the survival of the worms, the animals were prodded with a platinum wire every 2–3 days, and those that failed to respond were scored as dead. For analysis concerning mutant strains, the corresponding parent strain was used as a control in the same experiment.

For lifespan experiments involving RNAi, the plates also contained 1 mM IPTG (Acros, CAS 367-93-1) and 50 μg ml^{-1} ampicillin (Fisher, BP1760-25). RNAi was accomplished by feeding N2 worms HT115(DE3) bacteria expressing target-gene dsRNA from pL4440 (ref. 32); control RNAi was done in parallel for every experiment by feeding N2 worms HT115(DE3) bacteria expressing either GFP dsRNA or empty vector (which gave identical lifespan results).

Lifespan experiments with oligomycin (Cell Signaling, 9996) were performed as described for α-KG (that is, NGM plates with 1.5% DMSO and 49.5 μM FUDR; N2 worms; OP50 bacteria).

For lifespan experiments concerning *smg-1(cc546ts);pha-4(zu225)* and *smg-1(cc546ts)*[22,35], from egg to L4 stage the strains were grown at 24 °C, which inactivates the *smg-1* temperature-sensitive allele, preventing mRNA surveillance-mediated degradation of the *pha-4(zu225)* mRNA, which contains a premature stop codon, and thus produces a truncated but fully functional PHA-4 transcription factor[35]. Then at the L4 stage the temperature was shifted to 20 °C, which restores *smg-1* function and thereby results in the degradation of *pha-4(zu225)* mRNA. Treatment with α-KG began at the L4 stage.

All lifespan data are available in Extended Data Table 2, including sample sizes. The sample size was chosen on the basis of standards done in the field in published manuscripts. No statistical method was used to predetermine the sample size. Animals were assigned randomly to the experimental groups. Worms that ruptured, bagged (that is, exhibited internal progeny hatching), or crawled off the plates were censored. Lifespan data were analysed using GraphPad Prism; *P* values were calculated using the log-rank (Mantel–Cox) test.

Statistical analyses. All experiments were repeated at least two times with identical or similar results. Data represent biological replicates. Appropriate statistical tests were used for every figure. Data meet the assumptions of the statistical tests described for each figure. Mean ± s.d. is plotted in all figures unless stated otherwise.

Food preference assay. Protocol adapted from Abada *et al.*[36]. A 10 cm NGM plate was seeded with two spots of OP50 as shown in Extended Data Fig. 1e. After letting the OP50 lawns dry over 2 days at room temperature, vehicle (H_2O) or α-KG (8 mM) was added to the top of the lawn and allowed to dry over 2 days at room temperature. Approximately 50–100 synchronized adult day 1 worms were placed onto the centre of the plate and their preference for either bacterial lawn was recorded after 3 h at room temperature.

Target identification using DARTS. For unbiased target identification (Fig. 2a), human Jurkat cells were lysed using M-PER (Thermo Scientific, 78501) with the addition of protease inhibitors (Roche, 11836153001) and phosphatase inhibitors[37]. TNC buffer (50 mM Tris-HCl pH 8.0, 50 mM NaCl, 10 mM $CaCl_2$) was added to the lysate and protein concentration was then determined using the BCA Protein Assay kit (Pierce, 23227). Cell lysates were incubated with either vehicle (H_2O) or α-KG for 1 h on ice followed by an additional 20 min at room temperature. Digestion was performed using Pronase (Roche, 10165921001) at room temperature for 30 min and stopped using excess protease inhibitors with immediate transfer to ice. The resulting digests were separated by SDS–PAGE and visualized using SYPRO Ruby Protein Gel Stain (Invitrogen, S12000). The band with increased staining from the α-KG lane (corresponding to potential protein targets that are protected from proteolysis by the binding of α-KG) and the matching area of the control lane were excised, in-gel trypsin digested, and subjected to liquid chromatography-tandem mass spectrometry (LC-MS/MS) analysis as described previously[7,38]. Mass spectrometry results were searched against the human Swissprot database (release 57.15) using Mascot version 2.3.0, with all peptides meeting a significance threshold of $P < 0.05$.

For target verification by DARTS with western blotting (Fig. 2b), HeLa cells were lysed in M-PER buffer (Thermo Scientific, 78501) with the addition of protease inhibitors (Roche, 11836153001) and phosphatase inhibitors (50 mM NaF, 10 mM β-glycerophosphate, 5 mM sodium pyrophosphate, 2 mM Na_3VO_4). Chilled TNC buffer (50 mM Tris-HCl pH 8.0, 50 mM NaCl, 10 mM $CaCl_2$) was added to the protein lysate, and protein concentration of the lysate was measured by the BCA Protein Assay kit (Pierce, 23227). The protein lysate was then incubated with vehicle control (H_2O) or varying concentrations of α-KG for 3 h at room temperature with shaking at 600 r.p.m. in an Eppendorf Thermomixer. Pronase (Roche, 10165921001) digestions were performed for 20 min at room temperature, and stopped by adding SDS loading buffer and immediately heating at 70 °C for 10 min. Samples were subjected to SDS–PAGE on 4–12% Bis-Tris gradient gel (Invitrogen, NP0322BOX) and western blotted for ATP synthase subunits ATP5B (Sigma, AV48185), ATP5O (Abcam, ab91400) and ATP5A (Abcam, ab110273). Binding between α-KG and PHD-2 (encoded by *EGLN1*) (Cell Signaling, 4835), for which α-KG is a co-substrate[39], was confirmed by DARTS. GAPDH (Ambion, AM4300) was used as a negative control.

For DARTS using *C. elegans* (Extended Data Fig. 2a), wild-type animals of various ages were grown on NGM/OP50 plates, washed four times with M9 buffer, and immediately placed in the −80 °C freezer. Animals were lysed in HEPES buffer (40 mM HEPES pH 8.0, 120 mM NaCl, 10% glycerol, 0.5% Triton X-100, 10 mM β-glycerophosphate, 50 mM NaF, 0.2 mM Na_3VO_4, protease inhibitors (Roche, 11836153001)) using Lysing Matrix C tubes (MP Biomedicals, 6912-100) and the FastPrep-24 (MP Biomedicals) high-speed bench-top homogenizer in the 4 °C room (disrupt worms for 20 s at 6.5 m s^{-1}, rest on ice for 1 min; repeat twice). Lysed animals were centrifuged at 14,000 r.p.m. for 10 min at 4 °C to pellet worm debris, and supernatant was collected for DARTS. Protein concentration was determined by BCA Protein Assay kit (Pierce, 23223). A worm lysate concentration of 1.13 μg $μl^{-1}$ was used for the DARTS experiment. All steps were performed on ice or at 4 °C to help prevent premature protein degradation. TNC buffer (50 mM Tris-HCl pH 8.0, 50 mM NaCl, 10 mM $CaCl_2$) was added to the worm lysates. Worm lysates were incubated with vehicle control (H_2O) or α-KG for 1 h on ice and then 50 min at room temperature. Pronase (Roche, 10165921001) digestions were performed for

30 min at room temperature and stopped by adding SDS loading buffer and heating at 70 °C for 10 min. Samples were then subjected to SDS–PAGE on NuPAGE Novex 4–12% Bis-Tris gradient gels (Invitrogen, NP0322BOX), and western blotting was carried out with an antibody against ATP5B (Sigma, AV48185) that also recognizes ATP-2.

Complex V activity assay. Complex V activity was assayed using the MitoTox OXPHOS Complex V Activity Kit (Abcam, ab109907). Vehicle (H_2O) or α-KG was mixed with the enzyme before the addition of phospholipids. In experiments using octyl α-KG, vehicle (1% DMSO) or octyl α-KG was added with the phospholipids. Relative complex V activity was compared to vehicle. Oligomycin (Sigma, O4876) was used as a positive control for the assay.

Isolation of mitochondria from mouse liver. Animal studies were performed under approved University of California, Los Angeles animal research protocols. Mitochondria from 3-month-old C57BL/6 mice were isolated as described[40]. Briefly, livers were extracted, minced at 4 °C in MSHE plus BSA (70 mM sucrose, 210 mM mannitol, 5 mM HEPES, 1 mM EGTA, and 0.5% fatty acid free BSA, pH 7.2), and rinsed several times to remove blood. All subsequent steps were performed on ice or at 4 °C. The tissue was disrupted in ten volumes of MSHE plus BSA with a glass Dounce homogenizer (5–6 strokes) and the homogenate was centrifuged at 800*g* for 10 min to remove tissue debris and nuclei. The supernatant was decanted through a cell strainer and centrifuged at 8,000*g* for 10 min. The dark mitochondrial pellet was resuspended in MSHE plus BSA and re-centrifuged at 8,000*g* for 10 min. The final mitochondrial pellets were used for various assays as described later.

Submitochondrial particle ATPase assay. ATP hydrolysis by ATP synthase was measured using submitochondrial particles (see ref. 41 and references therein). Mitochondria were isolated from mouse liver as described earlier. The final mitochondrial pellet was resuspended in buffer A (250 mM sucrose, 10 mM Tris-HCl, 1 mM ATP, 5 mM $MgCl_2$ and 0.1 mM EGTA, pH 7.4) at 10 μg μl^{-1}, subjected to sonication on ice (Fisher Scientific Model 550 Sonic Dismembrator; medium power, alternating between 10 s intervals of sonication and resting on ice for a total of 60 s of sonication), and then centrifuged at 18,000*g* for 10 min at 4 °C. The supernatant was collected and centrifuged at 100,000*g* for 45 min at 4 °C. The final pellet (submitochondrial particles) was resuspended in buffer B (250 mM sucrose, 10 mM Tris-HCl and 0.02 mM EGTA, pH 7.4).

The SMP ATPase activity was assayed using the Complex V Activity Buffer as described eariler. The production of ADP is coupled to the oxidation of NADH to NAD^+ through pyruvate kinase and lactate dehydrogenase. The addition of α-KG (up to 10 mM) did not affect the activity of pyruvate kinase or lactate dehydrogenase when external ADP was added. The absorbance decrease of NADH at 340 nm correlates to ATPase activity. Submitochondrial particles (2.18 ng μl^{-1}) were incubated with vehicle or α-KG for 90 min at room temperature before the addition of activity buffer, and then the absorbance decrease of NADH at 340 nm was measured every 1 min for 1 h. Oligomycin (Cell signaling, 9996) was used as a positive control for the assay.

Assay for ATP levels. Normal human diploid fibroblast WI-38 (ATCC, CCL-75) cells were seeded in 96-well plates at 2×10^4 cells per well. Cells were treated with either DMSO (vehicle control) or octyl α-KG at varying concentrations for 2 h in triplicate. ATP levels were measured using the CellTiter-Glo luminescent ATP assay (Promega, G7572); luminescence was read using Analyst HT (Molecular Devices). In parallel, identically treated cells were lysed in M-PER (Thermo Scientific, 78501) to obtain protein concentration by BCA Protein Assay kit (Pierce, 23223). ATP levels were normalized to protein content. Statistical analysis was performed using GraphPad Prism (unpaired *t*-test).

The assay for ATP levels in *C. elegans* was carried out as follows. Synchronized day 1 adult wild-type *C. elegans* were placed on NGM plates containing either vehicle or 8 mM α-KG. On day 2 and 8 of adulthood, 9 replicates and 4 replicates, respectively, of about 100 worms were collected from α-KG or vehicle control plates, washed 4 times in M9 buffer, and frozen in −80 °C. Animals were lysed using Lysing Matrix C tubes (MP Biomedicals, 6912-100) and the FastPrep-24 (MP Biomedicals) high-speed bench-top homogenizer (disrupt worms for 20 s at 6.5 m s^{-1}, rest on ice for 1 min; repeat twice). Lysed animals were centrifuged at 14,000 r.p.m. for 10 min at 4 °C to pellet worm debris, and supernatant was saved for ATP quantification using the Kinase-Glo Luminescent Kinase Assay Platform (Promega, V6713) according to the manufacturer's instructions. The assay was performed in white opaque 96-well tissue culture plates (Falcon, 353296), and luminescence was measured using Analyst HT (Molecular Devices). ATP levels were normalized to the number of worms. Statistical analysis was performed using Microsoft Excel (*t*-test, two-tailed, two-sample unequal variance).

Measurement of oxygen consumption rates. Oxygen consumption rate (OCR) measurements were made using a Seahorse XF-24 analyser (Seahorse Bioscience)[42]. Cells were seeded in Seahorse XF-24 cell culture microplates at 50,000 cells per well in DMEM media supplemented with 10% FBS and 10 mM glucose, and incubated at 37 °C and 5% CO_2 overnight. Treatment with octyl α-KG or DMSO (vehicle control) was for 1 h. Cells were washed in unbuffered DMEM medium (pH 7.4, 10 mM glucose) just before measurement, and maintained in this buffer with indicated concentrations of octyl α-KG. OCR was measured three times under basal conditions and normalized to protein concentration per well. Statistical analysis was performed using GraphPad Prism.

Measurement of OCR in living *C. elegans* was carried out as follows. The protocol was adapted from those previously described[43,44]. Wild-type day 1 adult N2 worms were placed on NGM plates containing 8 mM α-KG or H_2O (vehicle control) seeded with OP50 or HT115 *E. coli*. OCR was assessed on day 2 of adulthood. On day 2 of adulthood, worms were collected and washed four times with M9 to rid the samples of bacteria (we further verified that α-KG does not affect oxygen consumption of the bacteria—therefore, even if there were any leftover bacteria after the washes, the changes in OCR observed would still be worm specific), and then the animals were seeded in quadruplicates in Seahorse XF-24 cell culture microplates (Seahorse Bioscience, V7-PS) in 200 μl M9 at ~200 worms per well. Oxygen consumption rates were measured seven times under basal conditions and normalized to the number of worms counted per well. The experiment was repeated twice. Statistical analysis was performed using Microsoft Excel (*t*-test, two-tailed, two-sample unequal variance).

Measurement of mitochondrial respiratory control ratio. Mitochondrial respiratory control ratio (RCR) was analysed using isolated mouse liver mitochondria (see ref. 15 and references therein). Mitochondria were isolated from mouse liver as described earlier. The final mitochondrial pellet was resuspended in 30 μl of MAS buffer (70 mM sucrose, 220 mM mannitol, 10 mM KH_2PO_4, 5 mM $MgCl_2$, 2 mM HEPES, 1 mM EGTA, and 0.2% fatty acid free BSA, pH 7.2).

Isolated mitochondrial respiration was measured by running coupling and electron flow assays as described[40]. For the coupling assay, 20 μg of mitochondria in complete MAS buffer (MAS buffer supplemented with 10 mM succinate and 2 μM rotenone) were seeded into a XF24 Seahorse plate by centrifugation at 2,000*g* for 20 min at 4 °C. Just before the assay, the mitochondria were supplemented with complete MAS buffer for a total of 500 μl (with 1% DMSO or octyl α-KG), and warmed at 37 °C for 30 min before starting the OCR measurements. Mitochondrial respiration begins in a coupled state 2; state 3 is initiated by 2 mM ADP; state 4o (oligomycin insensitive, that is, complex V independent) is induced by 2.5 μM oligomycin; and state 3u (FCCP-uncoupled maximal respiratory capacity) by 4 μM FCCP. Finally, 1.5 μg ml^{-1} antimycin A was injected at the end of the assay. The state 3/state 4o ratio gives the RCR.

For the electron flow assay, the MAS buffer was supplemented with 10 mM sodium pyruvate (complex I substrate), 2 mM malate (complex II inhibitor) and 4 μM FCCP, and the mitochondria are seeded the same way as described for the coupling assay. After basal readings, the sequential injections were as follows: 2 μM rotenone (complex I inhibitor), 10 mM succinate (complex II substrate), 4 μM antimycin A (complex III inhibitor) and 10 mM/100 μM ascorbate/tetramethylphenylenediamine (complex IV substrate).

ATP synthase enzyme inhibition kinetics. ATP synthesis enzyme inhibition kinetic analysis was performed using isolated mitochondria. Mitochondria were isolated from mouse liver as described earlier. The final mitochondrial pellet was resuspended in MAS buffer supplemented with 5 mM sodium ascorbate (Sigma, A7631) and 5 mM TMPD (Sigma, T7394).

The reaction was carried out in MAS buffer containing 5 mM sodium ascorbate, 5 mM TMPD, luciferase reagent (Roche, 11699695001), octanol or octyl α-KG, variable amounts of ADP (Sigma, A2754), and 3.75 ng μl^{-1} mitochondria. ATP synthesis was monitored by the increase in luminescence over time by a luminometer (Analyst HT, Molecular Devices). ATP-synthase-independent ATP formation, derived from the oligomycin-insensitive luminescence, was subtracted as background. The initial velocity of ATP synthesis was calculated from the slope of the first 3 min of the reaction, before the velocity begins to decrease. Enzyme inhibition kinetics was analysed by nonlinear regression least-squares fit using GraphPad Prism.

Assay for mammalian TOR pathway activity. Mammalian (m)TOR pathway activity in cells treated with octyl α-KG or oligomycin was determined by the levels of phosphorylation of known mTOR substrates, including S6K (T389), 4E-BP1 (S65), AKT (S473) and ULK1 (S757)[45–49]. Specific antibodies used: phospho (P)-S6K T389 (Cell Signaling, 9234), S6K (Cell Signaling, 9202S), P-4E-BP1 S65 (Cell Signaling, 9451S), 4E-BP1 (Cell Signaling, 9452S), P-AKT S473 (Cell Signaling, 4060S), AKT (Cell Signaling, 4691S), P-ULK1 S757 (Cell Signaling, 6888), ULK1 (Cell Signaling, 4773S) and GAPDH (Santa Cruz Biotechnology, 25778).

Assay for autophagy. DA2123 animals carrying an integrated GFP::LGG-1 translational fusion gene[50–52], were used to quantify levels of autophagy. To obtain a synchronized population of DA2123, we performed an egg preparation of gravid adults (by lysing ~100 gravid worms in 70 μl M9 buffer, 25 μl bleach and 5 μl 10 N NaOH) and allowed the eggs to hatch overnight in M9, causing starvation-induced L1 diapause. L1 larvae were deposited onto NGM treatment plates containing vehicle,

8 mM α-KG or 40 μM oligomycin, and seeded with either *E. coli* OP50, HT115(DE3) with an empty vector, or HT115(DE3)-expressing dsRNAs targeting *atp-2*, *let-363* or *ogdh-1* as indicated. When the majority of animals in a given sample first reached the mid-L3 stage, individual L3 larvae were mounted onto microscope slides and anaesthetized with 1.6 mM levamisole (Sigma, 31742). Nematodes were observed using an Axiovert 200M Zeiss confocal microscope with a LSM5 Pascal laser, and images were captured using the LSM Image Examiner (Zeiss). For each specimen, GFP::LGG-1 puncta (autophagosomes) in the epidermis, including the lateral seam cells and Hyp7, were counted in three separate regions of 140.97 μm^2 using 'analyze particles' in ImageJ[53]. Measurements were made blind to both the genotype and supplement. Statistical analysis was performed using Microsoft Excel (*t*-test, two-tailed, two-sample unequal variance).

The assay for autophagy in mammalian cells was carried out as follows. HEK-293 cells were seeded in 6-well plates at 2.5×10^5 cells per well in DMEM media supplemented with 10% FBS and 10 mM glucose, and incubated overnight before treatment with either octanol (vehicle control) or octyl α-KG for 72 h. Cells were lysed in M-PER buffer with protease and phosphatase inhibitors. Lysates were subjected to SDS–PAGE on a 4–12% Bis-Tris gradient gel with MES running buffer and western blotted for LC3 (Novus, NB100-2220). LC3 is the mammalian homologue of worm LGG-1, and conversion of the soluble LC3-I to the lipidated LC3-II is activated in autophagy, for example, upon starvation[54].

Pharyngeal pumping rates of *C. elegans* treated with 8 mM α-KG. The pharyngeal pumping rates of 20 wild-type N2 worms per condition were assessed. Pharyngeal contractions were recorded for 1 min using a Zeiss M2 BioDiscovery microscope and an attached Sony NDR-XR500V video camera at 12-fold optical zoom. The resulting videos were played back at 0.3× speed using MPlayerX and pharyngeal pumps were counted. Statistical analysis was performed using Microsoft Excel (*t*-test, two-tailed, two-sample unequal variance).

Assay for α-KG levels in *C. elegans*. Synchronized adult worms were collected from plates with vehicle (H_2O) or 8 mM α-KG, washed three times with M9 buffer, and flash frozen. Worms were lysed in M9 using Lysing Matrix C tubes (MP Biomedicals, 6912-100) and the FastPrep-24 (MP Biomedicals) high-speed bench-top homogenizer in the 4 °C room (disrupt worms for 20 s at 6.5 m s^{-1}, rest on ice for 1 min; repeat three times). Lysed animals were centrifuged at 14,000 r.p.m. for 10 min at 4 °C to pellet worm debris, and the supernatant was saved. The protein concentration of the supernatant was determined by the BCA Protein Assay kit (Pierce, 23223); there was no difference in protein level per worm in α-KG-treated and vehicle-treated animals (data not shown). α-KG content was assessed as described previously[55] with modifications. Worm lysates were incubated at 37 °C in 100 mM KH_2PO_4 (pH 7.2), 10 mM NH_4Cl, 5 mM $MgCl_2$ and 0.3 mM NADH for 10 min. Glutamate dehydrogenase (Sigma, G2501) was then added to reach a final concentration of 1.83 units ml^{-1}. Under these conditions, glutamate dehydrogenase uses α-KG and NADH to make glutamate. The absorbance decrease was monitored at 340 nm. The intracellular level of α-KG was determined from the absorbance decrease in NADH. The approximate molarity of α-KG present inside the animals was estimated using average protein content (~245 ng per worm, from BCA assay) and volume (~3 nl for adult worms 1.1 mm in length and 60 μm in diameter (http://www.wormatlas.org/hermaphrodite/introduction/Introframeset.html)).

For quantitative analysis of α-KG in worms using ultra-high-performance liquid chromatography-electrospray ionization-tandem mass spectrometry (UHPLC-ESI/MS/MS), synchronized day 1 adult worms were placed on vehicle plates with or without bacteria for 24 h, and then collected and lysed in the same manner as described earlier. α-KG analysis by LC/MS/MS was carried out on an Agilent 1290 Infinity UHPLC system and 6460 Triple Quadrupole mass spectrometer (Agilent Technologies) using an electrospray ionization (ESI) source with Agilent Jet Stream technology. Data were acquired with Agilent MassHunter Data Acquisition software version B.06.00, and processed for precursor and product ions selection with MassHunter Qualitative Analysis software version B.06.00 and for calibration and quantification with MassHunter Quantitative Analysis for QQQ software version B.06.00.

For UHPLC, 3 μl calibration standards and samples were injected onto the UHPLC system including a G4220A binary pump with a built-in vacuum degasser and a thermostatted G4226A high performance autosampler. An ACQUITY UPLC BEH Amide analytical column (2.1 × 50 mm, 1.7 μm) and a VanGuard BEH Amide Pre-column (2.1 × 5 mm, 1.7 μm) from Waters Corporation were used at the flow rate of 0.6 ml min^{-1} using 50/50/0.04 acetonitrile/water/ammonium hydroxide with 10 mM ammonium acetate as mobile phase A and 95/5/0.04 acetonitrile/water/ammonium hydroxide with 10 mM ammonium acetate as mobile phase B. The column was maintained at room temperature. The following gradient was applied: 0–0.41 min: 100% B isocratic; 0.41–5.30 min: 100–30% B; 5.30–5.35 min: 30–0% B; 5.35–7.35 min: 0% B isocratic; 7.35–7.55 min: 0–100% B; 7.55–9.55 min: 100% B isocratic.

For the MS detection, the ESI mass spectra data were recorded on a negative ionization mode by MRM. MRM transitions of α-KG and its ISTD $^{13}C_4$-α-KG (Cambridge Isotope Laboratories) were determined using a 1 min 37% B isocratic UHPLC method through the column at a flow rate of 0.6 ml min^{-1}. The precursor ion of $[M–H]^-$ and the product ion of $[M–CO_2–H]^-$ were observed to have the highest signal-to-noise ratios. The precursor and product ions are respectively 145.0 and 100.9 for α-KG, and 149.0 and 104.9 for ISTD $^{13}C_4$-α-KG. Nitrogen was used as the drying, sheath and collision gas. All the source and analyser parameters were optimized using Agilent MassHunter Source and iFunnel Optimizer and Optimizer software, respectively. The source parameters are as follows: drying gas temperature 120 °C, drying gas flow 13 l min^{-1}, nebulizer pressure 55 psi, sheath gas temperature 400 °C, sheath gas flow 12 l min^{-1}, capillary voltage 2,000 V, and nozzle voltage 0 V. The analyser parameters are as follows: fragmentor voltage 55 V, collision energy 2 V and cell accelerator voltage 1 V. The UHPLC eluants before 1 min and after 5.3 min were diverted to waste.

Membrane-permeable esters of α-KG. Octyl α-KG, a commonly used membrane-permeable ester of α-KG[55–58], was used to deliver α-KG across lipid membranes in experiments using cells and mitochondria. Upon hydrolysis by cellular esterases, octyl α-KG yields α-KG and the by-product octanol. We showed that, whereas octanol control has no effect (Extended Data Fig. 2e, f and Extended Data Fig. 6a), α-KG alone can bind and inhibit ATP synthase (Fig. 2a, b and Extended Data Fig. 2a, b; data not shown), decrease ATP and OCR (Fig. 2e, g), induce autophagy (Fig. 4b) and increase *C. elegans* lifespan (Figs 1, 3, Extended Data Figs 1, 5 and Extended Data Table 2). The existence and activity of esterases in our mitochondrial and cell culture experiments have been confirmed using calcein AM (C1430, Molecular Probes), an esterase substrate that fluoresces upon hydrolysis, and also by mass spectrometry (data not shown). The hydrolysis by esterases explains why distinct esters of α-KG, such as 1-octyl α-KG, 5-octyl α-KG, and dimethyl α-KG, have similar effects to α-KG (Extended Data Fig. 2g, h and Extended Data Table 2).

Synthesis of octyl α-KG. Synthesis of 1-octyl α-KG has been previously described[59]. Briefly, 1-octanol (0.95 ml, 6.0 mmol), DMAP (37 mg, 0.3 mmol) and DCC (0.743 g, 3.6 mmol) were added to a solution of 1-cyclobutene-1-carboxylic acid (0.295 g, 3.0 mmol) in dry CH_2Cl_2 (6.0 ml) at 0 °C. After it had been stirred for 1 h, the solution was allowed to warm to room temperature and stirred for another 8 h. The precipitate was filtered and washed with ethyl acetate (3 × 100 ml). The combined organic phases were washed with water and brine, and dried over anhydrous Na_2SO_4. Flash column chromatography on silica gel eluting with 80/1 hexane/ethyl acetate gave octyl cyclobut-1-enecarboxylate as a clear oil (0.604 g, 96%). To a −78 °C solution of this oil (0.211 g, 1.0 mmol) in CH_2Cl_2 (10 ml) was bubbled O_3/O_2 until the solution turned blue. The residual ozone was discharged by bubbling with O_2 and the reaction was warmed to room temperature and stirred for another 1 h. Dimethyl sulphide (Me_2S, 0.11 ml, 1.5 mmol) was added to the mixture and it was stirred for another 2 h. The CH_2Cl_2 was removed *in vacuo* and the crude product was dissolved in a solution of 2-methyl-2-butene (0.8 ml) in *t*-BuOH (3.0 ml). To this was added dropwise a solution containing sodium chlorite (0.147 g, 1.3 mmol) and sodium dihydrogen phosphate monohydrate (0.179 g, 1.3 mmol) in H_2O (1.0 ml). The mixture was stirred at room temperature overnight, and then extracted with ethyl acetate (3 × 50 ml). The combined organic phases were washed with water and brine, and dried over anhydrous Na_2SO_4. Flash column chromatography on silica gel eluting with 5/1 hexane/ethyl acetate gave octyl α-KG, which became a pale solid when stored in the refrigerator (0.216 g, 84%).

Synthesis of 5-octyl L-glutamate. L-Glutamic acid (0.147 g, 1.0 mmol) and anhydrous sodium sulphate (0.1 g) was dissolved in octanol (2.0 ml), and then tetrafluoroboric acid-dimethyl ether complex (0.17 ml) was added. The suspended mixture was stirred at 21 °C overnight. Anhydrous THF (5 ml) was added to the mixture and it was filtered through a thick pad of activated charcoal. Anhydrous triethylamine (0.4 ml) was added to the clear filtrate to obtain a milky white slurry. Upon trituration with ethyl acetate (10 ml), the monoester monoacid precipitated. The precipitate was collected, washed with additional ethyl acetate (2 × 5 ml), and dried *in vacuo* to give the desired product, 5-octyl L-glutamate (0.249 g, 96%) as a white solid. ^{1}H NMR (500 MHz, acetic acid-d_4): δ 4.12 (dd, J = 6.6, 6.6 Hz, 1H), 4.11 (t, J = 6.8 Hz, 2H), 2.64 (m, 2H), 2.26 (m, 2H), 1.64 (m, 2H), 1.30 (m, 10H), 0.89 (t, J = 7.0 Hz, 3H). ^{13}C NMR (125 MHz, acetic acid-d_4): δ 175.0, 174.3, 66.3, 55.0, 32.7, 30.9, 30.11, 30.08, 29.3, 26.7, 26.3, 23.4, 14.4.

Synthesis of 5-octyl D-glutamate. The synthesis of the opposite enantiomer, that is, 5-octyl D-glutamate, was carried out by the exact same procedure starting with D-glutamic acid. The spectroscopic data was identical to that of the enantiomeric compound.

Synthesis of 5-octyl α-KG. 1-Benzyl 5-octyl 2-oxopentanedioate was obtained as follows. To a solution of 5-octyl L-glutamate (0.249 g) in H_2O (6.0 ml) and acetic acid (2.0 ml) cooled to 0 °C was added slowly a solution of aqueous sodium nitrite (0.207 g, 3.0 mmol in 4 ml H_2O). The reaction mixture was allowed to warm slowly to room temperature and was stirred overnight. The mixture was concentrated.

The resulting residue was dissolved in DMF (10 ml) and $NaHCO_3$ (0.42 g, 5.0 mmol) and benzyl bromide (0.242 ml, 2.0 mmol) were added to the mixture. The mixture was stirred at 21 °C overnight and then extracted with ethyl acetate (3 × 30 ml). The combined organic phase was washed with water and brine and dried over anhydrous $MgSO_4$. Flash column chromatography on silica gel eluting with 7/1 hexanes/ethyl acetate gave the mixed diester 1-benzyl 5-octyl (*S*)-2-hydroxypentanedioate as a colourless oil. To this oil, dissolved in dichloromethane (10.0 ml), were added $NaHCO_3$ (0.42 g, 5.0 mmol) and Dess–Martin periodinane (0.509 g, 1.2 mmol), and the mixture was stirred at room temperature for 1 h and then extracted with ethyl acetate (3 × 30 ml). The combined organic phase was washed with water and brine and dried over anhydrous $MgSO_4$. Flash column chromatography on silica gel eluting with 5/1 hexanes/ethyl acetate gave the desired 1-benzyl 5-octyl 2-oxopentanedioate (0.22 g, 66%) as a white solid. ^{1}H NMR (500 MHz, $CDCl_3$): δ 7.38 (m, 5H), 5.27 (s, 2H), 4.05 (t, J = 6.5 Hz, 2H), 3.14 (t, J = 6.5 Hz, 2H), 2.64 (t, J = 6.5 Hz, 2H), 1.59 (m, 2H), 1.28 (m, 10H), 0.87 (t, J = 7.0 Hz, 3H). ^{13}C NMR (125 MHz, $CDCl_3$): δ 192.2, 171.9, 160.1, 134.3, 128.7, 128.6, 128.5, 67.9, 65.0, 34.2, 31.7, 29.07, 29.05, 28.4, 27.5, 25.7, 22.5, 14.0.

5-Octyl α-KG (5-(octyloxy)-2,5-dioxopentanoic acid) was obtained as follows. To a solution of 1-benzyl 5-octyl 2-oxopentanedioate (0.12 g, 0.344 mmol) in ethyl acetate (15 ml) was added 5% Pd/C (80 mg). Over the mixture was passed a stream of argon and then the argon was replaced with hydrogen gas and the mixture was stirred vigorously for 15 min. The mixture was filtered through a thick pad of Celite to give the desired product 5-octyl α-KG (0.088 g, 99%) as white solid. ^{1}H NMR (500 MHz, $CDCl_3$): δ 8.16 (br s, 1H), 4.06 (t, J = 6.5 Hz, 2H), 3.18 (t, J = 6.5 Hz, 2H), 2.69 (t, J = 6.0 Hz, 2H), 1.59 (m, 2H), 1.26 (m, 10H), 0.85 (t, J = 7.0 Hz, 3H). ^{13}C NMR (125 MHz, $CDCl_3$): δ 193.8, 172.7, 160.5, 65.5, 33.0, 31.7, 29.08, 29.06, 28.4, 27.8, 25.8, 22.5, 14.0.

31. Brenner, S. The genetics of *Caenorhabditis elegans*. *Genetics* **77,** 71–94 (1974).
32. Timmons, L. & Fire, A. Specific interference by ingested dsRNA. *Nature* **395,** 854 (1998).
33. Long, X. *et al.* TOR deficiency in *C. elegans* causes developmental arrest and intestinal atrophy by inhibition of mRNA translation. *Curr. Biol.* **12,** 1448–1461 (2002).
34. Sutphin, G. L. & Kaeberlein, M. Measuring *Caenorhabditis elegans* life span on solid media. *J. Vis. Exp.* **27,** 1152 (2009).
35. Gaudet, J. & Mango, S. E. Regulation of organogenesis by the *Caenorhabditis elegans* FoxA protein PHA-4. *Science* **295,** 821–825 (2002).
36. Abada, E. A. *et al. C. elegans* behavior of preference choice on bacterial food. *Mol. Cells* **28,** 209–213 (2009).
37. Lomenick, B., Jung, G., Wohlschlegel, J. A. & Huang, J. Target identification using drug affinity responsive target stability (DARTS). *Curr. Protoc. Chem. Biol.* **3,** 163–180 (2011).
38. Lomenick, B., Olsen, R. W. & Huang, J. Identification of direct protein targets of small molecules. *ACS Chem. Biol.* **6,** 34–46 (2011).
39. Stubbs, C. J. *et al.* Application of a proteolysis/mass spectrometry method for investigating the effects of inhibitors on hydroxylase structure. *J. Med. Chem.* **52,** 2799–2805 (2009).
40. Rogers, G. W. *et al.* High throughput microplate respiratory measurements using minimal quantities of isolated mitochondria. *PLoS ONE* **6,** e21746 (2011).
41. Alberts, B. *Molecular Biology of the Cell* 3rd edn (Garland, 1994).
42. Wu, M. *et al.* Multiparameter metabolic analysis reveals a close link between attenuated mitochondrial bioenergetic function and enhanced glycolysis dependency in human tumor cells. *Am. J. Physiol. Cell Physiol.* **292,** C125–C136 (2007).
43. Yamamoto, H. *et al.* NCoR1 is a conserved physiological modulator of muscle mass and oxidative function. *Cell* **147,** 827–839 (2011).
44. Pathare, P. P., Lin, A., Bornfeldt, K. E., Taubert, S. & Van Gilst, M. R. Coordinate regulation of lipid metabolism by novel nuclear receptor partnerships. *PLoS Genet.* **8,** e1002645 (2012).
45. Pullen, N. & Thomas, G. The modular phosphorylation and activation of p70s6k. *FEBS Lett.* **410,** 78–82 (1997).
46. Burnett, P. E., Barrow, R. K., Cohen, N. A., Snyder, S. H. & Sabatini, D. M. RAFT1 phosphorylation of the translational regulators p70 S6 kinase and 4E-BP1. *Proc. Natl Acad. Sci. USA* **95,** 1432–1437 (1998).
47. Gingras, A. C. *et al.* Hierarchical phosphorylation of the translation inhibitor 4E-BP1. *Genes Dev.* **15,** 2852–2864 (2001).
48. Sarbassov, D. D., Guertin, D. A., Ali, S. M. & Sabatini, D. M. Phosphorylation and regulation of Akt/PKB by the rictor-mTOR complex. *Science* **307,** 1098–1101 (2005).
49. Kim, J., Kundu, M., Viollet, B. & Guan, K. L. AMPK and mTOR regulate autophagy through direct phosphorylation of Ulk1. *Nature Cell Biol.* **13,** 132–141 (2011).
50. Kang, C., You, Y. J. & Avery, L. Dual roles of autophagy in the survival of *Caenorhabditis elegans* during starvation. *Genes Dev.* **21,** 2161–2171 (2007).
51. Hansen, M. *et al.* A role for autophagy in the extension of lifespan by dietary restriction in *C. elegans*. *PLoS Genet.* **4,** e24 (2008).
52. Alberti, A., Michelet, X., Djeddi, A. & Legouis, R. The autophagosomal protein LGG-2 acts synergistically with LGG-1 in dauer formation and longevity in *C. elegans*. *Autophagy* **6,** 622–633 (2010).
53. Schneider, C. A., Rasband, W. S. & Eliceiri, K. W. NIH Image to ImageJ: 25 years of image analysis. *Nature Methods* **9,** 671–675 (2012).
54. Kabeya, Y. *et al.* LC3, a mammalian homologue of yeast Apg8p, is localized in autophagosome membranes after processing. *EMBO J.* **19,** 5720–5728 (2000).
55. MacKenzie, E. D. *et al.* Cell-permeating α-ketoglutarate derivatives alleviate pseudohypoxia in succinate dehydrogenase-deficient cells. *Mol. Cell. Biol.* **27,** 3282–3289 (2007).
56. Zhao, S. *et al.* Glioma-derived mutations in IDH1 dominantly inhibit IDH1 catalytic activity and induce HIF-1α. *Science* **324,** 261–265 (2009).
57. Xu, W. *et al.* Oncometabolite 2-hydroxyglutarate is a competitive inhibitor of α-ketoglutarate-dependent dioxygenases. *Cancer Cell* **19,** 17–30 (2011).
58. Jin, G. *et al.* Disruption of wild-type IDH1 suppresses D-2-hydroxyglutarate production in IDH1-mutated gliomas. *Cancer Res.* **73,** 496–501 (2013).
59. Jung, M. E. & Deng, G. Synthesis of the 1-monoester of 2-ketoalkanedioic acids, for example, octyl α-ketoglutarate. *J. Org. Chem.* **77,** 11002–11005 (2012).

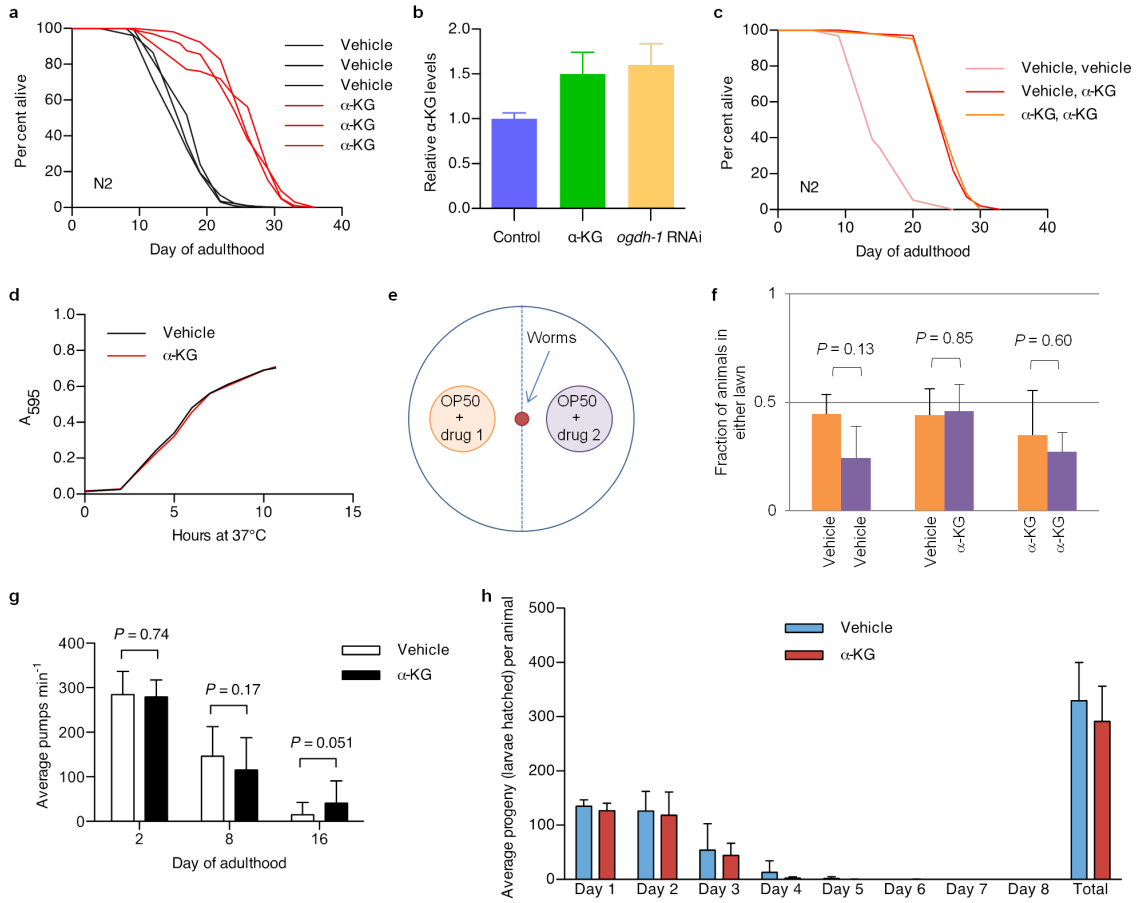

Extended Data Figure 1 | Supplementation with α-KG extends *C. elegans* adult lifespan but does not change the growth rate of bacteria, or food intake, pharyngeal pumping rate or brood size of the worms. **a**, Robust lifespan extension in adult *C. elegans* by α-KG. 8 mM α-KG increased the mean lifespan of N2 by an average of 47.3% in three independent experiments ($P < 0.0001$ for every experiment, by log-rank test). Experiment 1, mean lifespan (days of adulthood) with vehicle treatment (m_{veh}) = 18.9 ($n = 87$ animals tested), $m_{\alpha\text{-KG}} = 25.8$ ($n = 96$); experiment 2, $m_{veh} = 17.5$ ($n = 119$), $m_{\alpha\text{-KG}} = 25.4$ ($n = 97$); experiment 3, $m_{veh} = 16.3$ ($n = 100$), $m_{\alpha\text{-KG}} = 26.1$ ($n = 104$). **b**, Worms supplemented with 8 mM α-KG and worms with RNAi knockdown of α-KGDH (encoded by *ogdh-1*) have increased α-KG levels. Young adult worms were placed on treatment plates seeded with control HT115 *E. coli* or HT115-expressing *ogdh-1* dsRNA, and α-KG content was assayed after 24 h (see Methods). **c**, α-KG treatment beginning at the egg stage and that beginning in adulthood produced identical lifespan increases. Light red, treatment with vehicle control throughout larval and adult stages ($m = 15.6$, $n = 95$); dark red, treatment with vehicle during larval stages and with 8 mM α-KG at adulthood ($m = 26.3$, $n = 102$), $P < 0.0001$ (log-rank test); orange, treatment with 8 mM α-KG throughout larval and adult stages ($m = 26.3$, $n = 102$), $P < 0.0001$ (log-rank test). **d**, α-KG does not alter the growth rate of the OP50 *E. coli*, which is the standard laboratory food source for nematodes. α-KG (8 mM) or vehicle (H_2O) was added to standard LB media and the pH was adjusted to 6.6 by the addition of NaOH. Bacterial cells from the same overnight OP50 culture were added to the LB ± α-KG mixture at a 1:40 dilution, and then placed in the 37 °C incubator shaker at 300 r.p.m. The absorbance at 595 nm was read at 1 h time intervals to generate the growth curve. **e**, Schematic representation of food preference assay. **f**, N2 worms show no preference between OP50 *E. coli* food treated with vehicle or α-KG ($P = 0.85$, by *t*-test, two-tailed, two-sample unequal variance), nor preference between identically treated OP50 *E. coli*. **g**, Pharyngeal pumping rate of *C. elegans* on 8 mM α-KG is not significantly altered (by *t*-test, two-tailed, two-sample unequal variance). **h**, Brood size of *C. elegans* treated with 8 mM α-KG. Brood size analysis was conducted at 20 °C. Ten L4 wild-type worms were each singly placed onto an NGM plate containing vehicle or 8 mM α-KG. Worms were transferred one per plate onto a new plate every day, and the eggs laid were allowed to hatch and develop on the previous plate. Hatchlings were counted as a vacuum was used to remove them from the plate. Animals on 8 mM α-KG showed no significant difference in brood size compared with animals on vehicle plates ($P = 0.223$, by *t*-test, two-tailed, two-sample unequal variance). Mean ± s.d. is plotted in all cases.

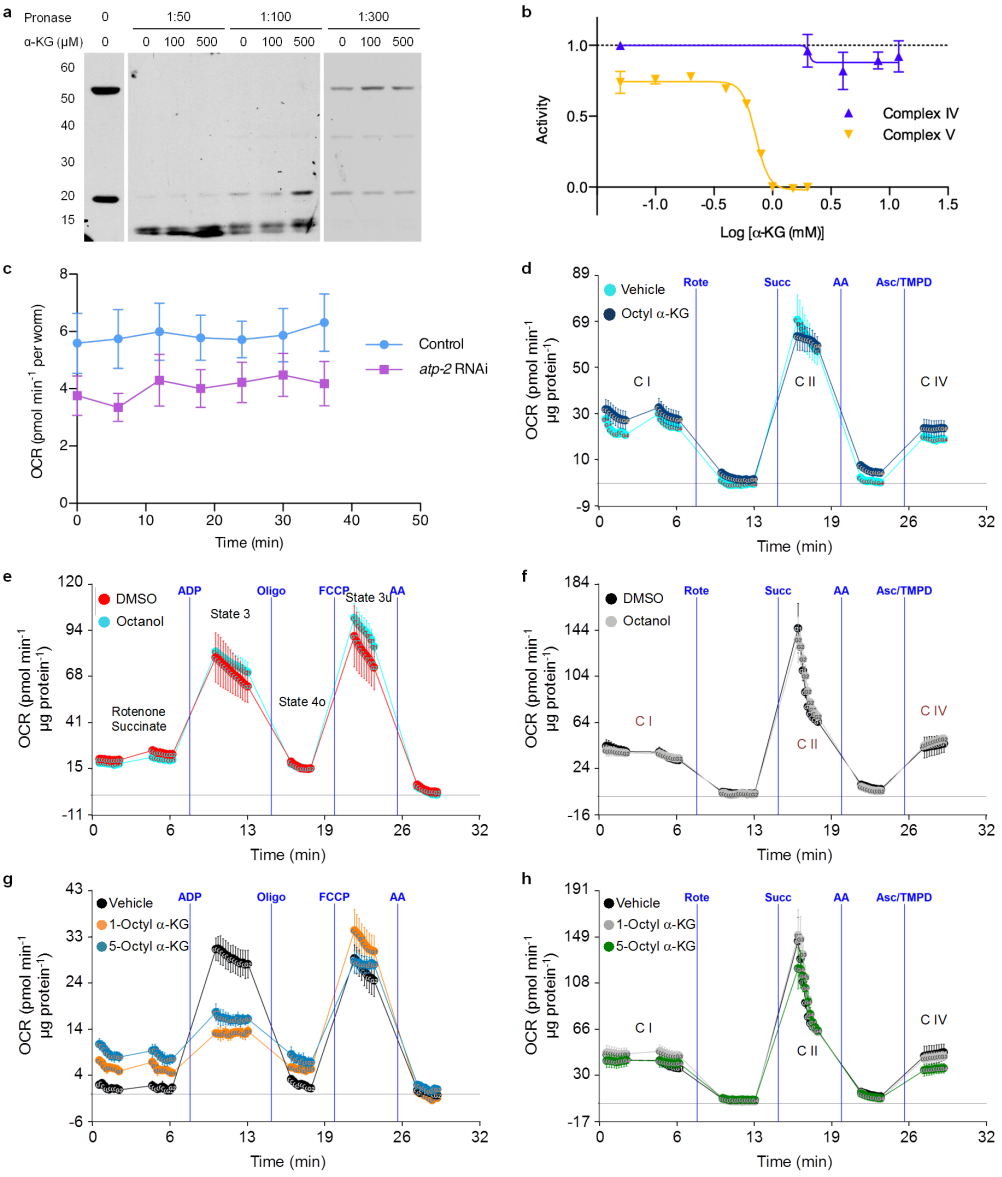

Extended Data Figure 2 | α-KG binds to the β subunit of ATP synthase and inhibits the activity of complex V but not the other ETC complexes. **a**, Western blot showing protection of the ATP-2 protein from Pronase digestion upon α-KG binding in the DARTS assay. The antibody for human ATP5B (Sigma, AV48185) recognizes the epitope $_{144}$IMNVIGEPIDERGPIKTKQFAPIHAEAPEFMEMSVEQEILVTGIKVVDLL$_{193}$ that has 90% identity to the *C. elegans* ATP-2. The lower molecular weight band near 20 kDa is a proteolytic fragment of the full-length protein corresponding to the domain directly bound by α-KG. **b**, α-KG does not affect complex IV activity. Complex IV activity was assayed using the MitoTox OXPHOS Complex IV Activity Kit (Abcam, ab109906). Relative complex IV activity was compared to vehicle (H_2O) controls. Potassium cyanide (Sigma, 60178) was used as a positive control for the assay. Complex V activity was assayed using the MitoTox Complex V OXPHOS Activity Microplate Assay (Abcam, ab109907). **c**, *atp-2* RNAi worms have lower oxygen consumption compared to control (*gfp* in RNAi vector), $P < 0.0001$ (*t*-test, two-tailed, two-sample unequal variance) for the entire time series (two independent experiments); similar to α-KG-treated worms shown in Fig. 2g. **d**, α-KG does not affect the electron flow through the ETC. Oxygen consumption rate (OCR) from isolated mouse liver mitochondria at basal (pyruvate and malate as complex I substrate and complex II inhibitor, respectively, in the presence of FCCP) and in response to sequential injection of rotenone (Rote; complex I inhibitor), succinate (Succ; complex II substrate), antimycin A (AA; complex III inhibitor), ascorbate/tetramethylphenylenediamine (Asc/TMPD; cytochrome *c* (complex IV) substrate). No difference in complex I (C I), complex II (C II) or complex IV (C IV) respiration was observed after 30 min treatment with 800 μM octyl α-KG, whereas complex V was inhibited (see Fig. 2h) by the same treatment (two independent experiments). **e**, **f**, No significant difference in coupling (**e**) or electron flow (**f**) was observed with either octanol or DMSO vehicle control. **g**, **h**, Treatment with 1-octyl α-KG or 5-octyl α-KG gave identical results in coupling (**g**) or electron flow (**h**) assays. Mean ± s.d. is plotted in all cases.

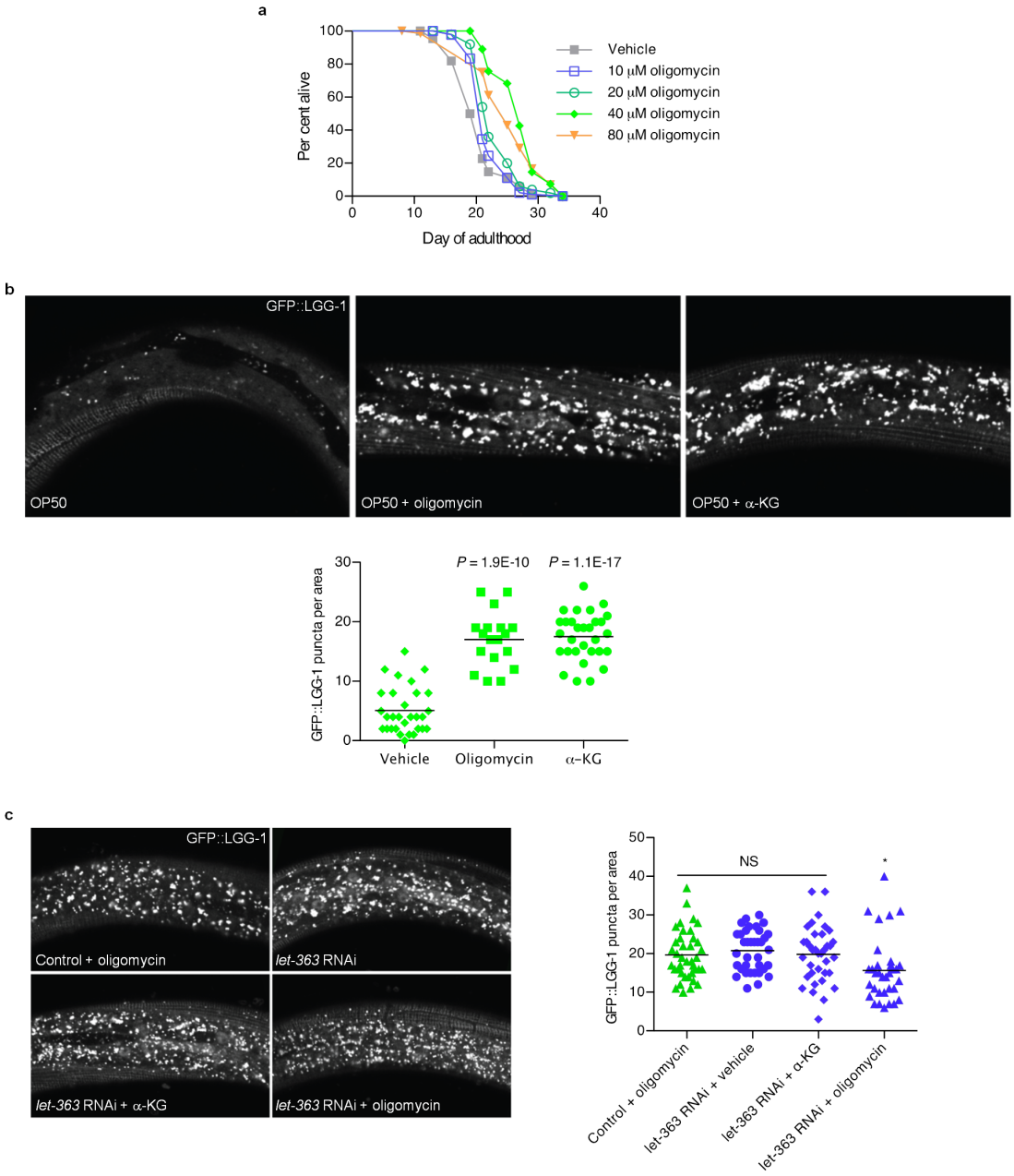

Extended Data Figure 3 | Treatment with oligomycin extends *C. elegans* lifespan and enhances autophagy in a manner dependent on *let-363*. **a**, Oligomycin extends the lifespan of adult *C. elegans* in a concentration-dependent manner. Treatment with oligomycin began at the young adult stage. 40 μM oligomycin increased the mean lifespan of N2 worms by 32.3% ($P < 0.0001$, by log-rank test); see Extended Data Table 2 for details. **b**, Confocal images of GFP::LGG-1 puncta in L3 epidermis of *C. elegans* with vehicle, oligomycin (40 μM) or α-KG (8 mM), and number of GFP::LGG-1-containing puncta quantified using ImageJ. Bars indicate the mean. Autophagy in *C. elegans* treated with oligomycin or α-KG is significantly higher than in vehicle-treated control animals (*t*-test, two-tailed, two-sample unequal variance). **c**, There is no significant difference (NS) between control worms treated with oligomycin and *let-363* RNAi worms treated with vehicle, nor between vehicle- and α-KG-treated *let-363* RNAi worms, consistent with independent experiments in Fig. 4b, c; also, oligomycin does not augment autophagy in *let-363* RNAi worms (if anything, there may be a small decrease, as indicated by an asterisk); by *t*-test, two-tailed, two-sample unequal variance. Bars indicate the mean. Photographs were taken at ×100 magnification.

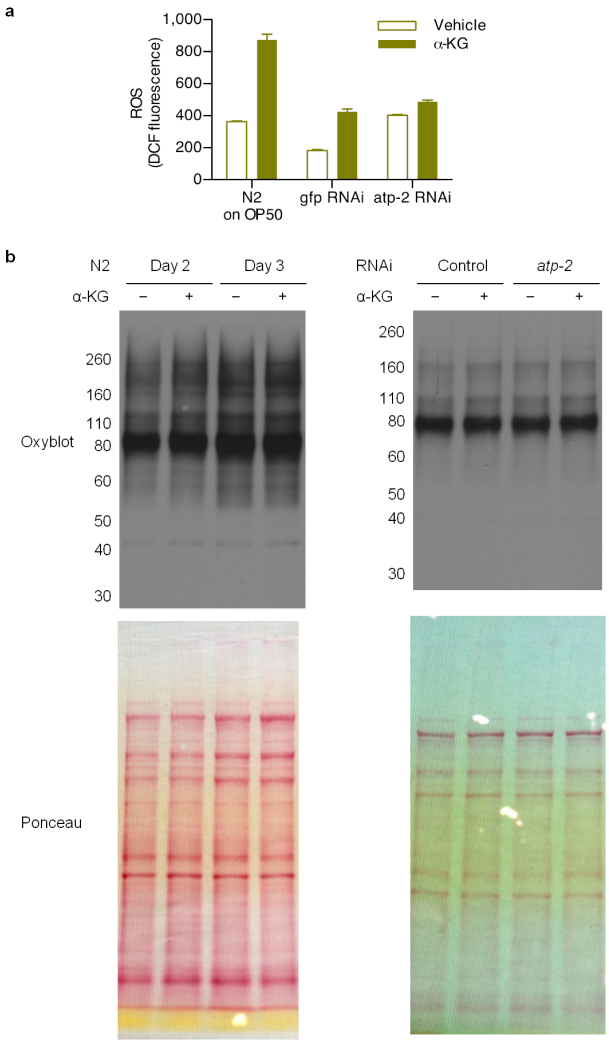

Extended Data Figure 4 | Analyses of oxidative stress in worms treated with α-KG or *atp-2* RNAi. a, The *atp*-2 RNAi worms have higher levels of 2′,7′-dichlorofluorescein (DCF) fluorescence than *gfp* control worms ($P < 0.0001$, by *t*-test, two-tailed, two-sample unequal variance). Supplementation with α-KG also leads to higher DCF fluorescence, in both HT115- (for RNAi) and OP50-fed worms ($P = 0.0007$ and $P = 0.0012$, respectively). Reactive oxygen species (ROS) levels were measured using 2′, 7′-dichlorodihydrofluorescein diacetate (H_2DCF-DA). As whole worm lysates were used, total cellular oxidative stress was measured here. H_2DCF-DA (Molecular Probes, D399) was dissolved in ethanol to a stock concentration of 1.5 mg ml^{-1}. Fresh stock was prepared every time before use. For measuring ROS in worm lysates, a working concentration of H_2DCF-DA at 30 ng ml^{-1} was hydrolysed by 0.1 M NaOH at room temperature for 30 min to generate 2′,7′-dichlorodihydrofluorescein (DCFH) before mixing with whole worm lysates in a black 96-well plate (Greiner Bio-One). Oxidation of DCFH by ROS yields the highly fluorescent DCF. DCF fluorescence was read at excitation/emission of 485/530 nm using SpectraMax MS (Molecular Devices). H_2O_2 was used as positive control (data not shown). To prepare the worm lysates, synchronized young adult animals were cultivated on plates containing vehicle or 8 mM α-KG and OP50 or HT115 *E. coli* for 1 day, and then collected and lysed as described in Methods. Mean ± s.d. is plotted. **b**, There was no significant change in protein oxidation upon α-KG treatment or *atp-2* RNAi. Oxidized protein levels were determined by OxyBlot. Synchronized young adult N2 animals were placed onto plates containing vehicle or 8 mM α-KG, and seeded with OP50 or HT115 bacteria that expressed control or *atp-2* dsRNA. Adult day 2 and day 3 worms were collected and washed four times with M9 buffer, and then stored at −80 °C for at least 24 h. Laemmli buffer (Biorad, 161-0737) was added to every sample and animals were lysed by alternate boil/freeze cycles. Lysed animals were centrifuged at 14,000 r.p.m. for 10 min at 4 °C to pellet worm debris, and supernatant was collected for OxyBlot analysis. Protein concentration of samples was determined by the 660 nm Protein Assay (Thermo Scientific, 1861426) and normalized for all samples. Carbonylation of proteins in each sample was detected using the OxyBlot Protein Oxidation Detection Kit (Millipore, S7150).

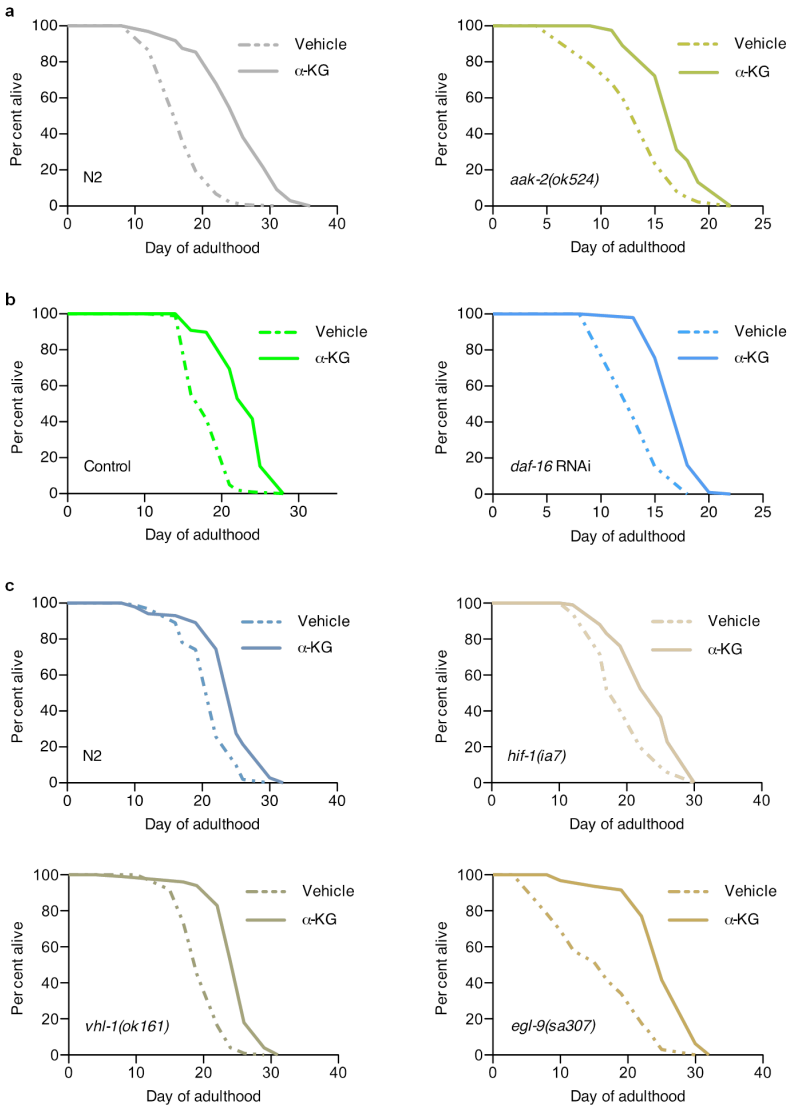

Extended Data Figure 5 | Lifespan extension by α-KG in the absence of *aak-2, daf-16, hif-1, vhl-1* or *egl-9*. **a**, Lifespans of α-KG-supplemented N2 worms, $m_{veh} = 17.5$ ($n = 119$), $m_{\alpha\text{-KG}} = 25.4$ ($n = 97$), $P < 0.0001$; or *aak-2(ok524)* mutants, $m_{veh} = 13.7$ ($n = 85$), $m_{\alpha\text{-KG}} = 17.1$ ($n = 83$), $P < 0.0001$. **b**, N2 worms fed *gfp* RNAi control, $m_{veh} = 18.5$ ($n = 101$), $m_{\alpha\text{-KG}} = 23.1$ ($n = 98$), $P < 0.0001$; or *daf-16* RNAi, $m_{veh} = 14.3$ ($n = 99$), $m_{\alpha\text{-KG}} = 17.6$ ($n = 99$), $P < 0.0001$. **c**, N2 worms, $m_{veh} = 21.5$ ($n = 101$), $m_{\alpha\text{-KG}} = 24.6$ ($n = 102$), $P < 0.0001$; *hif-1(ia7)* mutants, $m_{veh} = 19.6$ ($n = 102$), $m_{\alpha\text{-KG}} = 23.6$ ($n = 101$), $P < 0.0001$; *vhl-1(ok161)* mutants, $m_{veh} = 20.0$ ($n = 98$), $m_{\alpha\text{-KG}} = 24.9$ ($n = 100$), $P < 0.0001$; or *egl-9(sa307)* mutants, $m_{veh} = 16.2$ ($n = 97$), $m_{\alpha\text{-KG}} = 25.6$ ($n = 96$), $P < 0.0001$. *P* values were determined by the log-rank test. Number of independent experiments: N2 (8), *hif-1* (5), *vhl-1* (1) and *egl-9* (2); see Extended Data Table 2 for details. Two different *hif-1* mutant alleles[27] have been used: *ia4* (shown in Fig. 3g) is a deletion over several introns and exons; *ia7* (shown here) is an early stop codon, causing a truncated protein. Both alleles have the same effect on lifespan[27]. We tested both alleles for α-KG longevity and obtained the same results.

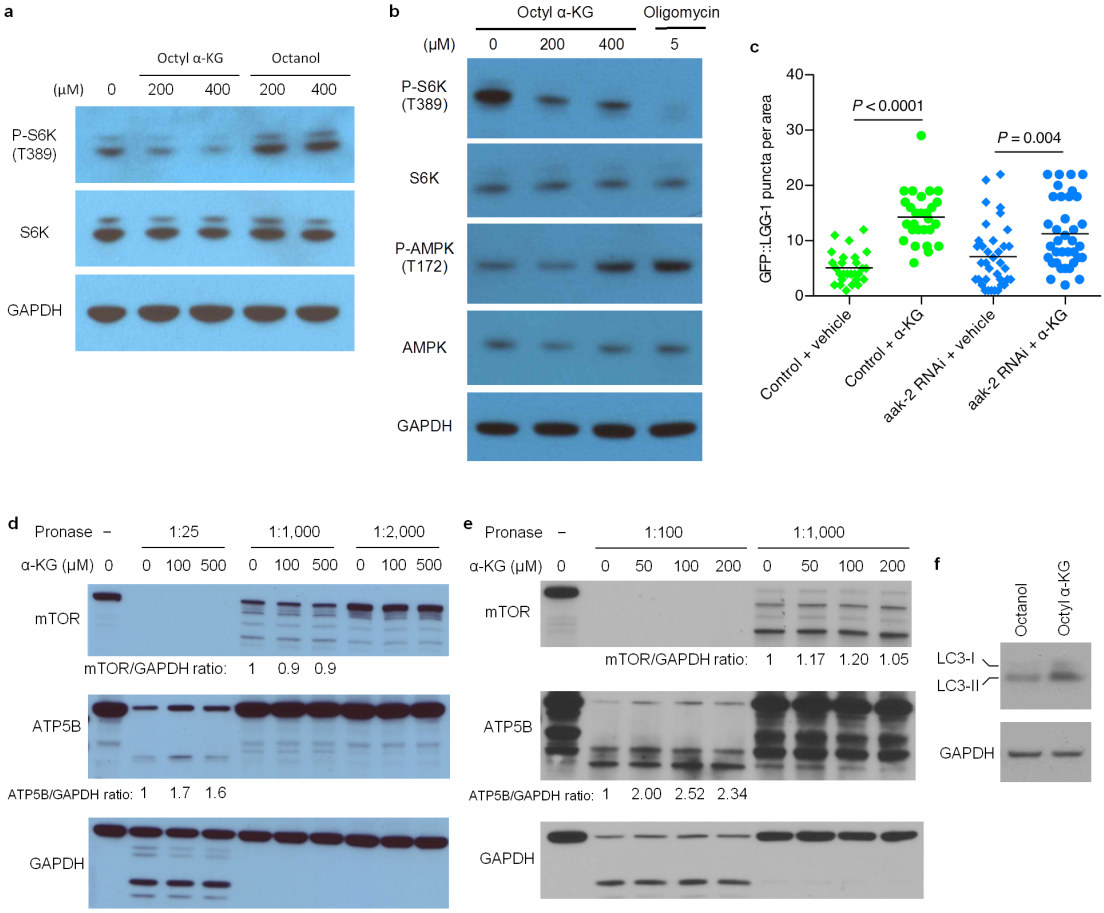

Extended Data Figure 6 | α-KG decreases TOR pathway activity but does not directly interact with TOR. **a**, Phosphorylation of S6K (T389) was decreased in U87 cells treated with octyl α-KG, but not in cells treated with octanol control. The same results were obtained using HEK-293 and MEF cells. **b**, Phosphorylation of AMPK(T172) is upregulated in WI-38 cells upon complex V inhibition by α-KG, consistent with decreased ATP content in α-KG-treated cells and animals. However, this activation of AMPK appears to require more severe complex V inhibition than the inactivation of mammalian TOR, as either oligomycin or a higher concentration of octyl α-KG was required for increasing phospho (P)-AMPK whereas concentrations of octyl α-KG comparable to those that decreased cellular ATP content (Fig. 2d) or oxygen consumption (Fig. 2f) were also sufficient for decreasing P-S6K. The same results were obtained using U87 cells. Samples were subjected to SDS–PAGE on 4–12% Bis-Tris gradient gel (Invitrogen, NP0322BOX) and western blotted with specific antibodies against P-AMPK T172 (Cell Signaling, 2535S) and AMPK (Cell Signaling, 2603S). **c**, α-KG still induces autophagy in *aak-2* RNAi worms; $^{**}P < 0.01$ (*t*-test, two-tailed, two-sample unequal variance). The number of GFP::LGG-1 containing puncta was quantified using ImageJ. Bars indicate the mean. **d**, **e**, α-KG does not bind to TOR directly as determined by DARTS. HEK-293 (**d**) or HeLa (**e**) cells were lysed in M-PER buffer (Thermo Scientific, 78501) with the addition of protease inhibitors (Roche, 11836153001) and phosphatase inhibitors (50 mM NaF, 10 mM β-glycerophosphate, 5 mM sodium pyrophosphate, 2 mM Na_3VO_4). Protein concentration of the lysate was measured by BCA Protein Assay kit (Pierce, 23227). Chilled TNC buffer (50 mM Tris-HCl pH 8.0, 50 mM NaCl, 10 mM $CaCl_2$) was added to the protein lysate, and the protein lysate was then incubated with vehicle control (DMSO) or varying concentrations of α-KG for 1 h (**d**) or 3 h (**e**) at room temperature. Pronase (Roche, 10165921001) digestions were performed for 20 min at room temperature, and stopped by adding SDS loading buffer and immediately heating at 95 °C for 5 min (**d**) or 70 °C for 10 min (**e**). Samples were subjected to SDS–PAGE on 4–12% Bis-Tris gradient gel (Invitrogen, NP0322BOX) and western blotted with specific antibodies against ATP5B (Santa Cruz, sc58618), mammalian TOR (Cell Signaling, 2972) or GAPDH (Ambion, AM4300). ImageJ was used to quantify the mammalian TOR/GAPDH and ATP5B/GAPDH ratios. Susceptibility of the mammalian TOR protein to Pronase digestion is unchanged in the presence of α-KG, whereas, as expected, Pronase resistance in the presence of α-KG is increased for ATP5B, which we identified as a new binding target of α-KG. **f**, Increased autophagy in HEK-293 cells treated with octyl α-KG was confirmed by western blot analysis of MAP1 LC3 (Novus, NB100-2220), consistent with decreased phosphorylation of the autophagy-initiating kinase ULK1 (Fig. 4a).

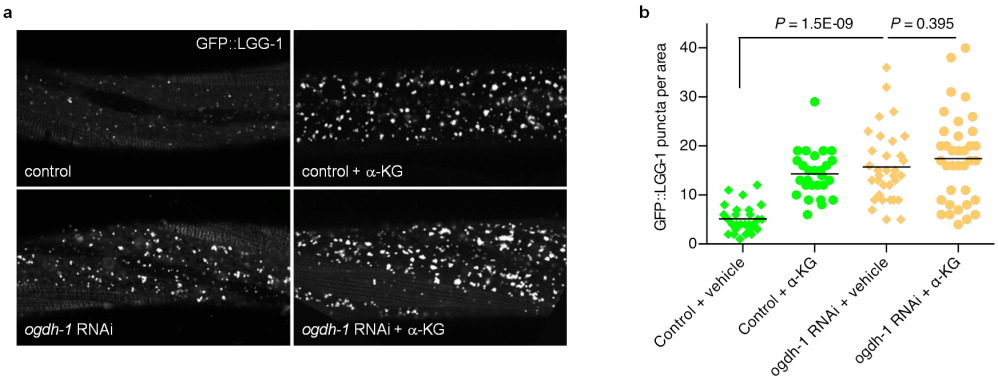

Extended Data Figure 7 | Autophagy is enhanced in *C. elegans* treated with *ogdh-1* RNAi. **a**, Confocal images of GFP::LGG-1 puncta in the epidermis of mid-L3 stage, control or *ogdh-1* knockdown *C. elegans* treated with vehicle or α-KG (8 mM). **b**, Number of GFP::LGG-1 puncta quantified using ImageJ. Bars indicate the mean. *ogdh-1* RNAi worms have significantly higher autophagy levels, and α-KG does not significantly augment autophagy in *ogdh-1* RNAi worms (*t*-test, two-tailed, two-sample unequal variance). Photographs were taken at ×100 magnification.

Extended Data Table 1 | Enriched proteins in the α-KG DARTS sample

Protein Symbol	Protein Name	Score	Control sample		α-KG sample		Enrichment
			Spectra	Peptides	Spectra	Peptides	
ATP5B	ATP synthase subunit beta	4088	23	9	121	15	5.3
HSPD1	60 kDa heat shock protein	2352	31	11	138	29	4.5
PKM2	Pyruvate kinase isozymes M1/M2	2203			56	7	
LCP1	Plastin-2	1865	14	8	76	13	5.4
ATP5A1	ATP synthase subunit alpha	1616	41	9	61	12	1.5
SHMT2	Serine hydroxymethyltransferase	1060	7	5	33	10	4.7
HSP90AA1	Heat shock protein HSP 90-alpha	952	29	8	44	8	1.5
EEF2	Elongation factor 2	943	4	2	37	9	9.3
DDX5	Probable ATP-dependent RNA helicase DDX5	652	7	3	33	10	4.7
HSPA8	Heat shock cognate 71 kDa protein	615	4	2	35	10	8.8

Only showing those proteins with at least 15 spectra in α-KG sample and enriched at least 1.5 fold.

Extended Data Table 2 | Summary of lifespan data

Strain	*m* (mean lifespan, days)		% difference	*P*-value	*n* (number of animals)	
	Vehicle	α-KG			Vehicle	α-KG
N2	18.9	25.8	36.3	< 0.0001	87	96
N2	17.5	25.4	45.6	< 0.0001	119	97
N2	16.3	26.1	60.2	< 0.0001	100	104
eat-2(ad1116)	22.8	22.9	0.5	0.79	59	40
daf-16(mu86)	16.3	18.8	15.1	< 0.0001	106	105
eat-2(ad1116)	21.1	24.0	13.4	0.23	39	59
daf-2(e1370)	38.0	47.6	25.1	< 0.0001	72	69
N2	13.2	22.3	69.8	< 0.0001	100	104
daf-16(mu86)	13.4	17.4	29.5	< 0.0001	71	72
daf-16 RNAi	14.3	17.6	22.9	< 0.0001	99	99
N2	16.1	19.1	19.3	0.0003	97	96
daf-2(e1370)	38.3	43.9	14.6	< 0.0001	109	101
aak-2(ok524)	13.7	17.1	24.3	< 0.0001	85	83
aak-2(ok524)	16.4	17.5	6.7	< 0.0001	97	97
aak-2 RNAi	16.2	19.9	23.3	< 0.0001	93	92
N2	15.6	26.3	68.8	< 0.0001	95	102
N2	15.6	26.3	68.5	< 0.0001	95	102
egl-9(sa307)	16.2	25.6	58.6	< 0.0001	97	96
egl-9(sa307)	19.5	27.3	40.3	< 0.0001	95	101
N2	14.7	21.6	46.9	< 0.0001	100	88
N2	14.0	20.7	47.9	< 0.0001	112	114
N2	21.5	24.6	14.6	< 0.0001	101	102
hif-1(ia4)	20.5	26.0	26.5	< 0.0001	85	71
hif-1(ia7)	19.6	23.6	20.4	< 0.0001	102	101
hif-1(ia4)	21.5	24.7	14.7	< 0.0001	88	87
N2	16.7	23.4	39.7	< 0.0001	104	103
N2	15.8	22.2	40.5	< 0.0001	104	94
N2	18.4	24.6	33.4	< 0.0001	99	89
vhl-1(ok161)	20.0	25.0	24.9	< 0.0001	98	100
hif-1(ia7)	12.4	17.3	38.9	< 0.0001	97	90
hif-1(ia7)	17.9	23.7	32.0	< 0.0001	58	55
N2	16.8	22.4	32.7	< 0.0001	104	101
N2	15.7	21.6	37.6	< 0.0001	85	99
smg-1(cc546ts)	18.4	23.8	29.5	< 0.0001	110	87
smg-1(cc546ts);pha-4(zu225)	14.2	13.5	-4.9	0.5482	94	109
smg-1(cc546ts);pha-4(zu225)	17.6	15.2	-14.0	0.0877	28	34
N2	13.6	20.7	51.8	< 0.0001	103	104
smg-1(cc546ts)	16.2	23.0	42.2	< 0.0001	114	121
smg-1(cc546ts);pha-4(zu225)	13.8	15.2	10.2	0.254	45	45
EV RNAi control	18.6	23.4	26.1	< 0.0001	94	91
atp-2 RNAi	22.8	22.5	-1.3	0.3471	97	94
EV RNAi control	18.8	22.7	20.6	< 0.0001	97	94
gfp RNAi control	18.5	23.1	25.3	< 0.0001	101	98
ogdh-1 RNAi	21.2	21.1	-0.7	0.65	98	100
let-363 RNAi	22.1	23.6	6.8	0.02	94	95
gfp RNAi control	20.2	27.7	37.4	< 0.0001	99	81
let-363 RNAi	25.1	25.7	2.1	0.9511	96	74
EV RNAi control	22.8	27.2	21.6	<0.0001	70	72
let-363 RNAi	27.4	27.2	-0.8	0.7239	64	80
EV RNAi control	19.7	24.3	23.8	< 0.0001	93	84
atp-2 RNAi	25.3	23.4	-7.4	< 0.0001	87	63

Strain	*m*		% difference	*P*-value	*n*		[Oligomycin]
	Vehicle	Oligomycin			Vehicle	Oligomycin	
N2	20.4	25.5	25.2	< 0.0001	88	72	80 μM
N2		27.0	32.3	< 0.0001		82	40 μM
N2		23.1	13.2	0.0005		50	20 μM
N2		22.0	7.9	0.0106		90	10 μM

Strain	*m*		% difference	*P*-value	*n*		Treatment
	Vehicle	Treatment			Vehicle	Treatment	
N2	14.5	16.9	16.8	0.0005	73	71	Octyl α-KG (500 μM)
N2	14.5	17.0	16.8	< 0.0001	73	60	α-KG
N2	14.0	18.8	33.9	< 0.0001	112	114	Dimethyl α-KG
N2	14.0	20.7	47.8	< 0.0001	112	114	α-KG
N2	15.7	21.6	37.6	< 0.0001	85	99	Disodium α-KG

Strain	*m*		% difference	*P*-value	*n*		Food source
	Vehicle	α-KG			Vehicle	α-KG	
N2	17.4	21.2	21.6	0.0001	108	55	Live OP50
N2	19.0	23.0	21.0	0.0003	88	46	Dead OP50 (γ-irradiated)

SUPPLEMENTARY NOTES

α-KG dehydrogenase knockdown. Similar to α-KG supplemented animals, animals with RNAi knockdown of α-KGDH (encoded by *ogdh-1*) also have increased endogenous levels of α-KG (Extended Data Fig. 1b). These animals are also long-lived (Fig. 1f). While it is possible that *ogdh-1* knockdown extends lifespan by affecting other unknown pathways, the simplest interpretation is that the increase in endogenous α-KG levels in these animals is sufficient for long life. Consistent with this model, lifespan of *ogdh-1* RNAi animals is not increased by α-KG supplementation. The *ogdh-1* RNAi worms also have higher level of autophagy with larger number of GFP::LGG-1 puncta compared to empty vector control, which cannot be augmented by addition of α-KG (Extended Data Fig. 7). While the results together strongly support the idea that the effect of α-KG in longevity is largely direct and worm autonomous, an important caveat is that *ogdh-1* knockdown may not necessarily give all the same effects as exogenous α-KG supplementation. For example, we found that whereas α-KG supplemented worms have normal brood size (Extended Data Fig. 1h) *ogdh-1* knockdown animals are sterile.

$$\alpha\text{-KG} + NAD^+ + CoA \rightarrow \text{Succinyl CoA} + CO_2 + NADH$$

Since α-KGDH catalyzes the above reaction in the TCA cycle, loss of α-KGDH activity would not only lead to α-KG accumulation but also diminish succinyl CoA and perturb NAD^+/NADH, as well as halt the TCA cycle. Defective α-KGDH function has been associated with severe neurological dysfunction[1].

Physiological regulation of α-KG levels. Although the concentration of α-KG was considered to be constant in the TCA cycle, we have found that one can in fact increase α-KG concentration in *C. elegans* either by supplementation or by knocking down the α-KGDH enzyme (Extended Data Fig. 1b). An increase in α-KG levels has also been observed in human HEK293 cells treated with α-keto-β-methyl-n-valeric acid, an inhibitor of α-KGDH[2]. Moreover, it has been documented that α-KG levels are subject to change under physiological conditions. For example, α-KG accumulates in starved bacteria and yeast cells[3]; in *E. coli* α-KG accumulates rapidly by up to 10-fold in response to nitrogen starvation[4-6] and in cyanobacteria α-KG is a signal of nitrogen status[7,8]. In metazoans the issue is harder to address, due to the enormous complexity involving multitudes of cell types, organs, and tissues. But there also appear to be regulations of α-KG levels in response to feeding and starvation. For instance, starved pigeons have ~50% higher α-KG in the liver[9]. Recently, it has emerged that physical exercise can also increase α-KG levels. For example, after acute exercise urine α-KG concentrations increased by 27% (ref. [10]) and serum α-KG concentrations increased by

over 50% (ref. [11]). We found that α-KG levels are elevated in starved *C. elegans* (Fig. 4d).

The biochemical basis for this increase in α-KG upon starvation may be explained; in gluconeogenesis, an increased rate of deamination of amino acids (to provide carbon) by the glutamate-linked transaminases in the liver will lead to an increased formation of α-KG. Consistently, caloric restriction has been shown to increase gluconeogenic and transaminase enzyme activities in mouse liver[12]. Dynamic regulations of α-KG occur in physiological scenarios and represent an exciting avenue for future studies.

Evolutionary conservation of the ATP synthase. ATP synthase (Complex V) is highly conserved throughout evolution, although the *C. elegans* mitochondrial genome lacks the ATP8 gene[13]. The sequence of ATP8 differs among animals, plants, and fungi. Functionally, the ATP8 subunit is not well studied and does not appear to be important for Complex V biology. α-KG binds to the highly conserved ATP-2 subunit, and elicits its effects (both biochemically and phenotypically) through ATP-2.

Comparison of ATP-2 inhibition by α-KG and by genetic means. Overall, α-KG appears to inhibit ATP-2 more mildly than either the knockdown of *atp-2* by RNAi or null alleles. For example, *atp-2* RNAi animals arrest development as larvae, as do *atp-2* null mutants[14,15]. In contrast, larvae treated with α-KG do not arrest. Further, null mutations in *atp-2* are associated with very slow pharyngeal pumping[15], whereas α-KG treatment is not (Extended Data Fig. 1g). On the other hand, α-KG treatment resembles RNAi of *atp-2* on most levels, including a decrease in ATP content (Fig. 2e, and data not shown), reduction of oxygen consumption (Fig. 2g and Extended Data Fig. 2c), induction of autophagy (Fig. 4b-c), increase in ROS (Extended Data Fig. 4), and extension of lifespan (Fig. 3a). Although α-KG supplementation and *atp-2* RNAi are associated with many similar phenotypes, the differences noted above likely reflect variable thresholds for responses to decreased ATP synthase activity in specific cells, biological processes, or developmental events. In fact, work by Tsang and Lemire postulated that low ATP-2 levels are sufficient to support many basic cellular and organismal processes, whereas higher levels of ATP-2 are required for energy-intensive processes such as development and reproduction[15]. The longevity benefit derived from mild inhibition of ATP-2 by α-KG offers hope for the future development of anti-aging therapies that are safe and effective.

Mode of inhibition of ATP synthase by α-KG. α-KG acts as an uncompetitive inhibitor of ATP synthase, decreasing both the effective V_{max} and K_m of the enzyme (Fig. 2i). As expected of an uncompetitive mechanism, inhibition of ATP synthase by α-KG works better at higher substrate concentrations. This mechanism may serve to

safeguard that ATP production would not be inhibited inappropriately. An uncompetitive inhibitory mechanism means that the inhibitor binds to the enzyme-substrate complex, but not to the free enzyme, resulting in an inactive enzyme-substrate-inhibitor complex. Thus, α-KG binds only after ATP synthase has formed a complex with its substrate; that is, the binding site of α-KG is created after, but away from, substrate binding. Consistently, using DARTS, we have mapped the binding site of α-KG in ATP synthase by mass spectrometry identification of protected peptides. The single most highly protected peptide, indicative of the putative α-KG binding site, is a 24-amino acid sequence corresponding to residues 433-456 of ATP5B. The peptide count for this region was 33 in α-KG treated samples, but undetectable in vehicle treated samples. This site is distinct from the Walker A motif for substrate (nucleotide) binding[16], or the Walker B motif important for Mg^{2+} binding and catalysis[16,17]. However, the site is exceptionally well conserved. For example, a comparison of human, bovine, and *C. elegans* orthologues shows that this region is 100% identical among the mitochondrial enzymes, and nearly identical to the sequences in Arabidopsis chloroplasts and *E. coli* (the latter having 4 non-identical, but similar, residues). Therefore, α-KG binding could be an important property of ATP5B that has evolved to regulate energy homeostasis by this endogenous metabolite. A precise understanding of the detailed mechanism of α-KG inhibition of ATP synthase will only be obtained when structural information is available.

Would known chemical inhibitors of the ETC have the similar lifespan extending effect as α-KG? Among the known chemical inhibitors of the ETC, only antimycin A[18], an inhibitor of Complex III, and oxaloacetate[19], which is a potent inhibitor of Complex II, have been reported in the context of lifespan studies; both were shown to extend *C. elegans* lifespan. A well-known, potent inhibitor of Complex V (ATP synthase) is oligomycin, which binds to the F_O subunit and blocks proton transport. Like α-KG, oligomycin also extends the lifespan of adult *C. elegans* (Extended Data Fig. 3a).

Involvement of *daf-16*/FOXO and *aak-2*/AMPK in α-KG longevity. Genetically, *daf-16*/FOXO (Fig. 3e, and Extended Data Fig. 5b) and *aak-2*/AMPK (Extended Data Fig. 5a) are not essential for lifespan extension by α-KG. However, in *aak-2* and *daf-1*6 mutant worms the longevity effect of α-KG appears to be smaller than in N2 (Extended Data Fig. 5a, and Fig. 3e), suggesting that AMPK and FOXO partially contribute to the longevity conferred by α-KG.

This is in contrast to oxaloacetate, which was found to require *aak-2*/AMPK and *daf-16*/FOXO for its longevity effect[19], suggesting that the mechanisms behind the lifespan extension by the two TCA cycle intermediates are distinct. Our finding is consistent with

the fact that the loss of function of *aak-2* suppresses the lifespan of the long-lived *daf-2* mutant[20], since α-KG also increases longevity of *daf-2* worms (Fig. 3b).

aak-2 encodes the catalytic (α) subunit of AMP-activated protein kinase (AMPK), the cellular sensor of low energy levels[21]. AMPK and TOR are two major regulators of cellular energy homeostasis. AMPK is activated by increased AMP:ATP ratios, e.g., in glucose deprivation and other metabolic stresses[21], whereas TOR is inactivated upon amino acid limitation and other nutrient stresses[22,23] and by decreased ATP (ref. [24]). There is also emerging evidence for complex crosstalk between the two pathways[25-28] and with FOXO and SIRT1 (refs. [29,30]).

Activation of AMPK leads to enhanced energy production, decreased energy expenditure, and redirection of cellular proper (e.g., through the induction of autophagy). However, the requirements for AMPK vary under different starvation stresses. For example, in mammalian cells AMPK is required for autophagy induction under glucose starvation but not amino acid starvation[31]. In *C. elegans*, AMPK/*aak-2* has been shown to mediate dietary restriction in *C. elegans* fed diluted bacteria but not dietary restriction in the *eat-2* model[20,29,32,33].

Consistent with decreased ATP content in α-KG treated cells and animals, P-AMPK is upregulated upon Complex V inhibition by α-KG (Extended Data Fig. 6b). However, this activation of AMPK appears to require more severe Complex V inhibition than the inactivation of mTORC1, as either oligomycin or 400 μM of octyl α-KG was required for increased P-AMPK whereas 200 μM of octyl α-KG was sufficient for decreased P-S6K (Extended Data Fig. 6b). Interestingly, P-Akt was also only mildly decreased by octyl α-KG treatment but was strongly diminished by oligomycin treatment (Fig. 4a). These differential effects by α-KG may explain why *aak-2*/AMPK is not essential for α-KG to extend lifespan even though the extent of life extension by α-KG may be smaller in the mutants. Consistent with the lifespan effects, we also found that α-KG treatment induced the formation of additional GFP::LGG-1 puncta in *aak-2* RNAi worms (***P* < 0.01) (Extended Data Fig. 6c).

What is the role of reactive oxygen species (ROS) in lifespan extension by α-KG?
The relationship between ROS and lifespan regulation is not well understood. Increased levels of ROS are thought to activate stress responses that protect the organism and ultimately enhance longevity. However, ROS *per se* does not correlate with lifespan. For example, increased ROS is found in both short-lived (e.g., *mev-1*, *gas-1*, and *sdhb-1*)[34] and long-lived (e.g., *sod-2*) mutants. The ROS levels in ATP synthase mutants or knockdowns are not well characterized. However, It has been reported that *atp-3* RNAi animals show a very slight, if any, increase in the level of protein oxidization levels

(which occurs as a result of damage from ROS) as assessed by Oxyblot[35]. We also observed a slight increase in the abundance of oxidized proteins in animals treated with α-KG by Oxyblot (Extended Data Fig. 4b). Likewise, when ROS levels were measured by DCF fluorescence, both α-KG treated and *atp-2* RNAi adults exhibited increased ROS levels (Extended Data Fig. 4a). Together, our data suggest that ROS levels are increased in both α-KG treated and *atp-2* RNAi animals, further substantiating the model that α-KG inhibits ATP-2 *in vivo*. However, we consider this increase in ROS levels unlikely to play a major role in the lifespan extension conferred by α-KG for the following reasons.

First, as described above, increased ROS does not necessarily dictate a longer lifespan. Second, it has previously been shown that supplementation of long-lived *eat-2* mutant animals with the prooxidant paraquat further extends their lifespan[36], whereas α-KG does not further extend the lifespan of *eat-2* mutants (Fig. 3c). Third, ROS has been shown to activate the TOR pathway[37,38], whereas α-KG has the opposite effect—inhibiting TOR and activating autophagy (Fig. 4b-c). Lastly, it has been postulated that the increased ROS in mitochondrial ETC mutants promotes longevity by increasing the activity of hypoxia-inducible factor 1 (HIF-1)[39], whereas α-KG longevity does not require HIF-1 (Fig. 3g, and Extended Data Fig. 5c).

References

1 Tretter, L. & Adam-Vizi, V. Alpha-ketoglutarate dehydrogenase: a target and generator of oxidative stress. *Philos Trans R Soc Lond B Biol Sci* 360, 2335-2345 (2005).

2 MacKenzie, E. D. *et al.* Cell-permeating alpha-ketoglutarate derivatives alleviate pseudohypoxia in succinate dehydrogenase-deficient cells. *Mol Cell Biol* 27, 3282-3289 (2007).

3 Brauer, M. J. *et al.* Conservation of the metabolomic response to starvation across two divergent microbes. *Proc Natl Acad Sci U S A* 103, 19302-19307 (2006).

4 Yuan, J. *et al.* Metabolomics-driven quantitative analysis of ammonia assimilation in E. coli. *Mol Syst Biol* 5, 302 (2009).

5 Radchenko, M. V., Thornton, J. & Merrick, M. Control of AmtB-GlnK complex formation by intracellular levels of ATP, ADP, and 2-oxoglutarate. *J Biol Chem* 285, 31037-31045 (2010).

6 Boogerd, F. C. *et al.* AmtB-mediated NH3 transport in prokaryotes must be active and as a consequence regulation of transport by GlnK is mandatory to limit futile cycling of NH4(+)/NH3. *FEBS Lett* 585, 23-28 (2011).

7 Muro-Pastor, M. I., Reyes, J. C. & Florencio, F. J. Cyanobacteria perceive nitrogen status by sensing intracellular 2-oxoglutarate levels. *J Biol Chem* 276, 38320-38328 (2001).
8 Forchhammer, K. Global carbon/nitrogen control by PII signal transduction in cyanobacteria: from signals to targets. *FEMS Microbiol Rev* 28, 319-333 (2004).
9 Kaminsky, Y. G., Kosenko, E. A. & Kondrashova, M. N. Metabolites of citric acid cycle, carbohydrate and phosphorus metabolism, and related reactions, redox and phosphorylating states of hepatic tissue, liver mitochondria and cytosol of the pigeon, under normal feeding and natural nocturnal fasting conditions. *Comp Biochem Physiol B* 73, 957-963 (1982).
10 Pechlivanis, A. *et al.* (1)H NMR-based metabonomic investigation of the effect of two different exercise sessions on the metabolic fingerprint of human urine. *J Proteome Res* 9, 6405-6416 (2010).
11 Brugnara, L. *et al.* Metabolomics approach for analyzing the effects of exercise in subjects with type 1 diabetes mellitus. *PLoS One* 7, e40600 (2012).
12 Hagopian, K., Ramsey, J. J. & Weindruch, R. Caloric restriction increases gluconeogenic and transaminase enzyme activities in mouse liver. *Exp Gerontol* 38, 267-278 (2003).
13 Okimoto, R., Macfarlane, J. L., Clary, D. O. & Wolstenholme, D. R. The mitochondrial genomes of two nematodes, Caenorhabditis elegans and Ascaris suum. *Genetics* 130, 471-498 (1992).
14 Curran, S. P. & Ruvkun, G. Lifespan regulation by evolutionarily conserved genes essential for viability. *PLoS Genet* 3, e56 (2007).
15 Tsang, W. Y., Sayles, L. C., Grad, L. I., Pilgrim, D. B. & Lemire, B. D. Mitochondrial respiratory chain deficiency in Caenorhabditis elegans results in developmental arrest and increased life span. *J Biol Chem* 276, 32240-32246 (2001).
16 Walker, J. E., Saraste, M., Runswick, M. J. & Gay, N. J. Distantly related sequences in the alpha- and beta-subunits of ATP synthase, myosin, kinases and other ATP-requiring enzymes and a common nucleotide binding fold. *EMBO J* 1, 945-951 (1982).
17 Abrahams, J. P., Leslie, A. G., Lutter, R. & Walker, J. E. Structure at 2.8 A resolution of F1-ATPase from bovine heart mitochondria. *Nature* 370, 621-628 (1994).
18 Dillin, A. *et al.* Rates of behavior and aging specified by mitochondrial function during development. *Science* 298, 2398-2401 (2002).
19 Williams, D. S., Cash, A., Hamadani, L. & Diemer, T. Oxaloacetate supplementation increases lifespan in Caenorhabditis elegans through an AMPK/FOXO-dependent pathway. *Aging Cell* 8, 765-768 (2009).

20 Apfeld, J., O'Connor, G., McDonagh, T., DiStefano, P. S. & Curtis, R. The AMP-activated protein kinase AAK-2 links energy levels and insulin-like signals to lifespan in C. elegans. *Genes Dev* 18, 3004-3009 (2004).
21 Hardie, D. G. AMP-activated/SNF1 protein kinases: conserved guardians of cellular energy. *Nat Rev Mol Cell Biol* 8, 774-785 (2007).
22 Wullschleger, S., Loewith, R. & Hall, M. N. TOR signaling in growth and metabolism. *Cell* 124, 471-484 (2006).
23 Laplante, M. & Sabatini, D. M. mTOR signaling in growth control and disease. *Cell* 149, 274-293 (2012).
24 Dennis, P. B. *et al.* Mammalian TOR: a homeostatic ATP sensor. *Science* 294, 1102-1105 (2001).
25 Kimura, N. *et al.* A possible linkage between AMP-activated protein kinase (AMPK) and mammalian target of rapamycin (mTOR) signalling pathway. *Genes Cells* 8, 65-79 (2003).
26 Gwinn, D. M. *et al.* AMPK phosphorylation of raptor mediates a metabolic checkpoint. *Mol Cell* 30, 214-226 (2008).
27 Shaw, R. J. LKB1 and AMP-activated protein kinase control of mTOR signalling and growth. *Acta Physiol (Oxf)* 196, 65-80 (2009).
28 Inoki, K., Kim, J. & Guan, K. L. AMPK and mTOR in cellular energy homeostasis and drug targets. *Annu Rev Pharmacol Toxicol* 52, 381-400 (2012).
29 Greer, E. L. *et al.* An AMPK-FOXO pathway mediates longevity induced by a novel method of dietary restriction in C. elegans. *Curr Biol* 17, 1646-1656 (2007).
30 Canto, C. *et al.* AMPK regulates energy expenditure by modulating NAD+ metabolism and SIRT1 activity. *Nature* 458, 1056-1060 (2009).
31 Kim, J., Kundu, M., Viollet, B. & Guan, K. L. AMPK and mTOR regulate autophagy through direct phosphorylation of Ulk1. *Nat Cell Biol* 13, 132-141 (2011).
32 Curtis, R., O'Connor, G. & DiStefano, P. S. Aging networks in Caenorhabditis elegans: AMP-activated protein kinase (aak-2) links multiple aging and metabolism pathways. *Aging Cell* 5, 119-126 (2006).
33 Greer, E. L. & Brunet, A. Different dietary restriction regimens extend lifespan by both independent and overlapping genetic pathways in C. elegans. *Aging Cell* 8, 113-127 (2009).
34 Van Raamsdonk, J. M. & Hekimi, S. Reactive Oxygen Species and Aging in Caenorhabditis elegans: Causal or Casual Relationship? *Antioxid Redox Signal* 13, 1911-1953 (2010).
35 Rea, S. L., Ventura, N. & Johnson, T. E. Relationship between mitochondrial electron transport chain dysfunction, development, and life extension in Caenorhabditis elegans. *PLoS Biol* 5, e259 (2007).

36 Yang, W. & Hekimi, S. A mitochondrial superoxide signal triggers increased longevity in Caenorhabditis elegans. *PLoS Biol* 8, e1000556 (2010).
37 Bae, G. U. *et al.* Hydrogen peroxide activates p70(S6k) signaling pathway. *J Biol Chem* 274, 32596-32602 (1999).
38 Radisavljevic, Z. M. & Gonzalez-Flecha, B. TOR kinase and Ran are downstream from PI3K/Akt in H2O2-induced mitosis. *J Cell Biochem* 91, 1293-1300 (2004).
39 Hwang, A. B. & Lee, S. J. Regulation of life span by mitochondrial respiration: the HIF-1 and ROS connection. *Aging (Albany NY)* 3, 304-310 (2011).

CHAPTER 3

The Relationship between Alpha-Ketoglutarate and the Mitochondrial Unfolded Protein Response, Autophagy, and other Aging-Regulatory Pathways

Abstract

Alpha-ketoglutarate (α-KG) is a tricarboxylic acid (TCA) cycle intermediate that extends the lifespan of *Caenorhabditis elegans* by directly binding to and inhibiting the ATP synthase. α-KG also inhibits the target of rapamycin (TOR) downstream, and cannot further extend the lifespan of dietary restricted (DR) animals or ATP synthase- or TOR-defective animals. Here, we examine the effect of α-KG on healthspan and stress resistance, as well as evaluate the relationship of α-KG mediated lifespan extension to the mitochondrial unfolded protein response (UPR^{mt}), autophagy, and germline signaling pathways. We find that α-KG increases oxidative stress resistance, but not heat stress resistance. Unlike genetic perturbations of the mitochondrial machinery, α-KG supplementation lengthens the healthspan of animals and does not induce the UPR^{mt}. α-KG further extends the lifespan of germline-deficient mutants, but does not extend the lifespan of autophagy-defective mutants.

Introduction

We have previously showed that *C. elegans* supplemented with α-KG live about 50% longer than untreated controls[1]. α-KG extends lifespan by inhibiting the ATP synthase and TOR[1]. In dietary restricted animals, α-KG treatment does not further extend lifespan[1], and α-KG

levels are increased under starvation[1,2]. Thus, the evidence points to α-KG being a key regulator of energy-producing and nutrient-sensing pathways in response to environmental cues. As α-KG binds to and inhibits the ATP synthase[1], it is informative to assess whether α-KG treatment causes the same phenotypes as genetic modulation of the mitochondrial electron transport chain (ETC).

Genetic modulation, either by mutation or RNA interference (RNAi), of components of the mitochondrial ETC leads to sickly phenotypes in *C. elegans*, including reduced swimming rate and movement speed[3,4]. Thus, genetic inhibition of the ETC increases lifespan but, with respect to locomotive vitality, decreases healthspan. The effect of mitochondrial ETC inhibitors, like α-KG, on the healthspan of animals is unclear.

It was thought that RNAi against ETC subunits had to occur in development in order to extend lifespan[3,5], and that treating with ETC RNAi during development alone was sufficient for lifespan extension[3]. However, some reported a longevity effect when ETC RNAi is introduced after the L4 stage[6]. For pharmacological inhibition of the ETC, such as with rotenone, oligomycin, or α-KG, treatment starting from the young adult or adult stages is sufficient for lifespan extension[1,7]. However, it is unknown whether α-KG treatment during development alone could extend lifespan.

According to evolutionary theories of aging, in particular the disposable soma theory[8], an increased somatic maintenance is conducive to a long lifespan. Consistently, many long-lived animals have an increased resistance to heat and/or oxidative stress[9-12]. However, not all long-lived animals exhibit an increased stress resistance. For example, *sod-2* mutants live longer, but have an increased sensitivity to oxidative stress[13]. With respect to mitochondrial inhibition, some long-lived mitochondrial mutants display resistance to oxidative stress[14,15], but others do not[16]. Rotenone increases oxidative stress resistance in *C. elegans*[17], but it has not been established whether α-KG would increase heat and/or oxidative stress resistance.

The UPR^{mt} is a mitochondrial stress response pathway that signals the nucleus to encode mitochondria-specific protein chaperones[18]. The UPR^{mt} is activated by RNAi or mutations in the ETC[19,20], apparently because of a stoichiometric imbalance in the ratio of mitochondrial to nuclear encoded proteins in the mitochondria[20]. The UPR^{mt} has been perpetrated as a key pathway responsible for the extended lifespan by mitochondrial inhibition[19,20]. However, a recent study, which uses a different gene to block UPR^{mt} induction, shows that the UPR^{mt} is not required for the longevity of *isp-1(qm150)* or *cco-1(RNAi)* animals[21]. Nonetheless, it is undefined whether α-KG, being an inhibitor of ATP synthase, would induce UPR^{mt}, and whether the UPR^{mt} is important for α-KG mediated longevity.

Autophagy is a catabolic mechanism that allows cells to degrade damaged proteins and organelles and recycle their building blocks for energy or the synthesis of new molecules. Autophagy is considered to be essential for the longevity of mitochondrial mutants/RNAi strains[22,23], although some disagree with this point[24]. We have shown that α-KG and oligomycin, like *atp-2* or *let-363*/TOR RNAi, induces autophagy in *C. elegans*[1], but it has not been determined whether autophagy is required for the lifespan extension by α-KG supplementation.

In this chapter, we present the relationship of α-KG induced longevity with UPR^{mt} and autophagy. We also show that α-KG increases healthspan and oxidative stress resistance.

Materials and Methods

Lifespan analysis. Lifespan assays were conducted as described in[1]. For lifespan experiments concerning α-KG treatment during development only, gravid worms were lysed by egg preparation (lysing ~100 gravid worms in 70 µl M9 buffer[25], 25 µl bleach (10% sodium hypochlorite solution), and 5 µl 10 N NaOH), and eggs were deposited onto α-KG plates without 5-fluoro-2'-deoxyuridine[26] (FUDR; Sigma, F0503) and allowed to develop at 20°C. About two days later, L4/young adult worms were picked onto vehicle plates with FUDR, and their lifespan

was compared to that of vehicle-treated worms. The *daf-2(e1370)* and *glp-1(e2141)* strains were obtained from the *Caenorhabditis* Genetics Center. The *hlh-30(tm1978)* strain was obtained from Professor Malene Hansen (Sanford-Burnham Medical Research Institute, La Jolla, California).

Healthspan analysis. To assess full body movement, worms were prodded with a platinum wire and those that exhibited full body movement (rather than just head movement, or no movement) were scored as having full body movement. To assess swimming speed, young adult worms were placed on vehicle or α-KG plates. At day 3 or day 12 of adulthood, ~25 live worms were picked and deposited into a well (from a 24 well plate) with 500 µl M9 buffer. The animals were then videotaped for 5 minutes using a Sony Handycam Video camera recorder (Sony HDR-PJ430V). To count body bends, the resulting videos were played back at 0.3x speed using VLC Media Player and body bends were counted. Statistical analysis was performed using Microsoft Excel (t-test, two-tailed, two-sample unequal variance).

Juglone resistance assay. The juglone resistance assay was performed as in [27] with some modifications. Synchronized, young adult wildtype N2 *C. elegans* were placed onto NGM/OP50 plates containing vehicle or α-KG (as described in "lifespan analysis"). On day 5 of their adulthood, the worms were picked onto plates containing 240 µM juglone (Sigma H47003). The survival of the worms was assessed at 40, 83, 124, 161, 195, and 256 minutes after initial exposure to juglone.

Thermotolerance assay. Thermotolerance was assessed as in [28] with some modifications. Survival at 30°C: the same procedure was used as in "lifespan analysis," except that the experiment was conducted at 30°C. Survival at 35.5°C: synchronized, young adult wildtype N2 *C. elegans* were placed onto NGM/OP50 plates containing vehicle or α-KG at 20°C. At day 4 of

adulthood, the worms were placed into a 35.5°C incubator, and survival was assessed every 2 hours.

Assessment of mitochondrial unfolded protein response. The *hsp-6* and *hsp-60* GFP-reporter strains (SJ4100 and SJ4058, respectively)[18] were obtained from the CGC. They contain a GFP reporter plasmid in which GFP is driven by the *hsp-6* or *hsp-60* promoter. *hsp-6p::gfp* encodes the first 10 amino acids of HSP-6 fused to GFP. *hsp-60p::gfp* encodes the first 7 amino acids of HSP-60 fused to GFP. SJ4058 and SJ4100 were used to assess the induction of the UPR^{mt}.

To obtain a synchronized population of worms, we performed an egg preparation of gravid adults (by lysing ~100 gravid worms in 70 µL M9 buffer[25], 25 µL bleach and 5 µL 10 N NaOH), and allowed the eggs to hatch overnight in M9 causing starvation induced L1 diapause. L1 larvae were deposited onto NGM treatment plates containing vehicle, 8 mM α-KG, or 40 µM oligomycin, and seeded with *E. coli* HT115(DE3) with either a control (empty) plasmid or a plasmid expressing dsRNAs targeting *atp-2*. When the majority of animals in a given sample first reached the mid L3 stage, multiple L3 larvae were mounted onto microscope slides and anesthetized with 1.6 mM levamisole (Sigma, 31742). Nematodes were observed using an Zeiss Axiovert 200M fluorescent microscope, and fluorescent images were captured at 10x magnification. In a separate experiment, SJ4058 or SJ4100 mid-L3 animals were collected and prepared for Western blotting as described[1]. Samples were then subjected to SDS-PAGE on NuPAGE Novex 4-12% Bis-Tris gradient gels (Invitrogen, NP0322BOX), and Western blotting was carried out with an antibody against GFP (Genscript, A01704-40) or tubulin (Abcam, ab6160).

Results

We previously showed that α-KG supplementation during both development and adulthood did not extend lifespan any better than supplementation in adulthood alone[1]. Since ETC RNAi during development alone was shown to be sufficient for lifespan extension[3], we tested whether α-KG would give a similar result. α-KG treatment during development alone had no effect on lifespan (Fig. 3.1). This is not due to an inability of α-KG to function in larvae, since we have shown that α-KG induces autophagy in larvae[1].

The extension of lifespan is most impressive when accompanied with an increase in healthspan. To determine whether α-KG delays the aging process, we measured the effect of α-KG on the age-related decline in body movement. α-KG retards the loss of full, coordinated whole-body movement and swimming speed with age (Fig. 3.2). Taken together, our data suggest that α-KG extends the healthspan of animals.

Since many long-lived animals have an increased resistance to stress[29], we determined whether α-KG increased resistance to heat or oxidative stress. α-KG increased the resistance of wildtype N2 animals to juglone, a redox-active quinone that can reduce O_2 to $O_2^{\bullet -}$ (superoxide anion) (Fig. 3.3a). On the other hand, α-KG did not increase the thermotolerance of wildtype animals when measured at 30°C or 35.5°C (Fig. 3.3b-c). This finding may be related to the fact that α-KG binds to multiple heat shock proteins/chaperones[1], but the significance of this binding is unknown at this time. Furthermore, the fact that α-KG does not increase thermotolerance suggests that the lifespan extension by α-KG does not involve heat shock proteins/chaperones. Consistently, *daf-2(e1370)* mutants, which extend lifespan in a manner different from that of α-KG[1], are thermotolerant (Fig. 3.3c), and the longevity of *daf-2(e1370)* animals is completely abolished by *hsf-1* (heat shock factor) RNAi[17]. On the other hand, the long-lifespan of *eat-2(ad1116)* animals (which is not additive with α-KG treatment[1]) was unaffected by *hsf-1* RNAi[17], and some reports show *eat-2(ad1116)* animals to be only modestly resistant to heat stress[30].

The relationship of α-KG mediated longevity to several key aging-regulatory pathways, namely, insulin/IGF-1 signaling, AMP-activated protein kinase, hypoxia sensing, TOR, DR, and

mitochondrial ETC, has been previously explored[1]. To evaluate the relationship of an additional key aging-regulatory pathway, we assessed the involvement of germline signaling in α-KG mediated longevity. In *C. elegans*, when the germline is ablated by a laser microbeam or with mutations that block germ-cell proliferation, animals live significantly longer[31,32]. We found that α-KG could further extend the lifespan of the long-lived *glp-1(e2141)* mutants (Fig. 3.4), which are sterile at the non-permissive temperature due to a block in germ-line proliferation[33]. Consistently, the longevity of *glp-1(e2141)* mutants is fully suppressed by the loss of *daf-16*[32], whereas α-KG can still extend lifespan in *daf-16* mutants[1].

Inhibition of the mitochondrial ETC, at least by RNAi, has been shown to upregulate the UPR^{mt}[18,19]. The UPR^{mt} is induced by a stoichiometric imbalance between nuclear and mitochondrial-encoded ETC proteins, and but its role in the lifespan extension by ETC RNAi is currently unsettled[19-21]. Since we provided evidence for the binding and inhibition of ATP synthase by α-KG[1], we asked whether α-KG would also induce the UPR^{mt}. Using a reporter strain for *hsp-6* or *hsp-60* expression[18], two mitochondrial associated protein chaperones that are specifically induced by the UPR^{mt}, we found that α-KG or oligomycin did not activate the UPR^{mt} (Fig. 3.5). In contrast, the UPR^{mt} is turned on in *atp-2(RNAi)* animals. Our results suggest that the lifespan extension by α-KG or oligomycin is probably not caused by the UPR^{mt}.

Inhibition of ATP synthase, either by α-KG, oligomycin, or RNAi, increased autophagy, as seen by the prevalence of GFP::LGG-1 puncta[1]. To investigate whether autophagy is necessary for the lifespan extension by α-KG, we used the *hlh-30(tm1978)* loss-of-function mutant strain. HLH-1 is a *C. elegans* orthologue of the basic helix-loop-helix (HLH) transcription factor EB (TFEB), a key transcriptional regulator of the autophagy process in mammals[34]. HLH-30 is a key transcription factor that regulates multiple genes with functions throughout the autophagy process, such as autophagosome formation, cargo degradation, fusion, and lysosomal degradation[22,35]. The knockdown of *hlh-1* suppressed the long lifespan of multiple longevity models, including DR, TOR inhibition, and reduced mitochondrial respiration[22]. We

found that α-KG could not extend the lifespan of *hlh-30(tm1978)* mutants (Fig. 3.6), suggesting that the induction of autophagy seen in α-KG treated animals may be important for their longevity.

Discussion

In this chapter, we showed that α-KG treatment does not extend lifespan when provided to worms during development only. With respect to lifespan extension, it is conceivable that small molecule inhibitors of the mitochondrial ETC have different timing requirements than ETC RNAi. In support of this, it was shown that treatment with rotenone (a complex I inhibitor) during adulthood alone extended lifespan, and interestingly, even treatment for just the first five days of adulthood prolonged lifespan to a similar extent as treatment throughout adulthood[7]. Furthermore, α-KG or oligomycin, both of which inhibit ATP synthase, extend lifespan when provided in adulthood alone[1].

We also showed that α-KG increases oxidative stress resistance, but not thermotolerance. At this moment, it is unknown whether the increased oxidative stress resistance of α-KG treated animals is important for their longevity. However, it has been shown that *skn-1*, a transcription factor that controls the response to oxidative stress, is not required for the longevity of *atp-3(RNAi)* animals (*atp-3* encodes for the ATP5O subunit of the mitochondrial ATP synthase)[5].

We observed that α-KG does not induce UPR^{mt}, whereas *atp-2* RNAi does. This is not surprising because α-KG is not expected to change the stoichiometric balance of mitochondrial– vs nuclear –encoded oxidative phosphorylation proteins. Consistently, α-KG does not reduce ATP-2 protein levels, whereas *atp-2* RNAi does (data not shown). Importantly, oligomycin, which is known to bind and inhibit ATP synthase, also does not induce UPR^{mt}. It is prudent to acknowledge that we only tested the concentrations of α-KG and oligomycin that were optimal

for prolonging lifespan, and that it is theoretically possible that lower or higher concentrations of these drugs would induce UPR^{mt}. Additionally, although our data suggest that the UPR^{mt} is not involved in the lifespan extension by α-KG, future studies to verify this point should test whether blocking known components of the UPR^{mt} (such as *atfs-1*[21]) would abolish the longevity effect of α-KG.

Finally, we provided evidence that the autophagy induction by α-KG is important for the longevity of α-KG treated animals. However, thus far, we have only worked with *hlh-30*, which encodes a transcription factor important for the upregulation of autophagy. Additional lifespan experiments, in which essential components of the autophagic process (e.g., *bec-1*[24]) are knocked down, should be carried out. As autophagy is induced by dietary restriction[24], our data further support a model in which α-KG is a key metabolite mediating lifespan extension by starvation/dietary restriction[1].

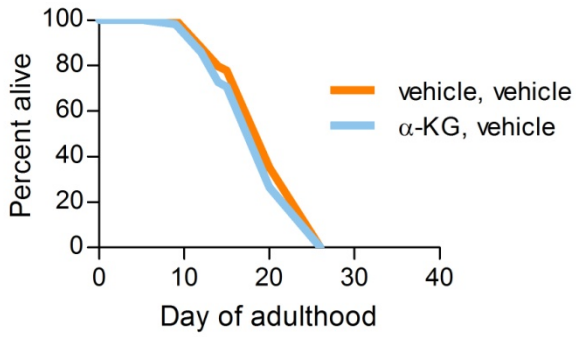

Figure 3.1. α-KG does not extend lifespan when administered to worms during development only. The lifespan of wildtype N2 *C. elegans* treated with α-KG during development only was compared with N2 treated with vehicle. m_{veh} = 20.6 (n = 108), $m_{\alpha\text{-KG}}$ = 19.5 (n = 106), P = 0.128 (log-rank test).

a

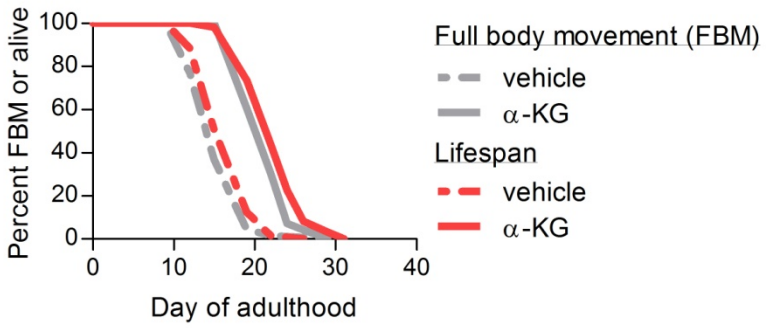

b

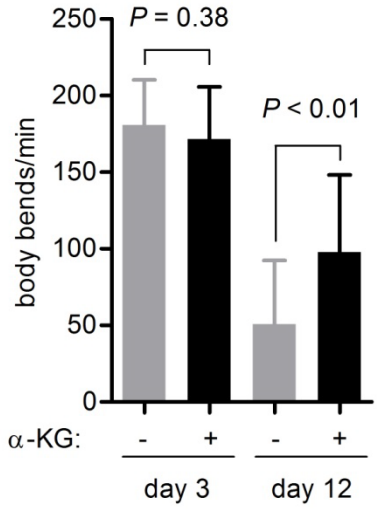

Figure 3.2. α-KG extends the healthspan of *C. elegans*, as assessed by locomotive assays. (a) α-KG extends the time that worms exhibit full body movement (FBM); m_{veh} = 16.0 (n = 139), $m_{\alpha\text{-KG}}$ = 21.7 (n = 167), $P < 0.0001$ (log-rank test). As expected, α-KG also extends the lifespan of these same worms; m_{veh} = 17.1 (n = 139), $m_{\alpha\text{-KG}}$ = 22.8 (n = 167), $P < 0.0001$ (log-rank test). m = mean lifespan (days); n = number of animals; veh = vehicle treated group. **(b)** α-KG suppresses the age-related decline in swimming speed.

a

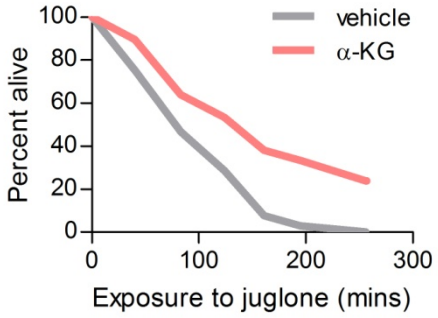

b

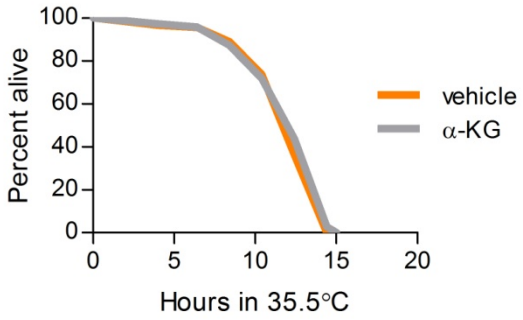

c

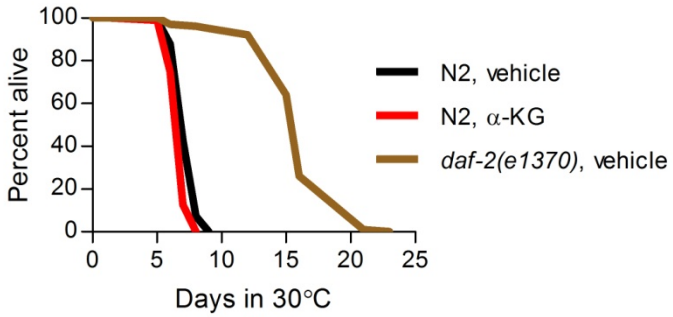

Figure 3.3. The effect of α-KG on the heat and oxidative stress resistance of wildtype N2 *C. elegans*. (a) α-KG increases resistance to juglone (median survival increased from 83 to 161 minutes, $P < 0.0001$, log-rank test). $n_{veh} = 105$; $n_{\alpha\text{-KG}} = 80$. **(b)** α-KG does not extend the lifespan of worms at 35.5°C; $m_{veh} = 12.2$ hours ($n = 91$), $m_{\alpha\text{-KG}} = 12.3$ hours ($n = 69$), $P = 0.3938$ (log-rank test). **(c)** α-KG does not extend the lifespan of worms at 30°C; $m_{veh} = 7.4$ days ($n = 98$), $m_{\alpha\text{-KG}} = 6.9$ days ($n = 96$), $P < 0.0001$ (log-rank test). As expected, *daf-2(e1370)* animals are thermotolerant ($P < 0.0001$,log-rank test); $m_{daf\text{-}2} = 16.5$ days ($n = 100$). *m* = mean lifespan; *n* = number of animals; veh = vehicle treated group.

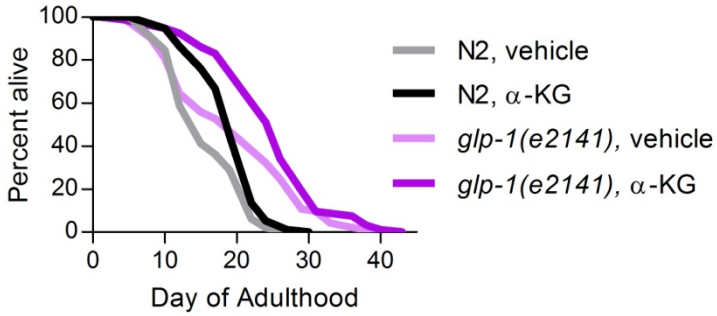

Figure 3.4. α-KG extends the lifespan of germline-less mutants. α-KG increases the lifespan of *glp-1(e2141)* mutants (P = 0.0016, log-rank test); m_{veh} = 20.2 (n = 93), $m_{\alpha\text{-KG}}$ = 25.3 (n = 94). Animals were raised from egg to L4 at 15°C, and then switched to 25 °C (the non-permissive temperature for *glp-1(e2141)*) at the young adult stage. For N2, m_{veh} = 16.1 (n = 97), $m_{\alpha\text{-KG}}$ = 19.1 (n = 96), P = 0.0003 (log-rank test). m = mean lifespan (days); n = number of animals; veh = vehicle treated group

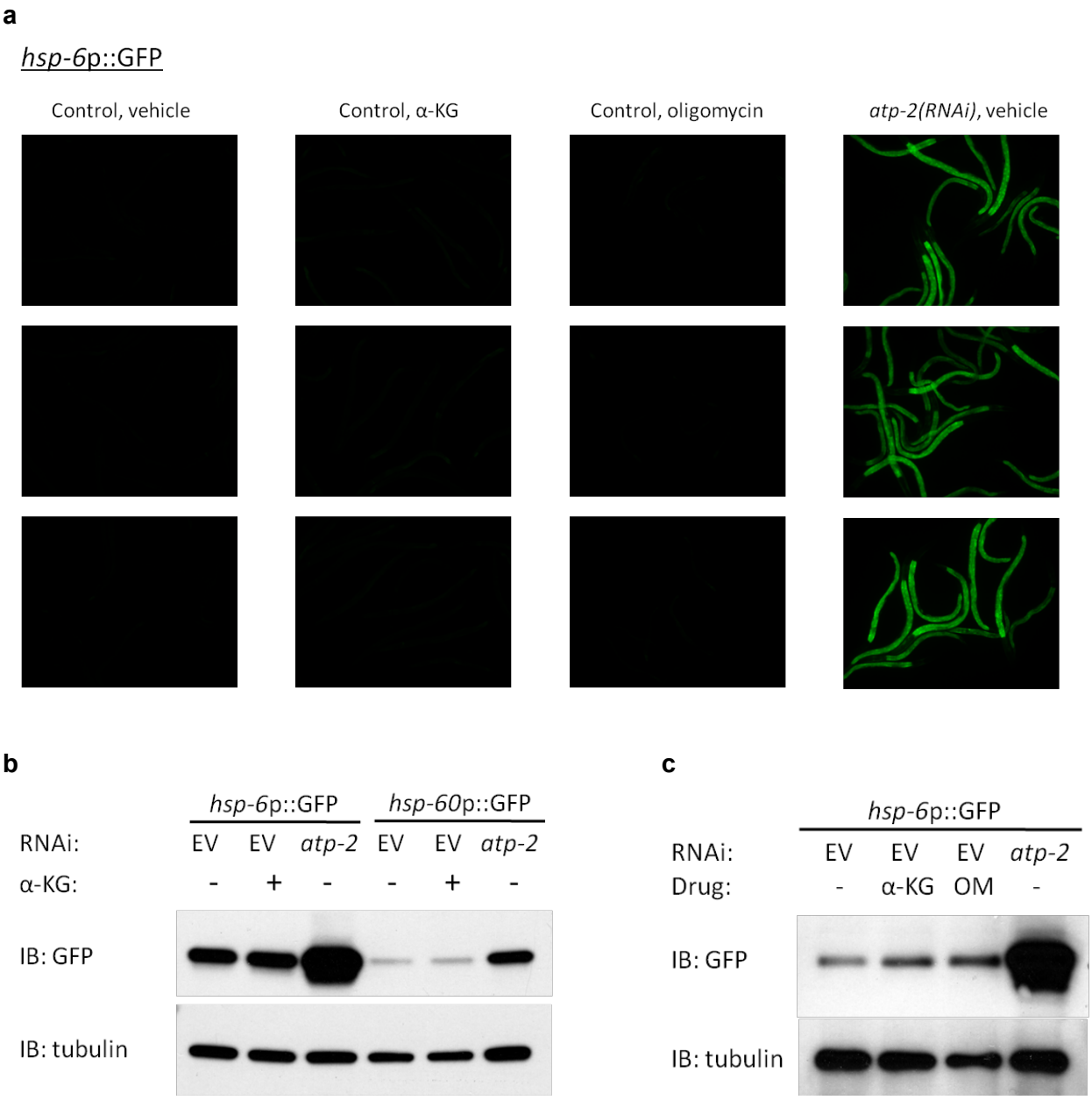

Figure 3.5. α-KG does not induce the mitochondrial unfolded protein response. Animals were fed control RNAi or *atp-2* RNAi, on plates containing vehicle, α-KG, or oligomycin (OM). **(a)** Three fluorescence images of mid-L3 *hsp-6*p::GFP worms, treated with the conditions shown, are depicted here. A low level of background GFP can be seen in the worms in the first three treatment conditions (i.e., control + vehicle, control + α-KG, or control + oligomycin). **(b,c)** Western blots showing the induction of UPR^{mt} in *atp-2(RNAi)* animals, but not in α-KG or oligomycin treated worms. EV, empty vector control RNAi.

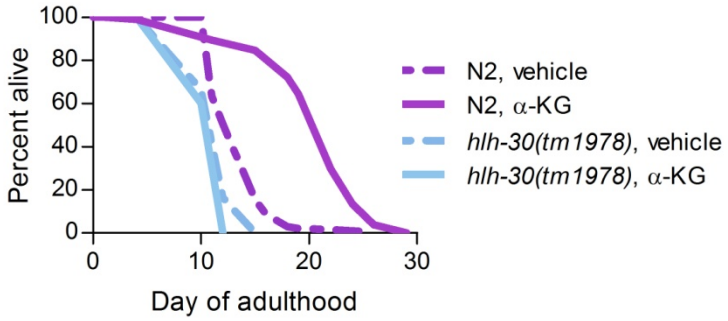

Figure 3.6. α-KG does not extend the lifespan of *hlh-30(tm1978)* mutants. α-KG does not extend the lifespan of *hlh-30(tm1978)* loss-of-function mutants (*P*=0.0025, log-rank test); m_{veh} = 11.8 (*n* = 110), $m_{\alpha\text{-KG}}$ = 11.2 (*n* = 123). For N2, m_{veh} = 13.6 (*n* = 103), $m_{\alpha\text{-KG}}$ = 20.7 (*n* = 104), *P* < 0.0001 (log-rank test). *m* = mean lifespan (days); *n* = number of animals; veh = vehicle treated group

References

1 Chin, R. M. *et al.* The metabolite alpha-ketoglutarate extends lifespan by inhibiting ATP synthase and TOR. *Nature*, doi:10.1038/nature13264 (2014).

2 Brauer, M. J. *et al.* Conservation of the metabolomic response to starvation across two divergent microbes. *Proc Natl Acad Sci U S A* **103**, 19302-19307, doi:10.1073/pnas.0609508103 (2006).

3 Dillin, A. *et al.* Rates of behavior and aging specified by mitochondrial function during development. *Science* **298**, 2398-2401, doi:10.1126/science.1077780 (2002).

4 Wong, A., Boutis, P. & Hekimi, S. Mutations in the clk-1 gene of Caenorhabditis elegans affect developmental and behavioral timing. *Genetics* **139**, 1247-1259 (1995).

5 Rea, S. L., Ventura, N. & Johnson, T. E. Relationship between mitochondrial electron transport chain dysfunction, development, and life extension in Caenorhabditis elegans. *PLoS Biol* **5**, e259, doi:10.1371/journal.pbio.0050259 (2007).

6 Curran, S. P. & Ruvkun, G. Lifespan regulation by evolutionarily conserved genes essential for viability. *PLoS Genet* **3**, e56 (2007).

7 Schmeisser, S. *et al.* Neuronal ROS signaling rather than AMPK/sirtuin-mediated energy sensing links dietary restriction to lifespan extension. *Mol Metab* **2**, 92-102, doi:10.1016/j.molmet.2013.02.002 (2013).

8 Kirkwood, T. B. Evolution of ageing. *Nature* **270**, 301-304 (1977).

9 Lithgow, G. J., White, T. M., Melov, S. & Johnson, T. E. Thermotolerance and extended life-span conferred by single-gene mutations and induced by thermal stress. *Proc Natl Acad Sci U S A* **92**, 7540-7544 (1995).

10 Honjoh, S., Yamamoto, T., Uno, M. & Nishida, E. Signalling through RHEB-1 mediates intermittent fasting-induced longevity in C. elegans. *Nature* **457**, 726-730 (2009).

11 Benedetti, M. G. *et al.* Compounds that confer thermal stress resistance and extended lifespan. *Exp Gerontol* **43**, 882-891, doi:10.1016/j.exger.2008.08.049 (2008).

12 Honda, Y. & Honda, S. The daf-2 gene network for longevity regulates oxidative stress resistance and Mn-superoxide dismutase gene expression in Caenorhabditis elegans. *FASEB J* **13**, 1385-1393 (1999).

13 Van Raamsdonk, J. M. & Hekimi, S. Deletion of the mitochondrial superoxide dismutase sod-2 extends lifespan in Caenorhabditis elegans. *PLoS Genet* **5**, e1000361, doi:10.1371/journal.pgen.1000361 (2009).

14 Yang, W. & Hekimi, S. Two modes of mitochondrial dysfunction lead independently to lifespan extension in Caenorhabditis elegans. *Aging Cell* **9**, 433-447, doi:10.1111/j.1474-9726.2010.00571.x (2010).

15 Feng, J., Bussiere, F. & Hekimi, S. Mitochondrial electron transport is a key determinant of life span in Caenorhabditis elegans. *Dev Cell* **1**, 633-644 (2001).

16 Van Raamsdonk, J. M. *et al.* Decreased energy metabolism extends life span in Caenorhabditis elegans without reducing oxidative damage. *Genetics* **185**, 559-571, doi:10.1534/genetics.110.115378 (2010).

17 Hsu, A. L., Murphy, C. T. & Kenyon, C. Regulation of aging and age-related disease by DAF-16 and heat-shock factor. *Science* **300**, 1142-1145 (2003).

18 Yoneda, T. *et al.* Compartment-specific perturbation of protein handling activates genes encoding mitochondrial chaperones. *J Cell Sci* **117**, 4055-4066, doi:10.1242/jcs.01275 (2004).

19 Durieux, J., Wolff, S. & Dillin, A. The cell-non-autonomous nature of electron transport chain-mediated longevity. *Cell* **144**, 79-91, doi:10.1016/j.cell.2010.12.016 (2011).

20 Houtkooper, R. H. *et al.* Mitonuclear protein imbalance as a conserved longevity mechanism. *Nature* **497**, 451-457, doi:10.1038/nature12188 (2013).

21 Bennett, C. F. *et al.* Activation of the mitochondrial unfolded protein response does not predict longevity in Caenorhabditis elegans. *Nat Commun* **5**, 3483, doi:10.1038/ncomms4483 (2014).

22 Lapierre, L. R. *et al.* The TFEB orthologue HLH-30 regulates autophagy and modulates longevity in Caenorhabditis elegans. *Nat Commun* **4**, 2267, doi:10.1038/ncomms3267 (2013).

23 Toth, M. L. *et al.* Longevity pathways converge on autophagy genes to regulate life span in Caenorhabditis elegans. *Autophagy* **4**, 330-338 (2008).

24 Hansen, M. *et al.* A role for autophagy in the extension of lifespan by dietary restriction in C. elegans. *PLoS Genet* **4**, e24, doi:10.1371/journal.pgen.0040024 (2008).

25 Brenner, S. The genetics of Caenorhabditis elegans. *Genetics* **77**, 71-94 (1974).

26 Sutphin, G. L. & Kaeberlein, M. Measuring Caenorhabditis elegans life span on solid media. *J Vis Exp*, doi:10.3791/1152 (2009).

27 De Castro, E., De Castro, S. H. & Johnson, T. E. Isolation of long-lived mutants in Caenorhabditis elegans using selection for resistance to juglone. *Free Radical Biology and Medicine* **37**, 139-145 (2004).

28 Hansen, M. *et al.* Lifespan extension by conditions that inhibit translation in Caenorhabditis elegans. *Aging Cell* **6**, 95-110 (2007).

29 Zhou, K. I., Pincus, Z. & Slack, F. J. Longevity and stress in Caenorhabditis elegans. *Aging (Albany NY)* **3**, 733-753 (2011).

30 Kaeberlein, T. L. *et al.* Lifespan extension in Caenorhabditis elegans by complete removal of food. *Aging Cell* **5**, 487-494, doi:10.1111/j.1474-9726.2006.00238.x (2006).

31 Arantes-Oliveira, N., Apfeld, J., Dillin, A. & Kenyon, C. Regulation of life-span by germ-line stem cells in Caenorhabditis elegans. *Science* **295**, 502-505, doi:10.1126/science.1065768 (2002).

32 Hsin, H. & Kenyon, C. Signals from the reproductive system regulate the lifespan of C. elegans. *Nature* **399**, 362-366, doi:10.1038/20694 (1999).

33 Priess, J. R., Schnabel, H. & Schnabel, R. The glp-1 locus and cellular interactions in early C. elegans embryos. *Cell* **51**, 601-611 (1987).

34 Settembre, C. *et al.* TFEB links autophagy to lysosomal biogenesis. *Science* **332**, 1429-1433, doi:10.1126/science.1204592 (2011).

35 Laplante, M. & Sabatini, D. M. mTOR signaling in growth control and disease. *Cell* **149**, 274-293, doi:10.1016/j.cell.2012.03.017 (2012).

CHAPTER 4

Lifespan Extension by Alpha-Ketoglutarate-Related Metabolites

Abstract

Alpha-ketoglutarate (α-KG), a tricarboxylic acid (TCA) cycle intermediate, extends lifespan by inhibiting the ATP synthase and target of rapamycin (TOR). α-KG is believed to be a key metabolite involved in dietary restriction (DR) induced longevity because it is elevated under DR and does not further extend the lifespan of DR animals. Consistently, previous evidence have shown that glutamate dehydrogenase and transaminase activities are increased in DR, such that the flux of amino acids to TCA cycle intermediates is escalated. On the other hand, under normal conditions, α-KG is a precursor of several amino acids. Here, we evaluate the effect of TCA cycle intermediates and α-KG-related amino acids on lifespan. We show that of the TCA cycle intermediates, only α-KG, succinate, pyruvate, and oxaloacetate extend lifespan. We also reveal that of the α-KG family of amino acids, only glutamate, glutamine, and proline can extend lifespan. Finally, we provide evidence that α-KG treatment only increases the levels of succinate, and not the levels of other closely related metabolites. As succinate and α-KG probably extend lifespan for different reasons, our results suggest that the longevity of α-KG treated animals is probably not due to the metabolism of α-KG into other metabolites.

Introduction

Aging and metabolism are closely linked. DR has been shown to extend lifespan in yeast, worms, flies, rodents, and primates[1-9]. In DR, proteins are catabolized and transaminase activities are enhanced, thereby increasing the flux from amino acids to TCA cycle intermediates[10-12]. Protein turnover is thought to be beneficial for lifespan extension because it rids the cell of damaged proteins that would otherwise accumulate. Previously, several metabolites of the TCA cycle have been shown to extend lifespan[13,14]. We found that α-KG extends lifespan by inhibiting the ATP synthase and TOR[15]. Based on our findings and those of others, here we test whether other TCA cycle intermediates would have any effect on lifespan. Additionally, in our previous work we showed that α-KG extends lifespan[15], but we did not examine the possible role of the α-KG family of amino acids in the lifespan extension seen. Therefore, here we determine what effect, if any, the α-KG family of amino acids (glutamate, glutamine, proline, and arginine), have on lifespan. We also perform metabolomics studies on human cells to evaluate the change in the levels of closely related metabolites in response to α-KG treatment. In this chapter, we analyze the lifespan of *C. elegans* treated with various TCA cycle intermediates or amino acids. We conclude with metabolomics data showing that α-KG treatment only increases the steady state levels of succinate, but not the other TCA cycle intermediates and amino acids.

Materials and Methods

Lifespan analysis. Lifespan assays were conducted as described in [15]. TCA cycle intermediates and amino acids were acquired from Sigma. Compounds were added to the nematode growth media after autoclaving but before solidification of the media. The pH of the media was adjusted with NaOH or HCl (as necessary) to match the pH of the vehicle plates.

Mass spectrometry-based analysis of metabolites. Metabolomics studies were conducted at the UCLA Metabolomics Center (University of California Los Angeles, Los Angeles, California). HEK-293 Cells were cultured for 24 h, rinsed with PBS, and medium containing 1,2-^{13}C-glucose (1 g/l) was added. After 24 h in the media with labeled glucose, cells were rinsed with ice-cold 150 mM NH_4AcO (pH 7.3) followed by addition of 400 µl cold methanol and 400 µl cold water. Cells were scraped off and transferred to an Eppendorf tube. 10 nmol norvaline and 400 µl chloroform were added to each sample. For the metabolite extraction, samples were vortexed for 5 min on ice, spun down, and the aqueous layer was transferred into a glass vial and dried. Metabolites were resuspended in 70% acetonitrile (ACN), and 5 µl of each sample was loaded onto a Phenomenex Luna 3u NH2 100A (150 x 2.0 mm) column. The chromatographic separation was performed on an UltiMate 300RSLC (Thermo Scientific) with mobile phases A (5 mM NH_4AcO, pH 9.9) and B (ACN) and a flow rate of 300 µl/min. The gradient ran from 15% A to 95% A over 18 min, 9 min isocratic at 95% A, and re-equilibration for 7 min. Metabolite detection was achieved with a Thermo Scientific Q Exactive mass spectrometer run in polarity switching mode (+3.0 kV / -2.25 kV). TraceFinder 3.1 (Thermo Scientific) was used to quantify metabolites as area under the curve using retention time and accurate mass measurements (≤ 3 ppm). Isotopomers were corrected for naturally occurring ^{13}C as described[16]. Relative amounts of metabolites were calculated by summing up all isotopomers of a given metabolite.

Results

α-KG is part of the TCA cycle, where it is produced from isocitrate by oxidative decarboxylation catalysed by isocitrate dehydrogenase. We tested whether other TCA cycle intermediates could extend lifespan as well. α-KG, succinate, and pyruvate reliably extended lifespan in two independent experiments (Fig. 4.1). Of the TCA cycle metabolites, oxaloacetate

and pyruvate have already been shown to extend lifespan[13,14], which was verified by our work (Fig. 4.1 and data not shown).

α-KG is also a precursor for several amino acids, including glutamate, glutamine, proline, and arginine (Fig. 4.2)[17]. Of those, only proline has been shown to extend lifespan[18], albeit without a well-defined mechanism. We show that glutamine, glutamate, and proline extend the lifespan of wildtype N2 *C. elegans*, but arginine does not (Fig. 4.3a-d,f). For comparison, we also show that methionine and leucine supplementation do not extend lifespan (Fig. 4.3e); this was somewhat expected since methionine restriction extends lifespan[19,20] and leucine abrogates the longevity effect of starvation in *C. elegans*[21].

Since α-KG can be metabolized into other TCA cycle intermediates and amino acids, including those that extend lifespan by themselves, it is important to study how α-KG treatment affects the levels of other closely related metabolites. To this end, we performed metabolomics studies on HEK-293 cells treated with octyl α-KG or vehicle control (octanol). We also cultured the cells in the presence of 1,2-^{13}C-glucose for 24 h in order to gain more information concerning the metabolism of glucose. The concentration of TCA cycle intermediates, several amino acids, and other metabolites were measured using LC-MS.

Consistent with hydrolysis of octyl α-KG yielding α-KG, cells treated with octyl α-KG have higher levels of α-KG (2.2 fold; $P = 4.9 \times 10^{-6}$) than octanol treated control cells (Fig. 4.4a). Because the only source of exogenous ^{13}C carbon in the experiment was the 1,2-^{13}C-labeled glucose and the majority of α-KG was unlabeled (M+0 isotopomer; Fig. 4.4b), this strongly suggests that the bulk of the increased α-KG came from the hydrolysis of exogenously provided octyl α-KG. Our data also demonstrate that intracellular α-KG levels can be accumulated by octyl α-KG treatment, as opposed to being quickly metabolized into other products.

Among the other TCA cycle intermediates, there was a small increase in succinate levels, but no significant change in the steady state levels of pyruvate, citrate, fumarate, or malate (Fig. 4.4a). There was also no change in the levels of glutamate, glutamine, proline, or

arginine, the α-KG-related amino acids (Fig. 4.4a). Consistent with data shown in [15], ATP levels are decreased in octyl α-KG treated cells (Fig. 4.4a). Also, the amount of the M+2 isotopomer of citrate did not change in octyl α-KG treated cells (Fig. 4.4b), indicating that the flux into the TCA cycle is not affected by octyl α-KG treatment. As α-KG probably works via a different mechanism than succinate to extend lifespan (discussed below), and octyl α-KG treatment does not increase the steady state levels of other TCA cycle intermediates (except succinate) or amino acids, our metabolomics data suggest that the biological effects of α-KG are attributable to α-KG itself, rather than metabolites of α-KG.

Discussion

In this chapter, we show that of the TCA cycle intermediates, only oxaloacetate, succinate, pyruvate, and α-KG extend lifespan. Additional work is required to clarify whether α-KG extends lifespan via the same mechanism as the other TCA cycle intermediates. However, we can speculate on this topic. First, oxaloacetate was shown to extend lifespan in a *daf-16* and *aak-2* dependent manner[14]. This differs from α-KG, which can still extend lifespan in *daf-16* or *aak-2* mutant or RNAi animals[15]. Second, pyruvate was suggested to increase lifespan by increasing reactive oxygen species (ROS) levels, as the addition of N-acetyl-L-cysteine (NAC) abolished the long lifespan of mutants with higher levels of pyruvate[13]. On the other hand, α-KG also increased ROS levels[15], but the importance of ROS to α-KG mediated longevity is unresolved at this time. Third, succinate drives electron flow through complex II of the electron transport chain (succinate is a substrate for complex II), whereas α-KG does not affect electron flow through complex II[15]. Also, succinate does not bind to the beta subunit of ATP synthase and does not inhibit ATP synthase, unlike α-KG (data not shown). The differences between our findings on α-KG and what is known about oxaloacetate and succinate suggest that the mechanism by which α-KG extends lifespan is distinct from that of oxaloacetate and succinate.

At this time, we cannot make any conclusions on whether pyruvate and α-KG promote longevity via a similar mechanism.

We also evaluated the effects of α-KG related amino acids on lifespan. We show that glutamine, glutamate, and proline, but not arginine, extend lifespan, but the mechanism by which they extend lifespan has not been studied further.

Finally, we have performed metabolomic analysis on octyl α-KG treated cells. Our data only show steady state levels of metabolites and only provides a hint into the metabolism of α-KG by cells. A flux experiment, in which cells are fed labeled α-KG and the metabolome is assessed at various time points, is necessary to determine exactly where the supplemental α-KG is going. Nonetheless, given the data that we have at this point, our current findings support the notion that α-KG mediated lifespan extension is not due to upregulation of other metabolites.

a

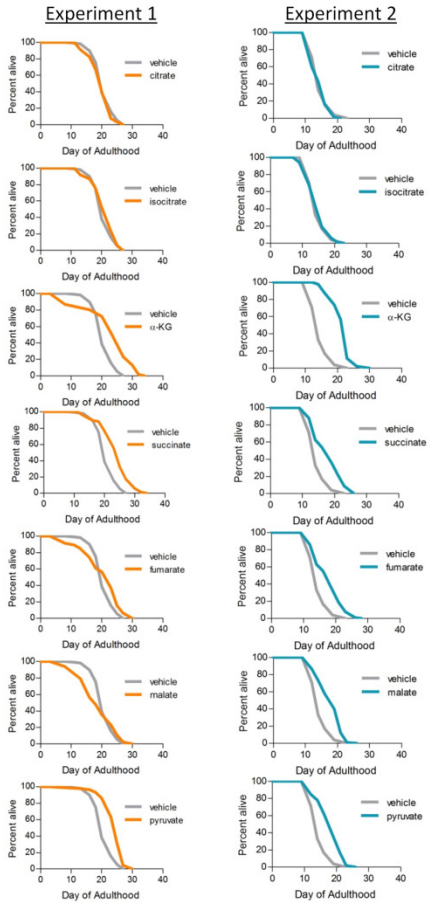

b

	Experiment 1			Experiment 2		
Treatment	**Percent increase in mean lifespan (compared to vehicle)**	***P*-value**	**n, number of animals**	**Percent increase in mean lifespan (compared to vehicle)**	***P*-value**	**n, number of animals**
Citrate	-3.2	0.246	91	-1.0	0.7199	100
Isocitrate	1.8	0.1978	99	0.4	0.6743	104
α-KG	11.1	< 0.0001	61	47.0	< 0.0001	88
Succinate	16.1	< 0.0001	68	22.7	< 0.0001	91
Fumarate	-0.5	0.0534	46	21.8	< 0.0001	92
Malate	-9.0	0.3907	48	22.4	< 0.0001	90
Pyruvate	16.7	< 0.0001	87	24.0	< 0.0001	105

Figure 4.1. Effect of tricarboxylic acid cycle intermediates on *C. elegans* lifespan. Results from screening the tricarboxylic acid cycle intermediates for an effect on lifespan. Two independent experiments are shown; all metabolites were given at a concentration of 8 mM. Lifespan curves are shown in (a); statistical data is shown in (b). Only α-KG, succinate, and pyruvate extended lifespan repeatedly in the two experiments.

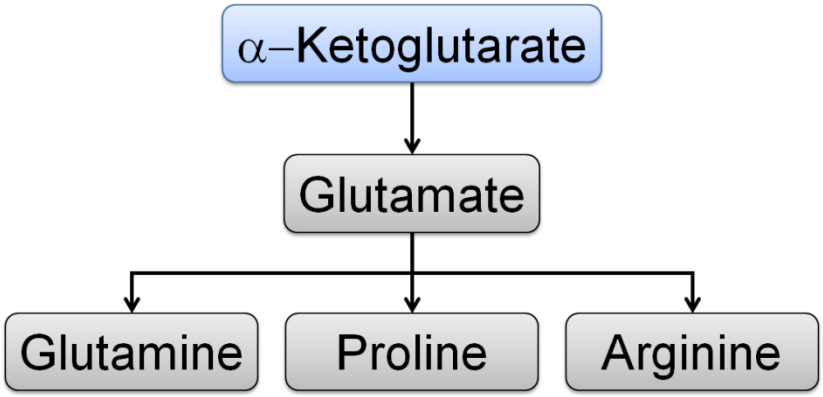

Figure 4.2. α-KG biosynthetic family of amino acids. Glutamate can be made from α-KG by glutamate dehydrogenase, and glutamine can be made from glutamate by glutamine synthetase. Proline and arginine are both synthesized via a multistep process from glutamate[17].

a

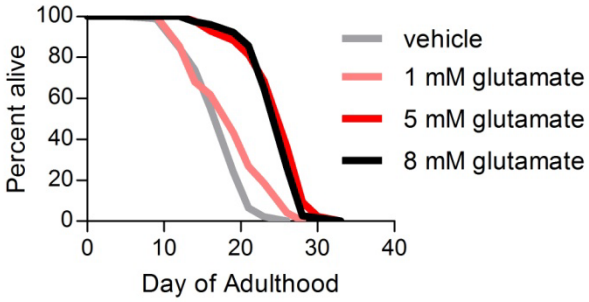

b

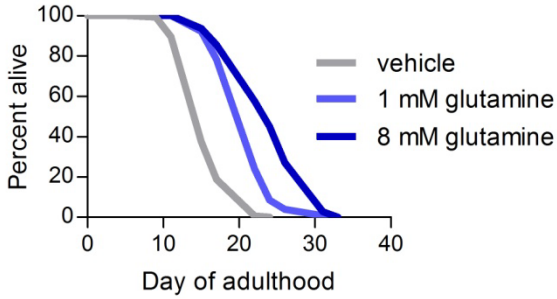

c

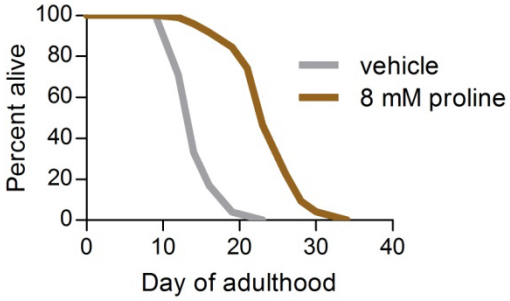

d

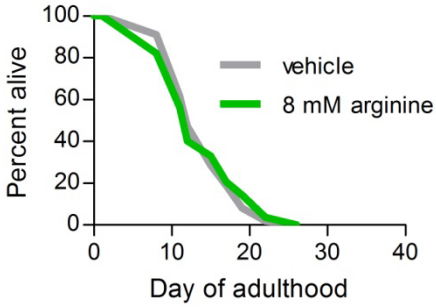

e

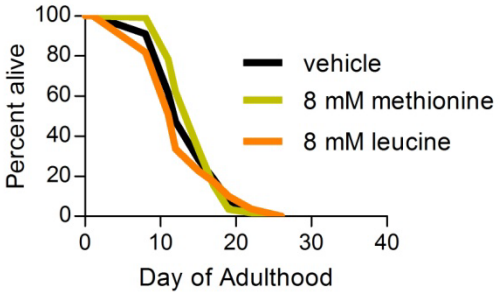

f

Amino acid	Concentration (mM)	Mean lifespan	Percent increase in mean lifespan over vehicle	*P*-value	Number of animals
L-glutamate	0	17.5	n/a	n/a	92
	1	19.0	8.5	0.0012	97
	5	25.2	44.0	< 0.0001	86
	8	25.0	43.0	< 0.0001	77
L-glutamine	0	16.3	n/a	n/a	144
	1	21.6	32.9	< 0.0001	129
	8	24.6	51.3	< 0.0001	111
L-proline	0	14.7	n/a	n/a	100
	8	24.0	63.3	< 0.0001	97
L-arginine	0	14.0	n/a	n/a	112
	8	13.8	-1.2	0.812	112
	0	14.0	n/a	n/a	112
L-methionine	8	14.7	5.2	0.4305	116
L-leucine	8	13.2	-5.9	0.3307	110

Figure 4.3. The effect of amino acid supplementation on *C. elegans* lifespan. (a-e) Glutamate, glutamine, or proline supplementation extended lifespan of wildtype N2 *C. elegans*, but arginine, methionine, or leucine did not. **(f)** Summary of data from a-e.

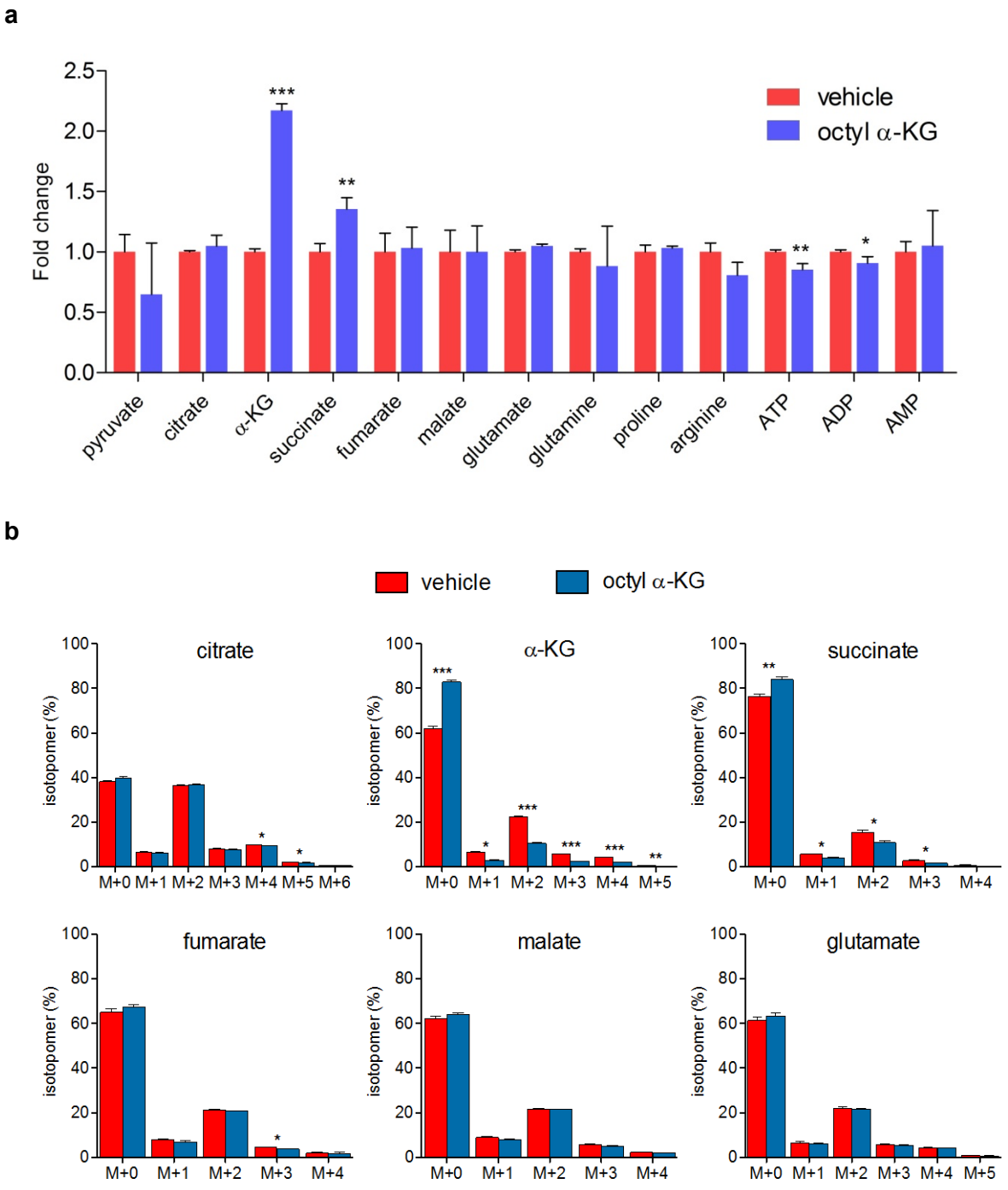

Figure 4.4. Metabolomic analysis of octyl α-KG treated cells. HEK293 cells were treated with 400 μM octyl α-KG and incubated in medium containing 1,2-^{13}C-glucose for 24 h. Relative amounts (a), as well as isotopomer distribution (b), of various metabolites were measured by mass spectrometry. Isotopomers were corrected for naturally occurring ^{13}C. (* P <0.05, ** P < 0.01, *** P < 0.001).

References

1 Lin, S. J., Defossez, P. A. & Guarente, L. Requirement of NAD and SIR2 for life-span extension by calorie restriction in Saccharomyces cerevisiae. *Science* **289**, 2126-2128 (2000).

2 Lakowski, B. & Hekimi, S. The genetics of caloric restriction in Caenorhabditis elegans. *Proc Natl Acad Sci U S A* **95**, 13091-13096 (1998).

3 Avery, L. The genetics of feeding in Caenorhabditis elegans. *Genetics* **133**, 897-917 (1993).

4 Greer, E. L. *et al.* An AMPK-FOXO pathway mediates longevity induced by a novel method of dietary restriction in C. elegans. *Curr Biol* **17**, 1646-1656, doi:10.1016/j.cub.2007.08.047 (2007).

5 Partridge, L., Green, A. & Fowler, K. Effects of egg-production and of exposure to males on female survival in Drosophila melanogaster. *Journal of Insect Physiology* **33**, 745–749 (1987).

6 Colman, R. J. *et al.* Caloric restriction delays disease onset and mortality in rhesus monkeys. *Science* **325**, 201-204 (2009).

7 Colman, R. J. *et al.* Caloric restriction reduces age-related and all-cause mortality in rhesus monkeys. *Nat Commun* **5**, 3557, doi:10.1038/ncomms4557 (2014).

8 Weindruch, R. & Walford, R. L. Dietary restriction in mice beginning at 1 year of age: effect on life-span and spontaneous cancer incidence. *Science* **215**, 1415-1418 (1982).

9 Weindruch, R., Walford, R. L., Fligiel, S. & Guthrie, D. The retardation of aging in mice by dietary restriction: longevity, cancer, immunity and lifetime energy intake. *J Nutr* **116**, 641-654 (1986).

10 Haigis, M. C. *et al.* SIRT4 inhibits glutamate dehydrogenase and opposes the effects of calorie restriction in pancreatic beta cells. *Cell* **126**, 941-954, doi:10.1016/j.cell.2006.06.057 (2006).

11 Hagopian, K., Ramsey, J. J. & Weindruch, R. Caloric restriction increases gluconeogenic and transaminase enzyme activities in mouse liver. *Exp Gerontol* **38**, 267-278 (2003).

12 Dhahbi, J. M. *et al.* Caloric restriction alters the feeding response of key metabolic enzyme genes. *Mech Ageing Dev* **122**, 1033-1048 (2001).

13 Mouchiroud, L. *et al.* Pyruvate imbalance mediates metabolic reprogramming and mimics lifespan extension by dietary restriction in Caenorhabditis elegans. *Aging Cell* **10**, 39-54 (2011).

14 Williams, D. S., Cash, A., Hamadani, L. & Diemer, T. Oxaloacetate supplementation increases lifespan in Caenorhabditis elegans through an AMPK/FOXO-dependent pathway. *Aging Cell* **8**, 765-768 (2009).

15 Chin, R. M. *et al.* The metabolite alpha-ketoglutarate extends lifespan by inhibiting ATP synthase and TOR. *Nature*, doi:10.1038/nature13264 (2014).

16 Yuan, J., Bennett, B. D. & Rabinowitz, J. D. Kinetic flux profiling for quantitation of cellular metabolic fluxes. *Nat Protoc* **3**, 1328-1340, doi:10.1038/nprot.2008.131 (2008).

17 Devlin, T. M. *Textbook of biochemistry : with clinical correlations*. 6th edn, (Wiley-Liss, 2006).

18 Zarse, K. *et al.* Impaired insulin/IGF1 signaling extends life span by promoting mitochondrial L-proline catabolism to induce a transient ROS signal. *Cell Metab* **15**, 451-465, doi:10.1016/j.cmet.2012.02.013 (2012).

19 Miller, R. A. *et al.* Methionine-deficient diet extends mouse lifespan, slows immune and lens aging, alters glucose, T4, IGF-I and insulin levels, and increases hepatocyte MIF levels and stress resistance. *Aging Cell* **4**, 119-125, doi:10.1111/j.1474-9726.2005.00152.x (2005).

20 Orentreich, N., Matias, J. R., DeFelice, A. & Zimmerman, J. A. Low methionine ingestion by rats extends life span. *J Nutr* **123**, 269-274 (1993).

21 Kang, C. & Avery, L. Systemic regulation of starvation response in Caenorhabditis elegans. *Genes Dev* **23**, 12-17, doi:10.1101/gad.1723409 (2009).

CHAPTER 5

Conclusions

The data presented in this dissertation examines the mechanism by which alpha-ketoglutarate (α-KG) extends lifespan. Specifically, we used DARTS (drug affinity response target stability)[1], an unbiased, label-free method for drug target identification, to discover a new binding target of α-KG, the beta subunit of ATP synthase[2]. We found that α-KG inhibited the activity of ATP synthase *in vitro* and *in vivo*, and reduced the ATP content and oxygen consumption of cells and animals[2]. In these respects, α-KG treatment gives similar results to the genetic inhibition (mutant or RNAi) of ATP synthase. However, α-KG supplementation differs from the genetic modulation of ATP synthase because α-KG does not arrest development, slow pharyngeal pumping, or induce the mitochondrial unfolded protein response[2] (also see Chapter 3). Interestingly, while we were working on the binding and inhibition of ATP synthase by α-KG, another group demonstrated that α-KG binds and inhibits an ATPase in bacteria[3].

Downstream of the interaction with ATP synthase, α-KG also inhibits the target of rapamycin (TOR), as evidenced by a decreased phosphorylation of TOR substrates and an increased autophagy[2]. The induction of autophagy by α-KG is probably important for the life prolonging effect of α-KG (Chapter 3). Consistent with TOR being an important mediator of dietary restriction (DR) induced longevity, α-KG could not further increase the lifespan of DR animals[2]. We also found that α-KG levels were increased in starved animals[2]. Taken together, our data suggest that α-KG is a key metabolite in DR induced longevity.

We also explored whether metabolites closely related to α-KG would have an effect on lifespan. Much of the tricarboxylic acid cycle (TCA) cycle intermediates did not extend lifespan.

Pyruvate, oxaloacetate, and succinate prolong lifespan, but the latter two most likely do not work through the same mechanism as α-KG (Chapter 4). Some α-KG-related amino acids extended lifespan as well, but at this time the mechanism by which those amino acids extend lifespan is unknown (Chapter 4). Furthermore, our metabolomics data show that α-KG treatment does not result in an increased steady state level of pyruvate, citrate, fumarate, malate, glutamate, glutamine, proline, or arginine, supporting the idea that α-KG mediated longevity is probably not due to the metabolism of α-KG into other closely related metabolites.

Although we have focused our efforts to characterize a new α-KG-binding target, α-KG has many other known functions, and it is possible that these may also play a role in the lifespan extension by α-KG. For instance, besides the prolyl 4-hydroxylase (as discussed in [2]), there are many other α-KG dependent oxygenases[4], and in addition to the TCA cycle, α-KG plays a role in the urea cycle, aiding in the removal of ammonia from the body. Next, α-KG was found to bind to a G protein coupled receptor[5,6] whose function has not been sufficiently explored. Finally, we found other novel binding targets of α-KG by DARTS[2], but we have not characterized the role of their binding to the longevity effect of α-KG.

Our discovery that α-KG extends the lifespan and healthspan of *C. elegans* is exciting, but the implications for human health are currently unknown. However, based on the current literature in mammals and lower organisms, we hypothesize that α-KG may have anti-aging (or anti-age-related disease) effects in humans. First, the mechanism by which α-KG extends lifespan in *C. elegans* is conserved in human cells[2]. Second, α-KG has been shown to be effective against age-related diseases in mammals; for example, α-KG inhibits tumor growth and angiogenesis in murine tumor xenograft models[7-9] and decreases the arterial stiffening that occurs in old mice[10]. Lastly, because α-KG is an endogenous metabolite, people have already been taking α-KG as a supplement, and α-KG levels are increased under starvation[2,11,12], we speculate that α-KG supplementation will be safe in humans.

As the elderly population continues to be the fastest growing age group[13], the incidence of age-related diseases will increase dramatically over the upcoming years. Thus, there is a great need to develop new and better strategies to treat or prevent aging and age-related diseases. Our work takes us one step closer to meeting this goal. For the future, we look forward to seeing the development of more potent and safer drugs, or perhaps even combination of drugs, to delay aging and combat the age-related decline in health.

References

1 Lomenick, B. *et al.* Target identification using drug affinity responsive target stability (DARTS). *Proc Natl Acad Sci U S A* **106**, 21984-21989 (2009).

2 Chin, R. M. *et al.* The metabolite alpha-ketoglutarate extends lifespan by inhibiting ATP synthase and TOR. *Nature*, doi:10.1038/nature13264 (2014).

3 Radchenko, M. V., Thornton, J. & Merrick, M. P(II) signal transduction proteins are ATPases whose activity is regulated by 2-oxoglutarate. *Proc Natl Acad Sci U S A* **110**, 12948-12953, doi:10.1073/pnas.1304386110 (2013).

4 Loenarz, C. & Schofield, C. J. Expanding chemical biology of 2-oxoglutarate oxygenases. *Nat Chem Biol* **4**, 152-156, doi:10.1038/nchembio0308-152 (2008).

5 Hebert, S. C. Physiology: orphan detectors of metabolism. *Nature* **429**, 143-145, doi:10.1038/429143a (2004).

6 He, W. *et al.* Citric acid cycle intermediates as ligands for orphan G-protein-coupled receptors. *Nature* **429**, 188-193, doi:10.1038/nature02488 (2004).

7 Matsumoto, K. *et al.* Antitumor effects of 2-oxoglutarate through inhibition of angiogenesis in a murine tumor model. *Cancer Sci* **100**, 1639-1647, doi:10.1111/j.1349-7006.2009.01249.x (2009).

8 Tennant, D. A. & Gottlieb, E. HIF prolyl hydroxylase-3 mediates alpha-ketoglutarate-induced apoptosis and tumor suppression. *J Mol Med (Berl)* **88**, 839-849, doi:10.1007/s00109-010-0627-0 (2010).

9 Harrison, A. P. & Pierzynowski, S. G. Biological effects of 2-oxoglutarate with particular emphasis on the regulation of protein, mineral and lipid absorption/metabolism, muscle performance, kidney function, bone formation and cancerogenesis, all viewed from a healthy ageing perspective state of the art--review article. *J Physiol Pharmacol* **59 Suppl 1**, 91-106 (2008).

10 Niemiec, T. *et al.* Alpha-ketoglutarate stabilizes redox homeostasis and improves arterial elasticity in aged mice. *J Physiol Pharmacol* **62**, 37-43 (2011).

11 Brauer, M. J. *et al.* Conservation of the metabolomic response to starvation across two divergent microbes. *Proc Natl Acad Sci U S A* **103**, 19302-19307, doi:10.1073/pnas.0609508103 (2006).

12 Kaminsky, Y. G., Kosenko, E. A. & Kondrashova, M. N. Metabolites of citric acid cycle, carbohydrate and phosphorus metabolism, and related reactions, redox and phosphorylating states of hepatic tissue, liver mitochondria and cytosol of the pigeon, under normal feeding and natural nocturnal fasting conditions. *Comp Biochem Physiol B* **73**, 957-963 (1982).

13 US Department of Health and Human Services, A. o. A. *Projected future growth of the older population*, <http://www.aoa.gov/Aging_Statistics/future_growth/future_growth.aspx#age> (2008).